Preformulation Development of a monovalent recombinant-based subunit vaccine, a multivalent recombinant-based subunit vaccine and a multivalent live attenuated viral vaccine

By

Vidyashankara Iyer Gowrishankara

B.S. Chemistry, University of Kansas, 2007

Submitted to the Bioengineering Graduate Program and the Graduate Faculty of the University of Kansas in partial fulfillment of the requirements for the degree of Doctor of Philosophy.

_____

Chairperson Charles Russell Middaugh

_____

David B. Volkin

_____

Jennifer Laurence

_____

Stevin Gehrke

_____

Michael Detamore

Dissertation Defended on October 4th 2012

The Dissertation Committee for Vidyashankara Iyer Gowrishankara certifies that this is the approved version of the following dissertation:

Preformulation Development of a monovalent recombinant-based subunit vaccine, a multivalent recombinant-based subunit vaccine and a multivalent live attenuated viral vaccine

_____

Chairperson Charles Russell Middaugh

Dissertation Approved on October 4th 2012

Preformulation Development of a monovalent recombinant-based subunit vaccine, a multivalent recombinant-based subunit vaccine and a multivalent live attenuated viral vaccine

Vidyashankara Iyer

The University of Kansas, 2012

ABSTRACT

The objective of this project is to explore of the use of the empirical phase diagram approach in the formulation development of several forms of vaccines that exist today such as recombinant based subunit vaccines and the traditional live attenuated viral vaccines. The chapters in this dissertation describe the formulation development of three vaccines. The first is a monovalent recombinant-based subunit vaccine targeted against that 2009 pandemic "swine" influenza (Chapter 1). The second is a trivalent vaccine consisting of three recombinantly produced proteins from S. pneumonia (Chapter 2). The third is a trivalent live viral canine vaccine targeted against canine distemper, parainfluenza and kennel cough caused by canine adenovirus type 2 (Chapter 3). The first aim in each chapter is the biophysical characterization of the individual biological entities. This was accomplished by initially by fully characterizing each of the antigens using multiple analytical techniques such as intrinsic tryptophan fluorescence and circular dichroism spectroscopy and static light scattering experiments among others. The ideal preformulation conditions were identified using the empirical phase diagram technique.

Influenza is a prevalent, highly contagious and sometimes fatal respiratory disease. Vaccination provides an effective approach to control the disease, but because of frequent changes in the structure of the major surface proteins, there is great need for a technology that permits rapid preparation of new forms of the vaccine each year in sufficient quantities. Recently, using a safe, simple, time- and cost-effective plant viral vector-based transient expression system, the hemagglutinin antigen of H1N1

influenza A strain (HAC1), an H1N1 influenza vaccine candidate, has been produced in Nicotiana benthamiana plants. As a step towards the generation of a commercially viable subunit influenza vaccine, we developed HAC1 formulations in the presence and absence of an aluminum salt adjuvant (Alhydrogel®), analyzed their properties, and assessed immunogenicity in an animal model. Biophysical properties of HAC1 were evaluated using several spectroscopic and light scattering techniques as a function of pH and temperature combined with data analysis using an empirical phase diagram approach. Excipients that were potent stabilizers of the recombinant protein were identified using intrinsic fluorescence spectroscopy. The adsorptive capacity and thermal stability of the protein on the surface of Alhydrogel® were then examined in the presence and absence of selected stabilizers using UV absorbance after centrifugation and intrinsic fluorescence spectroscopy, respectively. Immunogenicity studies conducted in mice demonstrated that the highest level of serum immune responses (hemagglutination-inhibiting antibody titers), with a 100% seropositive rates, were induced by HAC1 in the presence of Alhydrogel®, and this response was elicited regardless of the solution conditions of the formulation.

The preformulation of a trivalent recombinant protein based vaccine candidate for protection against Streptococcus pneumoniae is described both in the presence and absence of aluminum salt adjuvants. The biophysical properties of the three protein-based antigens, fragments of PsaA, StkP and PcsB, were studied using several spectroscopic and light scattering techniques. An empirical phase diagram was constructed to assess the overall conformational stability of the three antigens as a function of pH and temperatures. A variety of excipients were screened based on their ability to stabilize each antigen using intrinsic fluorescence spectroscopy and circular dichroism spectroscopy. Sorbitol, sucrose, and trehalose stabilized three proteins in solution. The addition of manganese also showed a drastic increase in the thermal stability of PsaA in solution. The adsorption and desorption processes of each of the antigens to aluminum salt adjuvants were evaluated and the stability of the adsorbed proteins were then assessed using intrinsic fluorescence spectroscopy and FTIR spectroscopy. All three proteins showed

good adsorption to Alhydrogel. PsaA was destabilized when adsorbed onto Alhydrogel and adding sodium phosphate showed a stabilizing effect. PcsB was found to be stabilized when adsorbed to Alhydrogel, and no destabilizing or stabilizing effects were seen in the case of StkP.

The empirical phase diagram based approach was utilized to rapidly identify stabilizing buffer conditions and excipients for potential use in a complex trivalent live-virus veterinary vaccine. The attenuated versions of canine distemper virus (CDV), canine parainfluenza virus (CPI) and the canine adenovirus type 2 (CAV2) were purified separately to enable study of the physical stability of the individual viruses. The CDV and CPI viruses were purified using centrifugation and/or sucrose gradient techniques, and CAV2 virus was isolated using ammonium sulfate precipitation. The integrity of the three viruses was confirmed by transmission electron microscopy and purity was assessed by SDS-PAGE. The structural properties and conformational stability of the three viruses were then studied using various spectroscopic and light scattering techniques. The data obtained from the various methods were then used to construct an empirical phase diagram to characterize the physical stability of the individual viruses as a function of pH and temperature. Potential stabilizers were then identified for each virus using an assay based on the aggregation state of the viral particles and the conformational state of the viral proteins. Sucrose and sorbitol were demonstrated to be promising common stabilizers for all three live attenuated viruses.

In conclusion, the empirical phase diagram approach was used to successfully formulate three vaccines in solution and while adsorbed on to the surface of aluminum salt adjuvants. The EPD proves to be a robust tool that can aid immensely in the early stages of formulation.

Dedicated to

Lord Hanuman,

My parents,

Sugantha and H.S. Gowrishankara,

My Aunt,

Radha

My brothers,

Mahesh and Radhakrishna,

And my Sister-in-law

Ramya

ACKNOWLDEGMENTS

I would like to acknowledge my advisor, Dr. Russ Middaugh, for his advice and guidance over the years. I would not have come this far without him. Russ is truly passionate about science. He is one of those rare people, with whom you can have a conversation about just anything – from the latest science to animal conservation. His dedication to educating students is unparalleled. There are very few people like him today. I am grateful to have known him and worked for him. I would also like to thank Dr. Sangeeta Joshi. She has been a great source of scientific knowledge and she has always found time to help me, scientifically or personally. Sangeeta is an amazing person and she is one of my closest friends and I am very fortunate to have worked for her. I would like to thank Dr. David Volkin for his help and encouragement over the years of my PhD. I will always cherish my time at the Macromolecule and Vaccine Stabilization Center. I want to take this opportunity to thank Drs. Jennifer Laurence, Michael Detamore, and Stevin Gehrke for their valuable time and advice and for serving on my committee.

Dr. Sampathkumar Krishnan was my mentor during my internship at Amgen Inc. I want to thank Dr. Krishnan for your guidance and for giving me the opportunity to work with him and the rest of the formulation group at Amgen.

I would also like to thank all my group members for the great times and memories. I would specifically like to thank Srivalli Telikepalli, Christopher Olsen, Yuhong Zeng, Prakash Manikwar, Rajoshi Chaudhry, Ranajoy Majumdar, Ryan Kramer, Ozam Kumru, Harshit Khasa and Neha Sahni. They are among my best friends I will always remember the times we spent together.

I would like to thank our collaborators at Fraunhofer Inc., Intercell AG, Intervet Inc. and PATH for their support, funding and contributions towards the development of the various vaccines outlined in this thesis.

I would also like to recognize and thank all the faculty members at Department of Bioengineering. I am honored to have been one of the first students to be accepted and graduate from this program.

I would like to thank my roommates Kannan Vetrivillalan, Arunsai Koppalan, Srinivas Kumar and Saurabh Srinivasan for their support. Graduate school has been a long journey and walking that road with friends is what made it really enjoyable and effortless. I would also like to thank some of my oldest friends who are always there when I need them. Yashas, Sridevi, Abheera, Gouri, Supriya, Vidya, Divya, Shruthi, Sathya, JD, Prashanth, Rajani, and Vignesh are among those who have played a crucial role in defining who I am. They are among those who have supported me immensely when I have needed them. I would also like to remember my dog, Chocky. I was reminded of him every day while I worked on the canine vaccine project.

Last, but not the least, I would like to thank my family. My father and mother went through a lot of hardship when I was younger. They would meet my teachers and principal regularly to follow up on my performance. My parents put in a lot of effort to make sure that I went to tuition and got a good education. They were instrumental in me getting admissions into the University of Kansas. There is no way that I would be here without them. I also want to thank my brothers, Mahesh and Radhakrishna, for their encouragement and support. Every time I almost gave up, my brothers have given me the boost that I needed to become productive again. I also want to thank my sister-in-law, Ramya Gopalakrishnan, for making the last few years very memorable to me and my family. I am going to be an uncle to a baby girl soon and we are very excited about having an addition to our family. I would also like to thank all of my uncles, aunts and my cousins. I also want to thank my grandparents, for they taught me the value of simplicity. My immense love for wildlife and animals is something that I inherited from my mother and grandfather, Sri Ananthanarayan Iyer of Coimbatore. My extended family includes over a 100 members and everyone is extremely supportive and wish for nothing but the best.

My salutations to my gurus, His Holiness, Sri Abhinava Vidya Theertha Mahaswamigal and His Holiness, Sri Bharathi Theertha Mahaswamigal of the Sringeri Sharada Peetam. My family and I have drawn immense strength and support from the Jagadguru. I was named after the Vidyashankara Temple at Sringeri, and I feel this symbolizes the eternal bond that my family has with Sringeri Sri Sharada Peetam for which I am grateful to my grandfather Sri Srikanta Iyer of Shimoga. Finally, I would like to recite the first few verses of Hanuman Chalisa. This is a source of great strength and it came to me at a time when I needed it most.

श्रीगुरु चरण् सरोजरज, नजिमनमुकुर सुधार ।
बरणौ रघुबर बमिल यश, जो दायक फलचार ॥

बुद्धहिीन तनु जानकै, सुमरौं पवन कुमार ।
बल बुद्धविद्या देहु मोहि, हरहु कलेश वकिार ॥

Table of Contents

Chapter 1

Introduction

Introduction

In combination with public health measures, vaccines have had the most profound beneficial effect on the quality of human health since the wide availability of potable water. With the use of vaccines in the last century, we have been able to completely eliminate diseases such as small pox and rinderpest.[1-3] Likewise polio is on the brink of extinction with the advent of the polio vaccine.[4] Diseases that have claimed millions of lives such as measles, mumps, rubella and pneumonia among several others have also been rendered harmless due to the development of vaccines. Table 1 lists a few diseases along with the effect that vaccines have had on the mortality caused by these diseases. Most of these vaccines have been developed by traditional methods, and are based on the use of attenuated or inactivated forms of the disease causing agent to prime the immune system[5]. The history of vaccines dates back several centuries when people in India and China used dried pus from people infected with small pox to inoculate healthy people.[6] Although not a vaccine as we know it today, this technique, which came to be known as variolation, dropped the mortality rates of small pox from 30% to about 2%.[3] Soon, the rest of the world would learn of this technique and it would even come to be used in the American war for independence.[3] The word "vaccine" comes from the use of vaccinia virus, which Edward Jenner used to protect against small pox. This was the first modern vaccine to be developed and it came at a time when scientists had even no idea of the existence of viruses.[7] But the lessons learned from the distribution mechanisms of the small pox vaccine helped Louis Pasteur unravel the concepts of attenuation or weakening of microorganisms when passaged through other cell cultures. This led to the development of vaccines against rabies and many very successful vaccines in the 20th century such as the ones against measles, mumps and rubella. Over the last century, we have learnt a lot about vaccines and how they work. This introductory chapter provides an overview of some basic immunology in addition to a brief description of the different types of vaccines, and the steps involved in the discovery and development of some of the basic types of vaccines.

Introduction to Immunology

Vaccines work by "teaching" the immune system to recognize harmful pathogens. To develop efficacious vaccines, it is crucial to understand how the immune system does this. The immune system has two branches – the innate immune system and the adaptive immune system, which describe non-specific and specific responses, respectively, towards invading pathogens.[8] The innate immune response provides the first line of defense against invading pathogen. There are four components to the innate immune system.

1. Anatomic barriers
2. Physiological barriers
3. Phagocytic mechanisms
4. Inflammation

Examples of anatomic barriers are the mucosal membranes and the skin that cover the interface between the environment and the body.[9] The skin consists of two distinct layers – the epidermis and the dermis. The epidermis consists of several layers of epithelial cells. The outermost layers are primarily filled with dead cells and keratin which keep the skin waterproof. This layer sloughs off and allows newer cells to take their place. The dermis is composed of connective tissue and contains blood vessels, sebaceous glands and sweat glands. The sebaceous glands secrete sebum maintaining the pH of the skin at about 3 to 5, which inhibits the growth of many microorganisms. Importantly, the dermis also contains antigen presenting cells as described later. The mucous membranes act as protective shields by entrapping pathogens in the mucus fibers from entering the body.

In addition to these anatomic barriers, an additional layer of protection is imparted by biological conditions such as temperature and pH.[10] Some organisms cannot grow well at physiological temperature (37^{o}C). The pH of the stomach is also instrumental in eliminating many of the microorganisms that we

ingest. Lysozyme, which is found in tears and saliva, is also useful in clearing harmful bacteria by causing damage to bacterial cell walls.

Apart from these physical barriers, the innate immune system also protects against infections at the cellular levels by recruiting cells such as macrophages, dendritic cells, and neutrophils.[10] Macrophages are among the most common cells of the innate system. These cells are known as monocytes, when in an inactivated state. They travel around the body sampling their immediate vicinity, waiting to become activated. There are a number of ways a monocyte can get activated to become a macrophage. Phagocytosis of bacteria or the use of pattern recognition receptors are among the most common ways that a macrophage may become activated.

Pattern recognition receptors (PRR's) are among the most interesting molecules in the innate immune system. These serve as one of the connections between innate and acquired immunity.[11,12] Our immune system has selected these molecules over millions of years of evolution to recognize molecules from potential pathogens. There are two types of PRR's – soluble and cell associated receptors. An example of soluble PRR's is C - reactive protein (CRP), which binds to several proteins on microbial membranes. These bound proteins then assist in activating complement and in recruiting macrophages to assist in phagocytosis of the microbe. Another example of soluble PRR's is the MBL or mannose binding lectin, which binds to mannose containing carbohydrates on cell walls of bacteria. These proteins help in opsinization of the bacteria and in activation of complement. The other type of PRR is the cell associated receptors. The most famous example of this class of PRR's are the toll-like receptors or TLRs. These represent a specific class of receptors that are associated with host immune cells, and may be present in either the interior or exterior of cells. There are 13 types of mammalian TLRs discovered so far.[13] To name and describe a few, TLR-4 binds to LPS on bacterial cell walls, TLR-3 binds to double stranded RNA typically found in viruses and TLR-9 binds to CPG sequences on bacterial DNA. When the TLR binds its target, it activates the cell on which it is expressed. Many recently identified adjuvants work by binding to TLRs and activating the innate immune system.[14]

The complement system is also a part of the innate immune system, which is often recruited by the adaptive system to clear pathogens from the body.[15,16] The complement system is made up of over 25 different proteins. When activated, a cascade of a reactions take place involving these small proteins and ultimately ends with the formation of a "membrane attack complex" or MAC.[17,18] This MAC forms a transmembrane channel in the pathogen, which leads to lysis of the target cell. Several different pathways have been identified leading to the activation of the complement system including the classical[19], lectin [20] and alternate pathway[21]. Additional information regarding the complement system may be obtained elsewhere. [11,16-19,21]

Inflammatory response can be considered as another branch of the innate immune system.[10] Inflammation is characterized by redness, swelling and pain. Activated macrophages secrete several important chemical factors into the extracellular space that promotes inflammation. For instance, macrophages secrete interleukin-1 which activates T-helper cells and also travels to the brain and induces a fever. The increased body temperature decreases pathogenic activity. C-reactive protein discussed on the previous page is a key biomarker for inflammation.

The cells of the innate immune system such as macrophages and neutrophils are largely non-specific and have no ability to perform self/non-self discrimination. They are, however, instrumental in activating the adaptive immune system. Macrophages and dendritic cells are largely responsible for processing and presenting antigen to cells of the adaptive immune system. Hence, these cells are also called antigen presenting cells (APCs). They present fragments of antigens on their major histocompatibility complex protein (MHC), for T-cells to recognize. MHCs are protein complexes that are expressed on almost all cells in the body and help the immune system differentiate between self and non-self entities.[22] There are two types of MHC designated MHC-I and MHC-II. Almost all nucleated cells in the body express MHC-1 while only professional antigen presenting cells express MHC-II. When a cell is infected by a pathogen, it tries to digest the pathogen in the lysosomal compartment. Here, the proteins from the pathogen are digested by proteases and the resulting peptides are complexed with the

MHC receptor and trafficked to the surface of the cell for recognition by T cells. MHC-I can bind most effectively to peptides that are about 9 amino acids long while MHC-II can bind peptides 13-18 amino acids in length. Generally, MHC-1 displays peptides that are derived from endogenous pathogens while MHC-II displays proteins derived from exogenous microorganisms. A more detailed description of MHC's, and their structure and function are described in depth elsewhere. [23-25]

The adaptive immune system contains a different set of cells that learn to recognize specific pathogens and effectively neutralize them.[26] The best characterized cells of the adaptive immune system are the B and T-cells. B-cells are largely responsible for the humoral, antibody response, while the T-cells primarily constitute the cellular response. These two classes of cells, however, assist in activating each other in the various stages on the adaptive immune response. For instance, T-Helper cells are essential in activating the B-Cells which eventually produce specific antibodies against the pathogen.

The antibody response is primarily the defense most vaccines today elicit. Table 2 lists some selected currently licensed vaccines along with the type of immune response they elicit.[27] Most subunit and inactivated viral vaccines primarily elicit an antibody response. Some of the live attenuated viral vaccines, however, produce both $CD8^+$ and $CD4^+$ activity in addition to the antibody response. B-cells mature in the bone marrow and express a unique antigen binding receptor on its surface.[26] This membrane bound highly selective antigen binding receptor is called a membrane antibody. Each B-cell expresses about 10,000 antibody molecules on its surface and each of these antibodies has the same specificity towards a specific antigen and is identical to the other antibodies on the same cell. The entire population of B cells in the human body can make up to 10^8 different antibodies. A naïve B-cell expresses a receptor that has affinity towards one specific antigen. Upon binding to the antigen, the B-cell is activated and differentiates into B-memory and plasma cells. Plasma cells are able to secrete large quantities of antibody in to the extracellular space. Antibodies have two biological functions. One is to bind to the pathogen and the second is to facilitate effector functions. An antibody molecule is composed of 2 heavy and 2 light chains. There are 5 types of antibodies in the body and they differ based on the 5 different

heavy chains used to make up the antibody. These are IgA, IgD, IgM, IgG and IgE classes. More detailed descriptions of the structure of these antibodies may be found elsewhere.[28] Once the antibodies bind to the pathogen, they signal macrophages and other immune cells for destruction of the pathogen by phagocytosis. Antibodies can also activate the complement system by the classical pathway, which then assists in the destruction of the pathogen or tumor. Additionally, antibodies can initiate a cellular response via antibody dependent cell-mediated cytotoxicity.

T-cells mature in the thymus and exist in a number of different types. The most common types are the T-helper cells and the cytotoxic T cells.[29,30] The T-helper (Th) cells have a CD4 receptor on their surface, which recognize peptides presented on MHC-II by APCs. This activates the Th cell, which then begins to proliferate and later develop into Th1 and Th2 cells. Th1 cells secrete cytokines to maximize the efficiency of macrophages and also activate other cytotoxic T cells, thereby assisting the cellular immune response.[31] Th2 cells go on to play an active role in the activation of B-cells, thereby initiating the humoral response.

The T cytotoxic cells (Tc) have a CD8 receptor on their surface, which recognizes peptides presented on MHC-I by all host cells.[32] This activates the Tc cells to become cytotoxic T cells (CTLs), which can then kill infected or modified cells directly by the use of various agents such as perforin and granzymes. Alternatively, CTLs can also induce apoptosis in target cell by interaction with FAS receptors. T-regulatory or Treg cells play a key role in regulating the immune response. They help by lowering the immune response when not needed, as in the case of self-antigens.

The hallmark of the adaptive immune system is the induction of memory.[33] Memory is brought about by the differentiation of B-cells and T-cells during their activation into B and T memory cells. These cells can live and circulate in the body for decades after the primary infection. In case of a second infection, these memory cells become activated and quickly proliferate and raise the appropriate immune response to neutralize the invading pathogen. Vaccines work by inducing memory. For instance,

immunization with a live attenuated strain of a virus causes a minor form of infection. Some infected host cells release several cytokines to attract macrophages and other immune cells to the site of infection. These macrophages then begin to digest the cells and viruses, and degrade them. Within the next couple of hours, the viral proteins are degraded into peptides and presented to T-helper cells in their MHC-II compartment. The Th cells are then activated and assist in the activation of B cells which secrete antibodies that help to neutralize the virus. In parallel, the infected cells present viral peptides to Tc cells in their MHC-I compartment. This activates the Tc cells to become cytotoxic T cells which then help eliminate viral infected cells. During the activation of the B and T cells, the progenitor cells also differentiate into B and T memory cells. These cells tend to circulate in regions where the virus was first encountered and the lymph codes. Should they encounter the same antigen again, they proliferate rapidly and work to rapidly eliminate the pathogen for the body.

Types of Vaccines

Modern vaccines come in several different types. Advances in technology and science have in a few cases enabled us to develop vaccines based on individual proteins from the pathogen. Many vaccines available today are those that were developed using traditional methods. These vaccines can be broadly divided into two categories – Whole organism based vaccines and subunit vaccines.[34-36] Whole organism vaccines employ attenuated or inactivated forms of a virus or bacteria that cause disease. Different strategies may be employed to achieve an attenuated strain of the disease causing agent. One approach is to use a similar viral strain that may be pathogenic in other animals but does not cause disease in humans. A classic example employs vaccinia which causes cowpox in humans, but protects humans from the more deadly smallpox without causing significant disease. Another example is the use of herpes virus from turkeys to control Marek disease in chickens. A second strategy attenuates a viral strain by mutating it by passaging the virus through cells obtained from another host. Examples of vaccines developed using this technique are the original rabies vaccine by Pasteur and the MMR vaccine against measles, mumps and

rubella. A third strategy is the use of a naturally occurring attenuated strain to protect against disease from the harmful strains. A good example of this is the use of weaker strains in the polio vaccine.

Traditional sub-unit vaccines are comprised of an inactivated form of a component of the pathogen as opposed to using the whole organism. In general, these are safer and have fewer side effects because they do not cause even mild disease. Examples of traditional sub-unit vaccines are the vaccines for tetanus and diphtheria. These bacteria are non-invasive, but the toxins they secrete can be deadly. These toxins can be "inactivated" by treatment with formalin or some other agent. These inactivated forms of the toxin, known as toxoids, can generate a neutralizing immune response against the toxin when injected into humans. Another example of a sub-unit vaccine is the split influenza vaccine. This vaccine is made by disrupting the virus by the use of various detergents and separating the two major surface antigens – haemagglutinin (HA) and neuraminidase (NA). The mixture of these two proteins is used in the seasonal flu vaccine. In some countries, an "adjuvant" is added to such vaccines to boost the immune response. [37,38]

Recombinant DNA technology has opened a number of possibilities in the area of vaccines.[31,33] Isolating and purifying a specific antigen from an infectious agent in large quantities has been a major challenge. This particular roadblock has now been overcome. It is now much easier to produce large quantities of pure antigen to enable their characterization and evaluation of their efficacy. With recombinant DNA technology, it has also become possible to insert a particular antigen in a suitable vector to increase the efficacy of the vaccine. A recombinant rabies vaccine (V-RG) for veterinary was developed by inserting a glycoprotein gene into the vaccinia virus.[39] Similar techniques are being tried with various other antigens. Currently, significant efforts involve the development of individual protein antigens as vaccines. These recombinant sub-unit vaccines have a well-defined structure and are often more stable than their live attenuated counter parts. These sub-unit vaccines can also be manufactured in bulk more easily. They do, however, have some disadvantages. Most isolated proteins have low intrinsic immunogenicity and cannot be used as vaccines by themselves. They require additives that boost their

immunogenicity. These additives are called “adjuvants” and will be discussed in detail later in this chapter. The human papilloma vaccine employs “virus-like particles” assembled from the recombinantly produced coat proteins of the human papilloma virus. The human papilloma vaccine also contains aluminum oxyhydroxide or Alhydrogel as an adjuvant to boost its immune response. A similar approach is used in the recombinant hepatitis B vaccines. DNA vaccines are relatively a new concept. This involves the use of a plasmid encoding a particular antigen as the vaccine. When cells start to take up such DNA, they can express the antigens with a resultant immune response. Significant interest has been spurred in this area because nucleic acid-based vaccines are able to elicit both a cellular response and humoral immune response. Most vaccines today, with the exception of live viruses elicit primarily a humoral response. Problematically, however, the cellular response is thought to be key in the development of vaccines towards TB, HIV and malaria among other diseases.

Discovery and Development of Vaccines

To develop more effective vaccines in the future, improvements can be made in at least two areas of vaccines development. One area deals with the identification of novel targets as vaccines candidates. The other concerns formulation and delivery aspects of vaccine development. Both of these areas have witnessed several breakthroughs in the past few decades. A brief introduction to some of the new methods used to identify vaccine targets is discussed below. The remainder of this chapter will be dedicated to the use of formulation to increase vaccine stability and efficacy.

Traditionally, vaccines candidates were discovered on a trial and error basis. Some were discovered before science even knew of the existence of viruses. For instance, the small pox and rabies vaccines created by Pasteur were developed before the microbial basis of disease was widely accepted.[7] Most of the vaccines used today were developed using traditional vaccinology technologies. Several of these were developed by inactivating or attenuating the pathogens, or in some cases, isolating the antigenic subunits. These approaches have been very successful in the past and have helped save tons of

millions of lives. There are, however, several examples where such techniques have failed due to safety concerns and low efficacy. Attenuated vaccines may revert back to virulent states and cause full blown disease in those vaccinated. Killed and attenuated whole organism vaccines may share protein sequence homology with human proteins, which may cause autoimmune disease. Identifying immunogenic subunits by classical methods is time consuming and often difficult. Today, antigen discovery is broadly based around two predictive methods. One is called Reverse Vaccinology and the other Antigenome technology. [40,41]

Reverse vaccinology uses bioinformatic analysis of the infectious agent's genome to select possible antigens. As multiple genomes of most human pathogens are now available in databases online, the initial information required to predict the first batch of vaccine candidates is freely available. This data is subjected to various predictive methods (bioinformatics, comparative genomics, proteomics, and DNA microarray analysis) to obtain a number of antigens that can be used in animal models to determine which are the most immunogenic. These initial predictive methods are primarily based on in silico analysis of the host genome. Additional methods are, however, constantly being implemented. The two most commonly used predictive methods are DNA sequence similarity searches such as FASTA or Psi-BLAST and protein location predictive algorithms such as PSort, SignalP or TMPRED. These algorithms provide us with similar, previously studied surface proteins that may be tested as antigens against the specific pathogen. Any "hits" obtained here are further refined with additional algorithm. The results from this part of the study are then studied in animal models to determine which antigens are the most immunogenic. One example of a potential vaccine created by this method is the multivalent recombinant MenB vaccine that is in phase III clinical trials. The Antigenome technology is a relatively newer. This technology combines the advantages of full pathogen genome coverage with serological antigen identification. The antigens characterized and formulated in Chapter 3 were discovered using Antigenome technology.

Adjuvants

The discovery of vaccine candidates is only the start of any vaccine development program. A whole new set of problems are usually encountered when one tries to make an actual vaccine from a specific antigen. These problems can broadly be classified into efficacy and stability problems. Most subunit vaccines are not highly immunogenic by themselves compared to their whole cell counterparts. To induce a robust immune response, multiple injections of the vaccine are often required and in many cases, the addition of an adjuvant is needed to increase the immunogenicity of the vaccine.[37,38] An adjuvant is a substance that can increase the immunogenicity of the antigen, but they do not confer immunity by themselves. The most commonly currently used adjuvants are the aluminum salts – aluminum oxyhydroxide (aluminum hydroxide) and aluminum hydroxyphosphate (aluminum phosphate). These were the first and only adjuvant to be approved for use in the United States until very recently. These adjuvants are known for their ability to induce a robust antibody response. Over the last half a century, hundreds of millions of doses of vaccines containing aluminum salt adjuvants have been administered. These adjuvants thus have an established safety and efficacy profile. These adjuvants are typically made by the precipitation of aluminum when a solution of alum (aluminum potassium sulfate) is titrated with a base such as ammonium hydroxide or sodium hydroxide.[42] The distinction between Alhydrogel and Adjuphos is in the degree of phosphate substitution for hydroxyl groups on the surface of the adjuvant.[38,43] This substitution imparts differences in surface charge leading to differential adsorption of antigens to the surface. This adsorption of the antigen to the surface of the adjuvant is thought to be required for the increase in immunogenicity imparted by the adjuvant, although this view has recently been challenged.[44] The major forces responsible for the adsorption of the antigen to the adjuvant are electrostatic interactions, hydrophobic forces and ligand exchange. Generally, since proteins and aluminum salt adjuvants are charged, electrostatic interactions often seem to be the major mechanism for adsorption of proteins to the adjuvant surface. At neutral pH, Alhydrogel (pI=11.4) is usually positively charged and Adjuphos (pI=4.5 to 5.5) is negatively charged. It is possible to optimize these interactions

by modifying formulation parameters such as pH, ionic strength and the addition of ions such as phosphate, and sulfate.

The adjuvanticity of the aluminum salts is characterized by an antibody response by the T helper type 2 cells as stated earlier. There are several proposed mechanisms of immunopotentiation by aluminum salt adjuvants.[45] The depot theory postulates that the aluminum adjuvant and the adsorbed antigen remain at the site of injection.[42] The slow release of antigen from the adjuvant stimulates antibody production. [38]Another theory predicts that the adjuvants cause inflammation at the site of injection, attracting antigen presenting cells (APC's) in large numbers. The APCs encounter the antigen at high concentration, thereby facilitating an immune response against it. Yet another theory postulates that there may be particulation of antigen on the surface of the adjuvant, which end up being internalized by macrophages via phagocytosis leading to an immune response. Recently it was proposed that the immune response may be raised by dendritic cells (DCs) and re-assortment of the DCs' lipid membrane upon interaction with the adjuvant.[46] This interactions leads to antigen being delivered in its soluble form to the dendritic cell, which is then processed in its MHC class II compartment which results in the activation of B-cells to raise an antibody response. It is possible that all of these mechanisms contribute to immunopotentiation by these adjuvants.

Adsorption of the antigen to the surface of the adjuvant has been shown to sometimes induce changes in the secondary and tertiary structure of the antigen and frequently to reduce their thermal stability.[47-49] This destabilization of the antigen has also been suggested as one of the causes for the adjuvanticity of aluminum salts since APCs are able to better degrade destabilized proteins.[47] The depot theory had originally led to the belief that adsorption of the antigen to the adjuvant was necessary for a robust immune response. This view has, however, been challenged in the recent years and there are a number of examples where the contrary appears to be true.[44] The importance of adsorption may be antigen specific and additional studies will need to be done in the future to clarify this. Current regulatory guidelines do, however, define a need for adsorption of the antigen as a general rule of thumb. The dose of adjuvant can also play an important role in the immunogenicity of the vaccine. Limits for the amount

of aluminum adjuvants in vaccines in injectibles are 1.25mg of aluminum per dose if the manufacturer can justify the need for the high concentration with safety and efficacy data (Code of Federal Regulations, 2003). Typically, most vaccines tend to contain less than 0.85mg of aluminum per dose. Table 3 lists select currently marketed vaccines that contain aluminum salt adjuvants along with their doses.[38]

Recently, with the release of Cervarix ®, AS04 was the second adjuvant to be licensed in the United States.[50] AS04 consists of monophosphoryl lipid A (MPL) adsorbed to aluminum hydroxide. MPL is a TLR4 agonist and is derived from the cell wall of gram-negative salmonella. This is detoxified by hydrolytic treatment and purified. AS04 is used as an adjuvant in the human pappilomavirus vaccine developed by GSK. In Europe, MF59 is the only other adjuvant that is approved for human use.[51] MF59 is an oil-in-water emulsion containing squalene. The squalene droplets are stabilized in water by the used of two surfactacts – tween-80 and sorbitan trioleate. MF-59 is used in the influenza vaccine, Fluad™. Some studies have indicated that the addition of MF59 as an adjuvant may provide a broader serological response than aluminum salt adjuvants. There are several other adjuvants used for veterinary purposes such as Freunds complete and incomplete adjuvants. The use of these adjuvants in humans, however, is unacceptable due to their toxicity.[38] Today, greater emphasis is being placed on the discovery and development of novel adjuvants to elicit robust cellular and antibody responses in both new and older vaccines.

Aluminum salt adjuvants will probably remain one of the most commonly used adjuvants in vaccines worldwide.[38,43,52] These adjuvants have a safety profile established over half a century and millions of doses. The transitions to newer adjuvants in vaccines require changes in regulatory policies and this has met with limited success.

Vaccine Stability

An antigen that can elicit an immune response towards its actual pathogen is the most common component of any vaccine. For instance, a live attenuated viral vaccine contains attenuated viral strains

while a sub-unit vaccine typically contains individual proteins or carbohydrates. In some cases, an adjuvant is added to boost the immune response as discussed earlier. The vaccines are, however, exposed to several environmental factors before being administered to patients. These include changes in temperature, exposure to light and physical stresses like shaking or stirring while being shipped. These factors may affect the stability of the antigen or the adjuvant and render them ineffective.[53] For instance, freezing of aluminum adjuvants causes coagulation of the salt. The resulting mixture cannot be readily re-dispersed upon thawing.[54] Changes in temperature can also inactivate viruses and causes changes in the secondary, tertiary and quaternary levels of constituent proteins. Apart from conformational changes, aggregation of viruses and purified protein are also a common concern. By studying the physical and chemical stability of the antigen, we can characterize the origin of instability in these antigens and take necessary measures to minimize degradation. The most common way this is done is by the addition of stabilizers.[55]

Proteins have several levels of structure. The primary structure is defined as the amino acid sequence. This linear chain of amino acids can then interact with itself causing the protein to fold in various shapes and sizes to give rise to the secondary and tertiary levels of structure in a protein. Local interactions give rise to the secondary structure in terms of helices and sheets while the details of the 3D structure constitute its tertiary structure. These individual protein units or monomers can interact with other individual protein units to form dimers and higher oligomers to give rise to quaternary structure. For instance, an antibody is made up of 4 sub-units. Two heavy chain molecules and two light chain molecules come together to form an antibody.[56] In this case, the monomers are held together by covalent (disulfide) bonds but it is often the case that the interactions between subunits are non-covalent in nature. All these levels of structure can be affected by environmental factors such as pH, temperature and ionic strength.[53,57-59] For example, the charge state of individual amino acids is dictated by the pH of its environment, which in turn effects their contributions to the various levels of structure in a protein. Ionic strength can weaken the electrostatic interactions while high salt concentrations can increase the strength

of apolar interactions. In vaccine development, ionic strength can also weaken interactions between the antigen and the adjuvant, which may be crucial for immunogenicity. Increases in temperature can weaken bonds stabilizing the protein which may cause irreversible unfolding of the protein. This unfolding may expose hydrophobic regions which can then interact with one another causing protein aggregation. These factors may also be involved in chemical degradation of the protein. For instance, deamidation of the asparagine residues in the protein can be stimulated at both high and low pH resulting in the formation of aspartic or iso-aspartic acid. Any of these factors may contribute to protein instability and loss in immunogenicity.[53,60] It is, therefore, very important to characterize a protein antigen to the fullest possible extent to enable selection of suitable formulation criteria to maintain the immunogenicity of the vaccine from manufacturing to administration. It is important to note that vaccines are shipped all over the world. They are desperately needed in the remote sites of the developing world where access to refrigerators may be limited. Effective formulations should ideally be able to keep the vaccines stable even at room temperatures in these cases. Unfortunately, this is currently not often the case.

The structural aspects of proteins are best defined by high resolution methods such as X-ray crystallography and NMR. These methods are, however, time consuming, and utilize large amounts of protein (which may not be available in the early stages of vaccine development). Therefore, low resolution methods such as circular dichroism (CD), fourier transform infrared (FTIR), ultraviolet (UV) absorbance and fluorescence spectroscopy and light scattering, and differential scanning calorimetry (DSC) are usually employed. Changes in data from such methods as a function of environmental stresses such as pH and temperature are useful in producing an information-rich stability profile for a biological entity as a function of the stresses applied. CD and FTIR spectroscopy can be used to study changes in the secondary structure of the protein, and intrinsic and extrinsic fluorescence spectroscopy as well as near UV CD and near UV absorption spectroscopy can be used to study the changes associated with tertiary structure. Aggregation events can be monitored using static and dynamic light scattering, size exclusion chromatography and a wide variety of other methods.

The use of these structural assays in combination can provide an overall picture of a protein's stability as a function of environmental stress. This can provide an idea of the most favorable and optimal conditions for a target protein. It also enables one to screen for suitable stabilizers that may enhance the stability of the protein. The most commonly used stabilizers are sugars, sugar alcohols, amino acids and surfactants.[61-63] Sugars and sugar alcohols such as sucrose and sorbitol stabilize proteins by preferential hydration.[63] Surfactants such a polysorbate-20 stabilize proteins by various non-specific interactions. For example, they coat hydrophobic surfaces such as the walls of a container and the air-water interface preventing protein adsorption and ultimately, aggregation of the protein.

Apart from the addition of stabilizers, other techniques may be used to slow or prevent protein degradation. The most common method is lyophilization (freeze drying) of the protein.[64-66] This technique involves removing most of the water in the formulation. Biological entities such as proteins and viruses usually exhibit enhanced stability in the dried state due to the reduction in reactive water as well as their internal motions. Though not common, protein sub-unit vaccines may sometimes be stabilized upon adsorption to adjuvants. In a molecular design approach, unstable regions of the proteins may be removed or certain amino acids replaced to further stabilize the antigen.

In addition, preservatives may be added to vaccine formulations to prevent the growth of other microorganisms.[67] Improvements in sterile manufacturing technologies over the last few decades have greatly reduced the need for preservatives in vaccines. Regulatory policies require manufacturers to include preservatives in multi-dose vials. Care should be taken to determine that these preservatives do not destabilize or degrade the antigen. There are four commonly used preservatives in vaccines. They are phenol, thimerosal, benzethonium chloride and 2-phenoxy-ethanol. The addition of thimerosal produced considerable controversy. Thimerosal was casually linked to the development of autism in children, despite the lack of any supportive scientific data. An in-depth and thorough study of the link between autism and thimerosal found no relationship between the two and the hypothesis has been definitely refuted.

Apart from the addition of adjuvants, stabilizers and preservatives, viral or subunit vaccines may also contain trace amounts of chemicals used to inactivate the viral or the toxin components.[67] The most commonly used chemicals used for this purpose are formaldehyde, formalin and β–propiolactone. In addition, some manufacturing and cell culture residuals may also be present in a final vaccine formulation in trace quantities.

In the course of this dissertation, I dedicate each chapter to the formulation development of three unique vaccines. Central to the formulation development of each of the vaccines are biophysical characterization of the different biological entities. The data obtained from the various techniques discussed above were incorporated into an empirical phase diagram (EPD), a form of stress-response diagram that will be described later. This was done to visualize pH and temperature ranges over which the antigens were most stable. This empirical phase diagram approach has been used before to successfully characterize several proteins.[68-77] After constructing an EPD for each of the antigens, an assay was developed to screen for potential stabilizers. Finally, the antigens were formulated with an adjuvant when required. The interactions between the antigen and the adjuvant were fully characterized and the stability of the antigen on the adjuvant surface was assessed by various spectroscopic methods. Chapter 2 deals with developing a stable formulation for a recombinantly produced hemagglutinin protein (HAC1) in the presence of Alhydrogel. This is intended for use a vaccine towards seasonal flu. The immunogenicity of HAC1 was tested in mice in the presence and absence of Alhydrogel. Phase I clinical trials for this vaccine was recently successfully completed and Phase II is currently underway. Chapter 3 outlines the formulation development of a recombinantly produced trivalent subunit protein vaccine against *S. Pneumonia*. The antigens used in this study were discovered using the Antigenome technology discussed earlier. Chapter 4 describes the development of a formulation for a trivalent live attenuated viral vaccine for dogs. The last chapter provides some conclusions and a summary of the work described in this dissertation.

References:

1. Roeder P 2011. Making a global impact: the eradication of rinderpest. The Veterinary record 169(25):650-652.
2. Zhang Y, Zhao K 1999. [Global eradication of small-pox: historical fact, experiences and enlightenment]. Zhonghua liu xing bing xue za zhi = Zhonghua liuxingbingxue zazhi 20(2):67-70.
3. F. Fenner DAH, I. Arita, Z. Jezek, I.D. Ladnyi. 1988. Smallpox and its eradication., ed.
4. Arita I, Francis DP 2011. Safe landing for global polio eradication: a perspective. Vaccine 29(48):8827-8834.
5. Josefsberg JO, Buckland B 2012. Vaccine process technology. Biotechnology and bioengineering 109(6):1443-1460.
6. Parrino J, Graham BS 2006. Smallpox vaccines: Past, present, and future. The Journal of allergy and clinical immunology 118(6):1320-1326.
7. Bordenave G 2003. Louis Pasteur (1822-1895). Microbes and infection / Institut Pasteur 5(6):553-560.
8. Moser M, Leo O 2010. Key concepts in immunology. Vaccine 28 Suppl 3:C2-13.
9. Madison KC 2003. Barrier function of the skin: "la raison d'etre" of the epidermis. The Journal of investigative dermatology 121(2):231-241.
10. Thomas J. Kindt RAG, Barbara A. Osborne 2004. Innate Immunity. Immunology, ed.
11. Hawlisch H, Kohl J 2006. Complement and Toll-like receptors: key regulators of adaptive immune responses. Molecular immunology 43(1-2):13-21.
12. Meylan E, Tschopp J, Karin M 2006. Intracellular pattern recognition receptors in the host response. Nature 442(7098):39-44.
13. Uematsu S, Akira S 2007. Toll-like receptors and Type I interferons. The Journal of biological chemistry 282(21):15319-15323.
14. Kaisho T AS 2002. Toll-like receptors as adjuvant receptors. Biochim Biophys Acta 1589(1):1-13.
15. Trouw LA, Daha MR 2011. Role of complement in innate immunity and host defense. Immunology letters 138(1):35-37.
16. Thomas J. Kindt RAG, Barbara A. Osborne 2004. The Complement System. Immunology, ed.
17. Muller-Eberhard HJ 1985. The killer molecule of complement. The Journal of investigative dermatology 85(1 Suppl):47s-52s.
18. Podack ER, Tschopp J 1984. Membrane attack by complement. Molecular immunology 21(7):589-603.
19. Daha NA, Banda NK, Roos A, Beurskens FJ, Bakker JM, Daha MR, Trouw LA 2011. Complement activation by (auto-) antibodies. Molecular immunology 48(14):1656-1665.
20. Turner MW 1996. The lectin pathway of complement activation. Research in immunology 147(2):110-115.
21. Gotze O, Muller-Eberhard HJ 1971. The C3-activator system: an alternate pathway of complement activation. The Journal of experimental medicine 134(3 Pt 2):90s-108s.
22. Martinez-Borra J, Lopez-Larrea C 2012. The emergence of the major histocompatilibility complex. Advances in experimental medicine and biology 738:277-289.
23. Natarajan K, Li H, Mariuzza RA, Margulies DH 1999. MHC class I molecules, structure and function. Reviews in immunogenetics 1(1):32-46.
24. Lechler RI 1988. Structure-function relationships of MHC class II molecules. Immunology Supplement 1:25-26.
25. Clark SS, Forman J 1983. Structure function relationship of class I MHC molecules. Survey of immunologic research 2(3):203-206.

26. Thomas J. Kindt RAG, Barbara A. Osborne 2004. Antigens and Antibodies. Immunology, ed.
27. Stanley Plotkin WO, Paul Offlt. 2008. Vaccine Immunology. Vaccines, ed.: Saunders Elsevier.
28. Thomas J. Kindt RAG, Barbara A. Osborne 2004. Organization and Expression of Immunoglobulin Genes. Immunology, ed.
29. Thomas J. Kindt RAG, Barbara A. Osborne 2004. T-Cell Receptor. Immunology, ed.
30. Thomas J. Kindt RAG, Barbara A. Osborne 2004. T-Cell Maturation, Activation and Differentiation. Immunology, ed.
31. Thomas J. Kindt RAG, Barbara A. Osborne 2004. Cytokines. Immunology, ed.
32. Thomas J. Kindt RAG, Barbara A. Osborne 2004. Cell-Mediated Cytotoxic Responses. Immunology, ed.
33. 2011. Remembering things past. Nature immunology 12(6):461.
34. Bagnoli RRaF. 2012. Overview of Vaccine Stratergies. Vaccine Design, ed.
35. Stanley Plotkin WO, Paul Offlt. 2008. A short history of vaccination. Vaccines, ed.: Saunders Elsevier.
36. Thomas J. Kindt RAG, Barbara A. Osborne 2004. Vaccines. Immunology, ed.
37. Leroux-Roels G 2010. Unmet needs in modern vaccinology: adjuvants to improve the immune response. Vaccine 28 Suppl 3:C25-36.
38. Stanley Plotkin WO, Paul Offlt. 2008. Adjuvants. Vaccines, ed.: Saunders Elsevier.
39. Cliquet F, Barrat J, Guiot AL, Cael N, Boutrand S, Maki J, Schumacher CL 2008. Efficacy and bait acceptance of vaccinia vectored rabies glycoprotein vaccine in captive foxes (Vulpes vulpes), raccoon dogs (Nyctereutes procyonoides) and dogs (Canis familiaris). Vaccine 26(36):4627-4638.
40. Sette A, Rappuoli R 2010. Reverse vaccinology: developing vaccines in the era of genomics. Immunity 33(4):530-541.
41. Meinke A, Henics T, Hanner M, Minh DB, Nagy E 2005. Antigenome technology: a novel approach for the selection of bacterial vaccine candidate antigens. Vaccine 23(17-18):2035-2041.
42. Glenny AT, Buttle GAH, Stevens MF 1931. Rate of disappearance of diphtheria toxoid injected into rabbits and guinea - pigs: Toxoid precipitated with alum. The Journal of Pathology and Bacteriology 34(2):267-275.
43. Singh M. 2007. Aluminum-Containing Vaccines. Vaccine Adjuvants and Delivery Systems, ed.: John Wiley & Sons.
44. Noe SM, Green MA, HogenEsch H, Hem SL Mechanism of immunopotentiation by aluminum-containing adjuvants elucidated by the relationship between antigen retention at the inoculation site and the immune response. Vaccine 28(20):3588-3594.
45. HogenEsch H 2002. Mechanisms of stimulation of the immune response by aluminum adjuvants. Vaccine 20 Suppl 3:S34-39.
46. Flach TL, Ng G, Hari A, Desrosiers MD, Zhang P, Ward SM, Seamone ME, Vilaysane A, Mucsi AD, Fong Y, Prenner E, Ling CC, Tschopp J, Muruve DA, Amrein MW, Shi Y Alum interaction with dendritic cell membrane lipids is essential for its adjuvanticity. Nature medicine 17(4):479-487.
47. Jones LS, Peek LJ, Power J, Markham A, Yazzie B, Middaugh CR 2005. Effects of adsorption to aluminum salt adjuvants on the structure and stability of model protein antigens. The Journal of biological chemistry 280(14):13406-13414.
48. Peek LJ, Martin TT, Elk Nation C, Pegram SA, Middaugh CR 2007. Effects of stabilizers on the destabilization of proteins upon adsorption to aluminum salt adjuvants. Journal of pharmaceutical sciences 96(3):547-557.
49. Wittayanukulluk A, Jiang D, Regnier FE, Hem SL 2004. Effect of microenvironment pH of aluminum hydroxide adjuvant on the chemical stability of adsorbed antigen. Vaccine 22(9-10):1172-1176.

50. Schwarz TF 2008. AS04-adjuvanted human papillomavirus-16/18 vaccination: recent advances in cervical cancer prevention. Expert review of vaccines 7(10):1465-1473.
51. O'Hagan DT, Rappuoli R, De Gregorio E, Tsai T, Del Giudice G 2011. MF59 adjuvant: the best insurance against influenza strain diversity. Expert review of vaccines 10(4):447-462.
52. Bagnoli RRaF. 2012. Adjuvants. Vaccine Design, ed.
53. Brandau DT, Jones LS, Wiethoff CM, Rexroad J, Middaugh CR 2003. Thermal stability of vaccines. Journal of pharmaceutical sciences 92(2):218-231.
54. Clapp T, Siebert P, Chen D, Jones Braun L 2011. Vaccines with aluminum-containing adjuvants: optimizing vaccine efficacy and thermal stability. Journal of pharmaceutical sciences 100(2):388-401.
55. Kamerzell TJ, Esfandiary R, Joshi SB, Middaugh CR, Volkin DB 2011. Protein-excipient interactions: mechanisms and biophysical characterization applied to protein formulation development. Advanced drug delivery reviews 63(13):1118-1159.
56. Wang W, Singh S, Zeng DL, King K, Nema S 2007. Antibody structure, instability, and formulation. Journal of pharmaceutical sciences 96(1):1-26.
57. Ausar SF, Foubert TR, Hudson MH, Vedvick TS, Middaugh CR 2006. Conformational stability and disassembly of Norwalk virus-like particles. Effect of pH and temperature. The Journal of biological chemistry 281(28):19478-19488.
58. Chi EY, Krishnan S, Randolph TW, Carpenter JF 2003. Physical stability of proteins in aqueous solution: mechanism and driving forces in nonnative protein aggregation. Pharmaceutical research 20(9):1325-1336.
59. Ausar SF, Rexroad J, Frolov VG, Look JL, Konar N, Middaugh CR 2005. Analysis of the thermal and pH stability of human respiratory syncytial virus. Molecular pharmaceutics 2(6):491-499.
60. Patro SY, Freund E, Chang BS 2002. Protein formulation and fill-finish operations. Biotechnology annual review 8:55-84.
61. Lee JC, Timasheff SN 1981. The stabilization of proteins by sucrose. The Journal of biological chemistry 256(14):7193-7201.
62. Uedaira H 2001. Role of hydration of polyhydroxy compounds in biological systems. Cell Mol Biol (Noisy-le-grand) 47(5):823-829.
63. Shimizu S, Smith DJ 2004. Preferential hydration and the exclusion of cosolvents from protein surfaces. J Chem Phys 121(2):1148-1154.
64. Nail SL, Jiang S, Chongprasert S, Knopp SA 2002. Fundamentals of freeze-drying. Pharmaceutical biotechnology 14:281-360.
65. Wang W 2000. Lyophilization and development of solid protein pharmaceuticals. International journal of pharmaceutics 203(1-2):1-60.
66. Chang LL, Pikal MJ 2009. Mechanisms of protein stabilization in the solid state. Journal of pharmaceutical sciences 98(9):2886-2908.
67. Stanley Plotkin WO, Paul Offlt. 2008. Vaccine additives and manufacturing residuals in United States-licensed vaccines. Vaccines, ed.: Saunders Elsevier.
68. Ramsey JD, Gill ML, Kamerzell TJ, Price ES, Joshi SB, Bishop SM, Oliver CN, Middaugh CR 2009. Using empirical phase diagrams to understand the role of intramolecular dynamics in immunoglobulin G stability. Journal of pharmaceutical sciences 98(7):2432-2447.
69. Zeng Y, Fan H, Chiueh G, Pham B, Martin R, Lechuga-Ballesteros D, Truong VL, Joshi SB, Middaugh CR 2009. Towards development of stable formulations of a live attenuated bacterial vaccine: a preformulation study facilitated by a biophysical approach. Hum Vaccin 5(5):322-331.
70. Peek LJ, Brandau DT, Jones LS, Joshi SB, Middaugh CR 2006. A systematic approach to stabilizing EBA-175 RII-NG for use as a malaria vaccine. Vaccine 24(31-32):5839-5851.
71. Kissmann J, Ausar SF, Rudolph A, Braun C, Cape SP, Sievers RE, Federspiel MJ, Joshi SB, Middaugh CR 2008. Stabilization of measles virus for vaccine formulation. Hum Vaccin 4(5):350-359.

72. Kissmann J, Ausar SF, Foubert TR, Brock J, Switzer MH, Detzi EJ, Vedvick TS, Middaugh CR 2008. Physical stabilization of Norwalk virus-like particles. Journal of pharmaceutical sciences 97(10):4208-4218.
73. Kissmann J, Joshi SB, Haynes JR, Dokken L, Richardson C, Middaugh CR H1N1 influenza virus-like particles: physical degradation pathways and identification of stabilizers. Journal of pharmaceutical sciences 100(2):634-645.
74. Rexroad J, Evans RK, Middaugh CR 2006. Effect of pH and ionic strength on the physical stability of adenovirus type 5. Journal of pharmaceutical sciences 95(2):237-247.
75. Kueltzo LA, Ersoy B, Ralston JP, Middaugh CR 2003. Derivative absorbance spectroscopy and protein phase diagrams as tools for comprehensive protein characterization: a bGCSF case study. Journal of pharmaceutical sciences 92(9):1805-1820.
76. Markham AP, Jaafar ZA, Kemege KE, Middaugh CR, Hefty PS 2009. Biophysical characterization of Chlamydia trachomatis CT584 supports its potential role as a type III secretion needle tip protein. Biochemistry 48(43):10353-10361.
77. Maddux NR, Joshi SB, Volkin DB, Ralston JP, Middaugh CR 2011. Multidimensional methods for the formulation of biopharmaceuticals and vaccines. Journal of pharmaceutical sciences.

Chapter 2

Formulation Development of a Plant-Derived H1N1 Influenza Vaccine Containing Purified Recombinant Hemagglutinin Antigen

Introduction

Influenza is one of the leading causes of respiratory infections worldwide and is associated with significant morbidity and mortality each year. There are several subtypes of the influenza virus that are currently circulating among humans.[1,2] An effective way to combat influenza is through vaccination using a trivalent vaccine produced in embryonated chicken eggs. Almost all commercially available vaccines contain two surface glycoproteins of influenza, hemagglutinin (HA) and neuraminidase (NA), as the key antigens, with HA being the dominant one of the two. Although this system has worked well over the past five decades, it has several well-recognized disadvantages.[1] One of the major disadvantages of this costly and time-consuming egg-based technology is that it is difficult to respond to a potential pandemic crisis in a timely manner, since a minimum of 3-6 months is required to generate an influenza vaccine.[2-5] The H1N1/09 virus was responsible for the 2009 swine flu epidemic. Significant morbidity and mortality associated with this disease were due to the lack of an effective vaccine.[6] More than 506,060 cases of the H1N1/09 infections have been reported worldwide, with over 6770 deaths.[7] These numbers may have been significantly underestimated, since it is no longer required to report all clinically diagnosed cases.

To prevent or effectively diminish the impact of influenza, it is imperative to have a system that can rapidly produce the vaccine when needed. Two relatively new technologies which are being tested to replace the egg-based production system are cell culture-based and recombinant protein (antigen)-based approaches.[5,8-11] The cell culture-based technology has its own limitations since the process still requires the production of re-assorted virus similarly to the egg-based technology[12,13] and has a number of other safety-associated concerns.[5] In contrast, the recombinant protein-based approach involves the use of purified viral surface antigens (HA

and/or NA) as the active component of the vaccine. HA is recognized as the key antigen in the host response induced by influenza vaccination and thus is a logical candidate for a recombinant influenza vaccine. Currently, there are no commercially available recombinant influenza vaccines, although many are in development, including purified HA-based as well as virus-like particle (VLP)-based vaccines.[5,8-11]

The currently available systems for the commercial production of recombinant protein vaccines include bacteria, yeast, insect and mammalian cell cultures. Although each of these systems has specific advantages, their application and use are limited due to insufficient scalability, safety concerns, high cost and target integrity. A much cheaper, safer and highly scalable alternative for recombinant subunit vaccine production is a plant-based system that can generate proteins in their native form with the desired properties.[14] A number of human and animal recombinant subunit vaccines have been produced in plants to date and have been demonstrated to be efficacious and safe in preclinical and clinical studies.[14,15]

In this report, we have conducted studies to formulate a recombinant HA protein (HAC1) from H1N1 influenza A (A/California/04/09 strain) produced in *Nicotiana benthamiana* plants as an early developmental step towards the generation of a commercially viable vaccine. In this work, we also test the utility of accelerated stability studies.

Materials and Methods

Plant-derived HA, HAC1, was produced by Fraunhofer CMB Inc. (Newark, DE)[16] and supplied as a frozen solution. For initial characterization studies, citrate phosphate (CP) buffers (20 mM, pH 3.0-8.0) with an ionic strength of 0.15 (adjusted with NaCl) were used. Imidazole buffer (10 mM, pH 7.0) containing 150 mM NaCl was used for excipient screening and adjuvant studies. For buffer exchange, protein was dialyzed at 4 °C using Slide-A-Lyzer® Dialysis

Cassettes, 10 kDa MWCO (Pierce, Rockford, IL). Alhydrogel® (2%) was obtained from Brenntag Biosector, Fredericksund, Denmark. All other reagents were of analytical grade. Protein concentration was determined by UV absorbance at 280 nm using an extinction coefficient of 1.36 ml/mg-cm for HAC1. Experiments in the presence of the adjuvant were conducted by adding Alhydrogel® to the protein (or the protein-excipient mixture).

Characterization of the physical stability of HAC1

Sample preparation

For each of the spectroscopic techniques, duplicate samples were prepared at different pH values (pH 3.0 to 8.0, at one pH unit intervals) by dilution of the stock material with 20 mM CP buffer of the appropriate pH. The ionic strength of each sample was kept constant at a value of 0.15 using NaCl. Protein solutions were studied at a concentration of 0.2 mg/ml for CD studies and 0.1 mg/ml for fluorescence studies.

Far-UV circular dichroism (CD) spectroscopy

CD spectra were acquired using a Jasco J-810 spectropolarimeter equipped with a 6-position peltier temperature-controlled sample cell holder (Jasco Inc., Easton, MD). The CD spectra were recorded from 260-190 nm with a scanning speed of 50 nm/min, a response time of 2 second and an accumulation of 3.To study thermal transitions (melting curves) of the proteins (in sealed cuvettes of 0.1 cm pathlength), the CD signal at 222 nm was monitored every 2.5 °C with a 3 minute equilibration over a 10 to 87.5 °C temperature range employing a temperature ramp of 15 °C/hr. A buffer baseline was subtracted from each spectrum.

Intrinsic tryptophan (Trp) fluorescence spectroscopy

Fluorescence spectra were acquired using a Photon Technology International (PTI) spectrofluorometer (Lawrenceville, NJ) equipped with a turreted 4-position peltier-controlled cell holder. An excitation wavelength of 295 nm was used to excite Trp residues and the emission spectra (>95% Trp emission) were collected from 310 to 400 nm. Light scattering was monitored using a second detector located at 180° to the emission detector, and was collected at 295 nm. Emission spectra were collected every 2.5 °C with a 3 minute equilibration period at each temperature over the temperature range of 10 to 87.5 °C in a 1 cm pathlength quartz cuvette. A buffer baseline was subtracted from each raw emission spectrum. Peak positions and intensities of the emission spectra were obtained using a mean spectral center of mass (MSM) method which increases the actual peak positions by about 8-10 nm, but yields a better signal to noise ratio and increased reproducibility.

ANS fluorescence spectroscopy

The accessibility of apolar sites on protein surfaces was monitored by fluorescence emission of the extrinsic probe 8-anilino-1-naphthalene sulfonate (ANS). Each sample contained an optimized 15-fold molar excess of ANS to protein. The ANS was excited at 375 nm and emission spectra were collected from 400-600 nm. Emission spectra were collected every 2.5 °C with a 3 min equilibration period over a temperature range of 10 to 87.5 °C. The ANS-buffer baseline at each corresponding pH was subtracted from raw emission spectra. Peak intensities of the emission spectra were obtained using the MSM method.

Empirical phase diagrams (EPDs)

EPDs were constructed as previously described.[17] CD molar ellipticity at 222 nm, intrinsic Trp fluorescence peak intensity and peak shift, light scattering intensity and ANS

fluorescence peak intensity data sets were used for construction of the empirical phase diagram. All calculations were performed using Matlab software (The MathWorks, Natick, MA). Briefly, the experimental data sets were represented as n-dimensional vectors in n x n density matrices, where n is the number of variables (e.g. CD, fluorescence, light scattering, etc.) at each pH-temperature combination. The density matrices were used to derive n sets of eigenvalues and eigenvectors. The three eigenvectors which corresponded to the highest eigenvalues were employed to re-expand the data into three dimensions, and each vector was assigned a color (red, green or blue). The resulting multi-colored plot represents contributions of each vector at a given pH/temperature value. Thus, regions of the plot with similar color indicate similar physical states of the protein. A detailed explanation of the calculations involved in construction of EPDs is presented elsewhere.[18,19]

Excipient screening

Prior to excipient screening, an accelerated stability assay based on intrinsic fluorescence and light scattering (using thermal transitions) was employed to select an optimal buffer system at pH 7.0. After observing insignificant differences in protein stability in the buffers tested including PBS, imidazole and citrate-phosphate, imidazole was chosen as the buffer for further experiments. For excipient screening, duplicate samples were prepared at pH 7.0 in 10 mM imidazole buffer. The ionic strength of all samples was kept constant at a value of 0.15 using NaCl. Protein solutions were studied at a concentration of 0.1 mg/ml for these studies. The intrinsic fluorescence assay was further used to screen for stabilizing compounds. Thermal transition plots of the protein in the presence of various GRAS (Generally Regarded as Safe) excipients were acquired using the PTI spectrofluorometer as described above. The excipients that shift the thermal transitions to higher temperatures are defined as stabilizers, while those that

shift the curves towards lower temperatures are considered destabilizers. Thus, the extent of stabilization and delay in aggregation of protein by the excipients were evaluated by their ability to shift the midpoint of the thermal transition temperature (T_m) of the protein to higher temperatures. The T_m values were obtained by normalizing the melting curve between 0 and 100 percent, i.e. the part of the curve before the transition initiates was set to 0, and the part of the curve after the transition is completed was set to 100. The temperature at which the melting curve crosses the 50% mark is then defined as the T_m.

Following identification of potential stabilizers, the concentration of the stabilizers was optimized. Once suitable concentrations of stabilizing compounds were obtained, the stabilizers were used in combinations to determine if any additive or synergistic effects could be obtained for stabilization of HAC1.

Adjuvant binding and stability studies

The adsorptive capacity of HAC1 in the presence of Alhydrogel® at various concentrations (0.04 – 0.36 mg/ml at 0.04 unit intervals) was determined by constructing a binding isotherm. The protein solutions in the presence of 0.2 mg/ml Alhydrogel® were tumbled in an end-over-end tube rotator at 4 °C for 20 minutes in imidazole buffer at pH 7.0. The samples were centrifuged using an IEC Micromax centrifuge at 2,500 x g for 1 minute to pellet the adjuvant. The amount of protein remaining in the supernatants (measured by UV absorbance spectroscopy) was used for the construction of binding curves. The ability of the protein to bind to Alhydrogel® in the presence of excipients was determined by the same procedure. In this case, Alhydrogel® was added to the protein-excipient solution.

Desorption of the protein from Alhydrogel® was monitored in the presence of several potential desorption agents including NaCl, guanidine hydrochloride, urea and sodium citrate.

The protein-Alhydrogel® pellets were prepared as described above. The pellets were washed with imidazole buffer (pH 7.0) to remove any protein present in the supernatant prior to addition of the desorption solution. The Alhydrogel® solutions were then tumbled in an end-over-end tube rotator at 4 °C for 20 minutes. The samples were centrifuged at 2,500 x g for 2 minutes to pellet the adjuvant. The amount of protein in the supernatant was used to measure the protein desorbed from the surface of the adjuvant.

The thermal stability of the protein bound to Alhydrogel® was monitored by intrinsic Trp fluorescence spectroscopy. Protein (180 μg/ml) was added to Alhydrogel® (0.5 mg/ml) by the procedure described above, which ensured >90% bound protein. The solution was transferred into a 1 mm cuvette and the adjuvant was allowed to settle for 4 hours. The use of a small pathlength cuvette enables us to obtain the fluorescence spectra of the protein while adsorbed to the adjuvant.[20] The pellet was then analyzed between 10 and 87.5 °C. The T_m values were obtained from the melting curves by intrinsic fluorescence spectroscopy. The effect of excipients on the stability on the adjuvant-bound protein was also tested. When tested with excipients, the adjuvant was always added last to the protein-excipient mixture.

A heat treatment ("annealing") of the protein was undertaken to see if this procedure offered any additional stability. Samples of the protein in the presence of the adjuvant were heated at 40, 50, or 60 °C for 10 minutes or 2 hours in a water bath. After the specified amount of time, they were allowed to cool to room temperature and then refrigerated at 4 °C until further experiments. The stability of the bound protein was tested as described above using intrinsic fluorescence spectroscopy. The stability of the annealed protein was studied in the presence of selected excipients as well.

Immunogenicity of selected formulations of HAC1 in mice

Immunogenicity of selected formulations of HAC1 was evaluated in mice using HAI antibody response as a parameter. Groups of 6-week–old Balb/c mice, 5 mice per group, were immunized with 18 μg/dose of HAC1 intramuscularly (i.m.) at 3-week intervals on study days 0 and 21. The HAC1 formulations tested were prepared in the buffer containing 10 mM imidazole and 150 mM NaCl, pH 7, and included three formulations without Alhydrogel®, two formulations with Alhydrogel® (0.5 mg/ml of aluminum), and heat-treated ("annealed") HAC1 with Alhydrogel® (to evaluate the effect of the heat treatment on the immunogenicity), as shown in Table 3. Animals in group 7 received HAC1 in saline with Alhydrogel® (1.8 mg/ml of aluminum), which has been previously shown to elicit robust HAI antibody responses in mice,[16] and group 8 received saline alone with 1.8 mg/ml of Alhydrogel® (a negative control group). Serum samples were collected prior to each immunization and at 2, 3 and 7 weeks after the second dose. Serum samples collected from immunized animals were first treated with a receptor-destroying enzyme (RDE; Denka Seiken Co. Ltd., Tokyo, Japan) and then tested in the HAI assay. The HAI assay was carried out using 0.75% turkey erythrocytes as described previously[21], with an initial serum dilution of 1:20 against the A/California/07/09 x 179A virus (CDC # 2009713114). Immunized animals with HAI antibody titers of ≥1:40 were defined as seropositive.

Statistical analysis of data was performed using a two-tailed F-test with equal variance and significance was considered at a p value <0.05. Mouse serum samples without detectable HAI were assigned a value of 10.

Results

Biophysical characterization of HAC1

The CD spectrum of HAC1 at pH 7.0 and 10 °C displays a broad negative peak between 205-225 nm with apparent double minima near 208 and 220 nm, indicating significant contributions from α-helices to the secondary structure of the protein (Figure 2.1). The CD spectrum at pH 7.0 is representative of what is seen at pH of 3.0-8.0 as well. The broad peak and significant negative ellipiticity at 215 nm, however, indicates the presence of some β-sheet as well. Decreases in the molar ellipiticity at 222 nm provide evidence for the loss of the α-helical secondary structure upon thermal stress (Figure 2.2). Only gradual transitions were evident at pH 3.0, 4.0, and 5.0, which initiate at relatively low temperatures (~ 20-30 °C) (Figure 2.2A-C). A small transition is seen near 30 °C at pH 6.0 (Figure 2.2D). In contrast, much sharper transitions are observed at pH 7.0 and 8.0 at 45-50 °C (Figure 2.2E-F).

Red shifts in protein Trp peak positions occur as buried Trp residues become exposed to a more polar environment and provide evidence for changes in the tertiary structure. Again, no sharp transitions are seen at pH 3.0, 4.0, and 5.0 (Figure 2.3). Instead, a very gradual shift is observed at these three pH values with peak positions at about 344 nm at 10 °C (note that the actual peak positions are ~ 10 nm lower). Sharp transitions are seen at pH 7.0 and 8.0 at about 50 °C, with the peak position at about 340 nm at 10 °C. At pH 6.0, the protein manifests a lower thermal stability compared to pH 7.0 and 8.0, with the peak position slightly red shifted to about 342 nm at 10 °C and transitions initiating above 30 °C.

Monitoring static light scattering intensity provides insight into the aggregation behavior of proteins in solution. Despite the absence of visible aggregates even after heating to 90 °C, the increasing static light intensity and corresponding transitions observed for HAC1 indicate formation of lower order aggregates with increases in temperature. At pH 3.0, 7.0, and 8.0, the aggregation transitions occur between 40-45 °C (Figure 2.4). At pH 6.0, the light scattering

intensity gradually increases without a sharp transition. The constant and low light scattering intensity throughout the entire temperature scan at pH 4.0 and 5.0 suggests that there is no detectable aggregate formation at these pH values.

At pH 3.0-5.0, ANS shows significant fluorescence intensity at low temperatures suggesting that the tertiary structure of HAC1 is already structurally altered (see Figure 2.5). A gradual decrease in ANS fluorescence intensity is observed at these pH values indicating release of ANS from the protein as it further unfolds and/or increasing fluorescence quenching at higher temperatures. The transition at pH 6.0 starts at 42 °C, while the transitions at pH 7.0 and 8.0 begin at higher temperature (52 °C) suggesting an increased conformational stability of HAC1 around neutral pH, similar to that observed by the other techniques. Again, the protein at pH 6.0 exhibits relatively increased stability compared to pH 3.0-5.0, but to a lesser extent than that seen at pH 7.0 and 8.0 as suggested by all of the biophysical studies.

An empirical phase diagram (EPD) was created by combining the data shown above to reflect secondary and tertiary structural changes, aggregation state, and the accessibility of apolar binding sites in the protein as a function of pH and temperature (Figure 2.6). The blue region at the lower, right-hand corner of the diagram encompassing pH 7.0 and 8.0 and temperatures below 50 °C can be considered the region in which the protein is found to be in its native conformation (region I). Intrinsic fluorescence, ANS fluorescence and light scattering data all confirm this observation. Region II represents an intermediate state of the protein at pH 6.0 and temperatures below 40 °C. Regions V and VI, present at pH 6.0, 7.0 and 8.0 at elevated temperatures, represent a physical state in which the protein is severely structurally altered and aggregated. Region III (green), present at pH 3.0-5.0 and below 50-60 °C, represents a state of the protein that is partially structurally altered, but remains in a non-aggregated state. As the

temperature is increased above 50 °C at pH 3.0-5.0, additional behavior (greenish blue) is apparent. At pH 3.0, this reflects a transition observed in the static light scattering plots and represents a severely disrupted and aggregated state of the protein. At pH 4.0 and 5.0, this region represents a severely structurally altered state as indicated by CD and fluorescence data but lacks the presence of aggregates.

Excipient screening

Based on the EPD and thermal melts generated from data acquired during biophysical characterization of HAC1, pH 7.0 was selected for excipient screening based on the optimal conformational stability and aggregation profile of HAC1 at this pH. A series of GRAS compounds from a library previously found to be of wide utility were screened by fluorescence spectroscopy for their ability to enhance HAC1 conformational stability and prevent aggregation. Among those compounds evaluated in the screening were a variety of carbohydrates, nonionic surfactants, amino acids, polyalcohols and cyclodextrins (Table 2.1). Examples of the relative shifts in the thermal unfolding curves of HAC1 in the presence of excipients are shown in Figure 2.7. The effect of excipients on the aggregation and conformational stability of HAC1 in imidazole buffer at pH 7.0 is summarized in Table 2.1 in the form of T_m values. Table 2.2 summarizes the effect of concentration of selected stabilizing excipients on both the aggregation and conformational stability of HAC1. The potential stabilizers identified include dextrose, sorbitol, glycerol, and Tween-80. As seen in Table 2.1, 20% sorbitol, 20% dextrose, and 20% sucrose produced the maximum increase in the conformational stability with a change in T_m of ~4 °C, while Tween-80 had the highest inhibitory effect on aggregation with a change of about 8 °C. The conformational destabilization caused by Tween-80, however, renders it potentially less useful as a stabilizer.

The effects of selected excipients were concentration dependent, except for glycerol and Tween-80 (Table 2.2). The use of these excipients at 20% concentration is beyond recommended limits due to high osmolarity values. Hence, the use of sorbitol, dextrose and sucrose was limited to a concentration of 15%. Tween-80 at concentrations lower than 0.1% was also tested due to its inhibitory effect on aggregation despite its conformation-destabilizing effect.

The effects of combinations of excipients on thermal transitions (both aggregation and conformational stability) are summarized in Table 2.3 (a) and (b). The combinations of selected excipients, however, did not yield significant improvements compared to 15% sorbitol alone with respect to the stabilization of HAC1. Some combinations of excipients such as 15% sucrose and 0.05% Tween-80 showed a stabilizing effect when analyzed by static light scattering. No significant effect, however, was observed using intrinsic fluorescence. This is presumably due to the non-specific interactions of tween-80 with the protein which inhibits aggregations. In contrast, this does not appear to protect a protein against changes in conformation.

Adjuvant binding studies

Adsorption and desorption studies of HAC1 with Alhydrogel®

The time required for the protein to adsorb onto the surface of an aluminum salt adjuvant varies for different proteins. Kinetic studies of HAC1 binding to Alhydrogel® revealed that the protein efficiently binds to Alhydrogel® at a protein concentration of 240 μg/ml and an adjuvant concentration of 0.5 mg/ml. In 10 mM imidazole buffer (pH 7.0, I=0.15, adjusted with NaCl), all of the protein binds to the adjuvant within the first 2 minutes of introducing the adjuvant (data not shown). The amount of protein bound to Alhydrogel® does not change significantly during the 20-minute period of testing.

The amount of protein that can be adsorbed onto the surface of Alhydrogel®, or the "adsorptive capacity" of Alhydrogel®, was determined by constructing adsorption isotherms. Adsorptive capacity is defined as the maximum amount of protein that can be adsorbed onto the surface of Alhydrogel®. In binding isotherms, 100 μg of Alhydrogel® is able to adsorb up to 160 μg of protein in 10 mM imidazole buffer (pH 7.0, I=0.15, adjusted with NaCl). In the studies conducted, saturation of protein binding was not attained and experiments with higher protein concentrations were not conducted.

An important study that the FDA requires in the development of a vaccine that involves aluminum salts is desorbing the protein from the surface of the adjuvant. The amount of desorbed protein depends on the desorptive media and the level of interaction between the protein and the adjuvant. Standard desorptive media such as 1 M NaCl and 1 M urea were not able to desorb significant amounts of protein (data not shown). Figure 2.8 shows the effects of the combination of urea/citrate and citrate alone on the desorption of three different concentrations of the protein adsorbed onto 100 μg of Alhydrogel®. A combination of 1.8 M urea and 0.9 M citrate was required to desorb about 80% of the protein from the surface of the adjuvant.

Effect of selected stabilizers on adsorption of HAC1 on Alhydrogel® surface

The adsorption of HAC1 to the surface of Alhydrogel® may be affected by the presence of the excipients that were identified as stabilizers of the protein in solution. The percent protein adsorbed to the adjuvant did not change significantly in the presence of the stabilizers (see **Figure 2.9**). Additional excipients including Tween-80 and phosphate were tested as well (data not shown), and no significant loss in the adsorption of HAC1 to the adjuvant surface was found.

Effect of Alhydrogel adsorption on HAC1 stability

Intrinsic Trp fluorescence spectroscopy was used to analyze changes in the tertiary structure of the protein adsorbed to the surface of Alhydrogel®. At 10 °C, the emission peak maximum for HAC1 in solution is at 332 nm, which indicates substantially buried Trp residues (Figure 2.10). The emission peak maximum does not change until about 45 °C, and slowly transitions to about 337 nm by 55 °C. This transition at 45 °C represents a surface-induced stability perturbation in the tertiary structure of HAC1, since the T_m of HAC1 in solution is about 54 °C. When the protein is adsorbed to Alhydrogel, the steep transition near 54 °C observed in solution is replaced by a very broad and gradual transition that actually initiates as low as 25 °C (Figure 2.10). In the presence of sorbitol, dextrose and sucrose, there is no significant stabilization of HAC1 on the adjuvant. Tween-80 and phosphate were also tested to see if they might help stabilize the adsorbed protein. Figure 2.11 shows the effect of the presence of 5 mM phosphate, 15% sorbitol and 0.1% Tween-80 as well as 5 mM phosphate alone on the stability of HAC1 adsorbed onto Alhydrogel®. At 10 °C, the position of the emission peak maxima is similar to that of HAC1 in solution in both cases. The broad, gradual transitions, however, still exist. HAC1 in the presence of 15% sorbitol, 0.1% Tween-80 and 5 mM phosphate showed a thermal melting profile closest to that seen in solution. In this case, the transition starts at about 35 °C with the T_m for the adsorbed protein found to be about 49 °C. This represents a 5 °C destabilization induced by the adsorption of HAC1 onto the surface of Alhydrogel®, compared to the 10 °C destabilization described above.

Heat treatment, or "annealing", of the protein was undertaken for 10 minutes at 40, 50 or 60 °C to see if this could produce a stabilization effect. The position of the emission peak

maxima was found to be near 334 nm, which suggests a slight change in structure compared to the non-annealed protein (Figure 2.12). When annealed at 40 °C, however, the protein retains this conformation until about 40 °C, with the position of the emission peak gradually increasing. The T_m for this transition was approximately 54 °C, the same as seen for HAC1 in solution in the absence of stabilizers. The extent of this retention of the conformation is not seen when the protein was annealed at 50 or 60 °C.

Of the formulations tested in this study, five were selected for further evaluation in animals based on their ability to best delay the transitions seen by intrinsic fluorescence. These formulations included the compounds, sorbitol, sucrose, phosphate and Tween-80. Fifteen percent sorbitol with 5mM phosphate and 0.1% tween-80 was used since it showed a profile closest to that seen in solution. HAC1 in the presence of 5mM phosphate was also used in the animal studies since the phosphate produced slight stabilization of the adsorbed protein. Finally, heat-treated HAC1 at 40 °C was also included in animal studies to test if an un-stabilized protein might be more immunogenic.

Immunogenicity of the selected formulations in mice

An immunogenicity study in mice was conducted to evaluate effects of formulations on HAC1-elicited protective correlates of immunity. In the absence of Alhydrogel®, mice immunized with HAC1 formulations with 15% sorbitol or 10% dextrose (groups 1 and 3) showed higher serum hemagglutination-inhibition (HAI) antibody titers on study day 35 compared to the HAC1 formulation with 10% sorbitol and 5% sucrose (group 2, p <0.001). In groups 1 and 3, mean HAI titers reached the values of 1:304 (± 138) and 1:154 (± 68), respectively, on study day 35, and 100% and 80% of the immunized animals, respectively, showed HAI titers of ≥1:40 (Table 2.5). These titers slightly decreased by study day 70 (Figure

2.13). In group 3, the mean HAI titer was 1:26 (± 8) on study day 35 and only 40% of animals reached HAI titers of ≥1:40 (Table 2.5). In the presence of Alhydrogel® (groups 4–7), mean HAI titers were significantly higher than those observed in the groups immunized without Alhydrogel®, and were either maintained or slightly increased through study day 35 to 70 with a 100% seropositive rate (Figure 2.13). No statistically significant difference was observed among the groups immunized with Alhydrogel®, except that in group 6 the mean HAI titer was lower than in groups 5 and 7 (p <0.05) on study day 35.

Discussion

HAC1 is an H1N1 influenza vaccine candidate containing the recombinant HA protein from H1N1 influenza virus A/California/04/09 strain produced in a plant-based system. Only the ectodomain of HA is used in HAC1 with the last 77 residues that aid in anchoring the protein to the lipid membrane of the virus removed. In this study, we applied a composite biophysical approach to characterize HAC1 and identify stabilizers. The signals from various spectroscopic and light scattering techniques have been used to monitor changes in the physical structure of HAC1 when exposed to stresses such as pH and temperature. The CD spectra of HAC1 show predominantly α-helical structure, although there is an indication of the presence of some β-sheet character as well. CD secondary structural analysis using K2D2 showed that HAC1 contained 77% of α-helix and about 1% β-sheet.[22] This is consistent with the published crystal structure of HA.[23] Thermal transitions indicate a gradual loss in the secondary structure with increases in temperature at pH 3.0, 4.0, and 5.0. The CD thermal transition at pH 6.0 manifests a sudden change in the secondary structure at about 30 °C, which is raised to about 45-50 °C at pH 7.0 and 8.0. The intrinsic Trp fluorescence melts show emission peak maxima for HAC1 at about 344 nm at pH 3.0, 4.0, 5.0 and 6.0, and about 340 nm at pH 7.0 and 8.0, when analyzed using the

MSM method, which overestimates the peak position by about 8-12 nm. This confirms that HAC1 is not completely structurally disrupted at any pH tested, but rather exists in a partially perturbed state, with its Trp residues relatively buried under all pH conditions examined. No cooperative transitions were detected at pH 3.0, 4.0 and 5.0. At pH 6.0, a thermal transition was observed at about ~40 °C and this transition initiates at ~50 °C for pH 7.0 and 8.0. Static light scattering and extrinsic ANS fluorescence also revealed similar trends in the protein's thermal transitions. ANS was found to bind to HAC1 at low temperature at pH 3.0, 4.0, and 5.0 presumably due to the partially altered structure.

All the data collected for HAC1 was combined in the form of an EPD to better represent the effect of temperature and pH on the protein. The three distinct regions in the EPD presumably reflect the conformational changes that HA undergoes when influenza virus infects a cell [24-26]. At physiological pH, the protein is in its native form. HA binds to sialic acid residues on the cell surface, which causes the host cell to internalize the virus into an endosomal compartment. When the pH of the endosome drops below 6.0, the conformation of HA alters, resulting in the exposure of apolar regions. This new form attaches itself to the endosomal membrane. As the pH further drops to about 5.0, HA again changes its structure causing the membrane of the virus to fuse with that of the endosome, propelling viral RNA into the cytoplasm. Thus, the conformational changes that occur at different pH values during natural virus infection appear to be reflected in the EPD.

Since HAC1 was found to be most stable at pH 7.0 and 8.0, pH 7.0 was chosen to screen for stabilizers and further formulation studies. Imidazole buffer was selected for the screening studies. Since phosphate can convert aluminum hydroxide into aluminum phosphate and citrate is known to dissolve the aluminum salt adjuvants, both of which can affect antigen binding

properties, citrate phosphate buffer was not used for further studies. Surfactants such as Tween-80, sugars and sugar alcohols such as dextrose and sorbitol showed the highest degree of stabilization with respect to aggregation with an increase in T_m of ~7 ^oC. Although Tween-80 stabilized the protein against aggregation, it did not significantly protect it against thermally induced conformational changes at concentrations of 0.05 - 0.1%. It has been suggested that polyalcohol and sugars delay or inhibit aggregation by enhancing the stability of native-like protein structures. Extensive studies have been reported on this kind of stabilization through nonspecific processes such as preferential hydration.[27-29] The potential for stabilization via specific interactions, however, cannot be eliminated due to similarities in the chemical structure between some stabilizers and sialic acid which is a natural ligand for the HA protein. Destabilization and enhanced aggregation of HAC1 in the presence of a polyanion (dextran sulfate) is presumably due to the formation of HA-polyanion complexes. Tween-80 is known to often exert protective effects on protein aggregation through direct interaction with the protein or via its effect on air and water interfaces. In this case, however, the conformational destabilization caused by Tween-80 renders it potentially less useful in formulation development. Sorbitol, dextrose, and sucrose produced the highest increases in T_m values. Concentrations of 15% or below were selected for combination studies to minimize high osmolarity values.

When using aluminum salt adjuvants, the antigen is typically adsorbed onto the surface of the adjuvant. A high level of unbound protein adjuvanted with Alhydrogel® has been associated with hypersensitivity reactions as shown for some malaria antigens in clinical trials.[30-32] Several ideas have been proposed over that last 80 years to explain the mechanism of immunopotentiation by aluminum salt adjuvants. The depot theory postulates that the aluminum adjuvant and the adsorbed antigen remain at the site of injection.[33] The slow release of antigen

from the adjuvant stimulates antibody production. Another theory suggests that the adjuvant causes inflammation at the site of injection, attracting antigen presenting cells (APCs).[34] A third idea postulates that particulation of an antigen may occur on the surface of the adjuvant, which results in antigen internalization by macrophages via phagocytosis leading to an enhanced immune response. Recently, it was proposed that upon interaction of dendritic cells (DCs), the key APCs, with an adjuvant, DCs' lipid membrane undergoes re-assortment which leads to the antigen being delivered in its soluble form into DC followed by processing in the MHC class II compartment, which ultimately shows a high preference for activation of $CD4^+$ T-cells that in turn activate B-cells and increase an antibody response.[35] It is possible that some these mechanisms contribute to immunopotentiation by aluminum salt adjuvants. Recent studies have also suggested that in some cases retention of an antigen on an adjuvant is not essential for immunopotentiation.[36] Nevertheless, adsorbing the antigen onto the surface of the aluminum salt adjuvant is a common approach to produce an optimal immunogenic effect.

The PI of HAC1 is around 6.5. This gives the protein a negative charge at pH 7.0. Due to simple electrostatic interactions, HAC1 should adsorb onto positively charged Alhydrogel®. This is in a good agreement with the experimental data. Other interactions such as van der Waals forces may play an important role in the adsorption process as well. Here, almost all of the protein is found to be bound to Alhydrogel® within the first 2 minutes of introduction. The adsorption isotherm demonstrates a very high adsorption capacity for HAC1 with 100 μg of Alhydrogel® able to adsorb 160 μg of HAC1. The inability of NaCl to desorb the protein from the surface of Alhydrogel® suggests that the binding is not purely electrostatic in nature. The presence of strong desorptive agents such as a combination of urea and citrate resulted in desorption of about 80% of the protein from the surface of Alhydrogel®. The stability of the

protein, however, was found to be decreased when adsorbed onto the surface of Alhydrogel®. Several studies have demonstrated that adsorption of a protein onto the surface of aluminum salts generally has a negative effect on the thermal stability of the protein.[20,37] When the protein is heated, there is a gradual change in the position of the emission peak maximum, replacing the cooperative unfolding transition that occurs at about 45 °C in solution with one 10 °C less. This may be due to a time-dependent optimization of interactions between the protein and the surface of the adjuvant. In a few cases, it was possible to partially overcome this effect. This decreased stability may also lead to enhanced chemical degradation. Deamidation is especially a concern. This is due to the high pH in the microenvironment of the protein on the surface of Alhydrogel®. The positively charged surface of the adjuvant repels protons and attracts OH^- ions, thereby increasing pH and making deamidation more likely to occur. The high surface pH can be countered by using sodium phosphate. Sodium phosphate can partially convert the positively charged surface of Alhydrogel® to aluminum phosphate lowering the surface pH. As seen is this study, sodium phosphate at a concentration of 5 mM was, in fact, able to stabilize the adsorbed protein to some extent. Actual studies of the chemical stability of HAC1 have not yet been conducted.

The effects of adding excipients and/or stabilizers on the immunogenicity of the HAC1 vaccine were also evaluated. The addition of 15% sorbitol or 10% dextrose resulted in the induction of higher serum HAI antibody titers in mice compared to the addition of 10% sorbitol and 5% sucrose. This suggests that sorbitol or dextrose may have a stabilizing effect, as described in the Results section, and improve the immunogenicity of the HAC1 vaccine. Serum HAI titers, however, gradually decreased from study day 35 through study day 70, while the HAI titers in mice immunized with HAC1 plus Alhydrogel® were maintained at same levels up to

study day 70, perhaps due to a depot effect of the aluminum adjuvant. In previous studies, we reported the ability of the plant-produced HAC1, at doses of 15 or 5 µg in saline plus Alhydrogel® (1:10 [w:w] of aluminum), to elicit HAI antibody titers ≥1:40 in 100% of immunized mice. In addition, immunization with 15 or 5 µg of HAC1 in the absence of Alhydrogel® elicited HAI antibody titers ≥1:40 in 83 or 50% of mice, respectively. According to the FDA's recommendation[38], however, the amount of aluminum in a dose of a biological product should not exceed 1.14 mg, if determined by calculation on the basis of the amount of aluminum compound added. Therefore, in the current study, we investigated whether vaccine formulations containing a lower, more acceptable amount of aluminum or no aluminum adjuvant at all could still elicit significant antibody responses. The results obtained indicate that immunization with HAC1 plus a lower amount (0.5 mg/ml) of aluminum can still elicit significant HAI antibody responses with 100% of animals generating HAI antibody titers ≥1:40. Interestingly, in the absence of Alhydrogel, the addition of 15% sorbitol resulted in the generation of equal or greater HAI responses compared to those induced by HAC1 in saline without Alhydrogel® as reported on previously. These results need to be further investigated in a dose-reduction study to determine how the buffer and excipients tested in the current study affected the robustness of the HAI antibody responses, particularly with regard to the lower amount of Alhydrogel® tested. In addition, no statistically significant differences in HAI titers were observed between the group of mice immunized with heat-treated HAC1 plus Alhydrogel® and the other HAC1/Alhydrogel® groups. Similar results were observed when total IgG titers elicited by the different immunizations were analyzed (data not shown). Although our results demonstrate that heat-induced structural changes did not affect the immunogenicity of HAC1 in terms of the magnitude of total IgG and HAI responses induced, comparison of virus-

neutralization antibody titers between animals immunized with structurally altered HAC1 versus non-denatured HAC1 would provide important additional information about the high temperatures have on the immunogenicity of HAC1. In summary, the results of this study demonstrate that the amount of Alhydrogel® in the HAC1 vaccine could be spared down to 0.5 mg/ml, the same amount of aluminum used in GARDASIL, the FDA-approved human papillomavirus vaccine (Merck & Co., Inc., Whitehouse Station, NJ).

References

1. Plotkin SA OW. 2004. Vaccines. 4 ed.: Saunders.
2. Gerdil C 2003. The annual production cycle for influenza vaccine. Vaccine 21(16):1776-1779.
3. Sheridan C 2004. Next generation flu vaccine boosted by Chiron debacle. Nat Biotechnol 22(12):1487-1488.
4. Stephenson I, Nicholson KG, Wood JM, Zambon MC, Katz JM 2004. Confronting the avian influenza threat: vaccine development for a potential pandemic. Lancet Infect Dis 4(8):499-509.
5. Wang K, Holtz KM, Anderson K, Chubet R, Mahmoud W, Cox MM 2006. Expression and purification of an influenza hemagglutinin--one step closer to a recombinant protein-based influenza vaccine. Vaccine 24(12):2176-2185.
6. Delaney JW, Fowler RA 2009 influenza A (H1N1): a clinical review. Hosp Pract (Minneap) 38(2):74-81.
7. Jean Maritz LMaWP 2010. Pandemic influenza A (H1N1) 2009: the experience

of the first six months. Clinical Chemistry and Laboratory Medicine 48(1):11-21.
8. Cox MM, Hollister JR 2009. FluBlok, a next generation influenza vaccine manufactured in insect cells. Biologicals 37(3):182-189.
9. Cox MM, Patriarca PA, Treanor J 2008. FluBlok, a recombinant hemagglutinin influenza vaccine. Influenza Other Respi Viruses 2(6):211-219.
10. Kissmann J, Joshi SB, Haynes JR, Dokken L, Richardson C, Middaugh CR H1N1 influenza virus-like particles: physical degradation pathways and identification of stabilizers. Journal of pharmaceutical sciences 100(2):634-645.
11. McPherson CE 2008. Development of a novel recombinant influenza vaccine in insect cells. Biologicals 36(6):350-353.
12. Robertson JS, Naeve CW, Webster RG, Bootman JS, Newman R, Schild GC 1985. Alterations in the hemagglutinin associated with adaptation of influenza B virus to growth in eggs. Virology 143(1):166-174.
13. Schild GC, Oxford JS, de Jong JC, Webster RG 1983. Evidence for host-cell selection of influenza virus antigenic variants. Nature 303(5919):706-709.
14. Yusibov V, Streatfield SJ, Kushnir N Clinical development of plant-produced recombinant pharmaceuticals: Vaccines, antibodies and beyond. Hum Vaccin 7(3):313-321.
15. Musiychuk K, Stephenson N, Bi H, Farrance CE, Orozovic G, Brodelius M, Brodelius P, Horsey A, Ugulava N, Shamloul AM, Mett V, Rabindran S, Streatfield SJ, Yusibov V 2007. A launch vector for the production of vaccine antigens in plants. Influenza Other Respi Viruses 1(1):19-25.
16. Shoji Y, Chichester JA, Jones M, Manceva SD, Damon E, Mett V, Musiychuk K, Bi H, Farrance C, Shamloul M, Kushnir N, Sharma S, Yusibov V Plant-based rapid production of recombinant subunit hemagglutinin vaccines targeting H1N1 and H5N1 influenza. Hum Vaccin 7 Suppl:41-50.
17. Fan H, Ralston J, Dibiase M, Faulkner E, Middaugh CR 2005. Solution behavior of IFN-beta-1a: an empirical phase diagram based approach. J Pharm Sci 94(9):1893-1911.
18. Kueltzo LA, Ersoy B, Ralston JP, Middaugh CR 2003. Derivative absorbance spectroscopy and protein phase diagrams as tools for comprehensive protein characterization: a bGCSF case study. Journal of pharmaceutical sciences 92(9):1805-1820.
19. Maddux NR, Joshi SB, Volkin DB, Ralston JP, Middaugh CR Multidimensional methods for the formulation of biopharmaceuticals and vaccines. J Pharm Sci.
20. Peek LJ, Martin TT, Elk Nation C, Pegram SA, Middaugh CR 2007. Effects of stabilizers on the destabilization of proteins upon adsorption to aluminum salt adjuvants. Journal of pharmaceutical sciences 96(3):547-557.
21. Shoji Y CJ, Bi H, Musiychuk K, de la Rosa P, Goldschmidt L, Horsey A, Ugulava N, Palmer GA, Mett V, Yusibov V. 2008. Plant-expressed HA as a seasonal influenza vaccine candidate. Vaccine 26(23):2930-2934.

22. Perez-Iratxeta C, Andrade-Navarro MA 2008. K2D2: estimation of protein secondary structure from circular dichroism spectra. BMC Struct Biol 8:25.
23. Lin T, Wang G, Li A, Zhang Q, Wu C, Zhang R, Cai Q, Song W, Yuen KY 2009. The hemagglutinin structure of an avian H1N1 influenza A virus. Virology 392(1):73-81.
24. Cross KJ, Langley WA, Russell RJ, Skehel JJ, Steinhauer DA 2009. Composition and functions of the influenza fusion peptide. Protein Pept Lett 16(7):766-778.
25. Harrison SC 2005. Mechanism of membrane fusion by viral envelope proteins. Adv Virus Res 64:231-261.
26. Harrison SC 2008. Viral membrane fusion. Nat Struct Mol Biol 15(7):690-698.
27. Shimizu S, Smith DJ 2004. Preferential hydration and the exclusion of cosolvents from protein surfaces. J Chem Phys 121(2):1148-1154.
28. Uedaira H 2001. Role of hydration of polyhydroxy compounds in biological systems. Cell Mol Biol (Noisy-le-grand) 47(5):823-829.
29. Lee JC, Timasheff SN 1981. The stabilization of proteins by sucrose. The Journal of biological chemistry 256(14):7193-7201.
30. Edelman R, Wasserman SS, Kublin JG, Bodison SA, Nardin EH, Oliveira GA, Ansari S, Diggs CL, Kashala OL, Schmeckpeper BJ, Hamilton RG 2002. Immediate-type hypersensitivity and other clinical reactions in volunteers immunized with a synthetic multi-antigen peptide vaccine (PfCS-MAP1NYU) against Plasmodium falciparum sporozoites. Vaccine 21(3-4):269-280.
31. Keitel WA, Kester KE, Atmar RL, White AC, Bond NH, Holland CA, Krzych U, Palmer DR, Egan A, Diggs C, Ballou WR, Hall BF, Kaslow D 1999. Phase I trial of two recombinant vaccines containing the 19kd carboxy terminal fragment of Plasmodium falciparum merozoite surface protein 1 (msp-1(19)) and T helper epitopes of tetanus toxoid. Vaccine 18(5-6):531-539.
32. Kaslow DC 2002. Transmission-blocking vaccines. Chem Immunol 80:287-307.
33. Glenny AT, Buttle GAH, Stevens MF 1931. Rate of disappearance of diphtheria toxoid injected into rabbits and guinea - pigs: Toxoid precipitated with alum. The Journal of Pathology and Bacteriology 34(2):267-275.
34. McKee AS, Munks MW, MacLeod MK, Fleenor CJ, Van Rooijen N, Kappler JW, Marrack P 2009. Alum induces innate immune responses through macrophage and mast cell sensors, but these sensors are not required for alum to act as an adjuvant for specific immunity. J Immunol 183(7):4403-4414.
35. Flach TL, Ng G, Hari A, Desrosiers MD, Zhang P, Ward SM, Seamone ME, Vilaysane A, Mucsi AD, Fong Y, Prenner E, Ling CC, Tschopp J, Muruve DA, Amrein MW, Shi Y Alum interaction with dendritic cell membrane lipids is essential for its adjuvanticity. Nat Med 17(4):479-487.
36. Noe SM, Green MA, HogenEsch H, Hem SL Mechanism of immunopotentiation by aluminum-containing adjuvants elucidated by the relationship between antigen retention at the inoculation site and the immune response. Vaccine 28(20):3588-3594.
37. Jones LS, Peek LJ, Power J, Markham A, Yazzie B, Middaugh CR 2005. Effects of adsorption to aluminum salt adjuvants on the structure and stability of model protein antigens. The Journal of biological chemistry 280(14):13406-13414.
38. FDA US. CFR - Code of Federal Regulations Title 21., ed.

Chapter 3

Preformulation Characterization of an Aluminum Salt Adjuvanted Trivalent Recombinant Protein based Vaccine Candidate against Streptococcus pneumoniae

Introduction

Streptococcus pneumoniae is the leading cause of pneumonia, bacteremia, and meningitis in the United States and worldwide. Systemic infections and invasive pneumococcal disease (IPD) are caused by the spread of the bacteria in the blood stream. It is estimated in the US alone, that over 40,000 lives are lost to *S. pneumoniae*-related diseases with pneumococci being responsible for over 500,000 cases of pneumonia each year.[1] Furthermore, pneumonia is the leading cause of childhood death and claims the lives of about 1.4 million children under the age of five every year, which is more than HIV, tuberculosis and malaria combined. *S. pneumoniae* is estimated to be the cause of over a third of those cases of pneumonia.[2,3] Current vaccines against the pathogen include a polysaccharide vaccine, and a carbohydrate conjugate vaccine.[4,5] The polysaccharide vaccine is approved for use in adults (65 years or older) and protects against up to 23 different serotypes of the bacteria. Unfortunately, this vaccine is poorly immunogenic in children below the age of 2 years, and in the elderly, especially those with compromised immune systems.[5,6] The conjugate vaccine is more immunogenic and approved for use in children[7,8] , and was recently approved by FDA for use in adults 50 years of age and older. This vaccine, however, does not protect against all serotypes of the pathogen.[4,5] The geographical distribution of the pathogen also makes it hard to identify a single efficacious vaccine for the entire world. There is a high level of complexity involved with the manufacturing of the conjugate vaccines, making them expensive and less-accessible to the majority of the world population who are most in need.

These limitations have spurred research into the development of a cost effective vaccine that is targeted against the majority of pneumococcal serotypes. Protein-based vaccines are among one of the approaches currently being taken towards producing a cheaper and more cross protective vaccine. Several surface proteins from *Streptococcus pneumoniae* are being evaluated for use as antigens in such vaccines. The pneumococcal surface protein A (PspA), pneumococcal surface protein C (PspC), pneumococcal surface adhesion A (PsaA), and serine-threonine protein kinase (StkP), as well as other essential proteins such as protein required for cell wall separation of group B streptococcus (PcsB) and pneumolysin (Ply) are

attractive candidates for use as vaccine antigens[4]. StkP and PcsB have previously been identified as antigens by the ANTIGENome technology.[9] Vaccines consisting of protein antigens are expected to be more immunogenic than their conjugate counterparts, especially in children and the elderly. They are also expected to address the coverage problem since 98-100% of the serotypes contain one or more of these surface proteins. In addition, a vaccine based on a few protein antigens is likely easier and cheaper to manufacture than multivalent carbohydrate-conjugate vaccines. There may also be the added advantages of using protein antigens from a stability point of view because they may be more easily characterized. Highly purified, recombinant protein antigens are usually not highly immunogenic by themselves and therefore usually require an adjuvant to boost their immunogenicity. The most common adjuvants used in the world today are aluminum hydroxide (Alhydrogel®) and aluminum phosphate (Adjuphos®). Protein antigens are typically adsorbed to the surface of these aluminum salt adjuvants for maximum effectiveness.

In this paper, we describe the biophysical characterization, stabilization and initial formulation development evaluations of a trivalent recombinant protein based vaccine against *Streptococcus pneumoniae* consisting of PsaA , StkP and PcsB fragments (furthermore mentioned as SP1650, SP1732 and SP2216 respectively) in the presence of aluminum salt adjuvants (Alhydrogel®, Adjuphos®).

Materials and Methods

The three purified antigens SP1650 (PsaA), SP1732 (StkP), and SP2216 (PcsB) were supplied by Intercell AG (Vienna, Austria) as frozen solutions in a 10 mM Tris buffer containing 70 mM sodium chloride, at pH 7.5. The SP1732 solution also contained 0.2% (w/v) polysorbate-20. For the initial biophysical characterization, all three of the proteins were dialyzed into 20 mM citrate phosphate (CP) buffers (pH 5.5, 6.0, 6.5, 7.0, 7.5 and 8.0) with a total ionic strength of 0.15 (adjusted with NaCl). All excipients were purchased from Sigma-Aldrich (St. Louis, MO). For excipient screening and adjuvant studies, 10 mM sodium acetate buffer (containing 0.067% w/v polysorbate-20) was used for all three proteins. All other reagents were of analytical grade. Protein concentration was determined by UV

absorbance at 280 nm using an extinction coefficient of 1.1 ml/mg-cm for SP1650, 0.468 ml/mg-cm for SP1732 and 0.1 ml/mg-cm for SP2216.

Characterization of Physical Stability:

Sample preparation:

For each of the spectroscopic techniques, duplicate samples were prepared at different pH values (pH 3 to 8, at one unit intervals) by dilution of the stock material with 20 mM CP buffer of the appropriate pH. The ionic strength of samples was kept constant at 0.15 using appropriate amounts of NaCl. Protein solutions were studied at a concentration of 0.2 mg/ml for the CD studies, 0.1 mg/ml for the fluorescence studies and 0.3 mg/ml for second derivative UV absorbance studies.

Far-UV Circular Dichroism (CD) Spectroscopy:

CD spectra were acquired using a Jasco J-810 spectropolarimeter equipped with a 6-position peltier temperature controlled sample cell holder. CD spectra were obtained from 260-190 nm. Melting curves of the proteins were constructed by plotting the CD signal at 222 nm at a 2.5^{o}C interval between 10 and 87.5^{o}C. Secondary structure analysis was done using CDNN software v2.1 after baseline correction of the obtained spectra (200-260nm).

Intrinsic Tryptophan (Trp) Fluorescence Spectroscopy:

Intrinsic fluorescence spectra were acquired using a Photon Technology International (PTI) spectrofluorometer (Lawrenceville, NJ) equipped with a turreted 4-position peltier-controlled cell holder. The Trp residues in the protein were excited at 295 nm, and the emission spectra were collected from 310 to 400 nm. Light scattering data were also collected at 295 nm using a second detector located at 180^{O} angle to the emission detector. Fluorescence spectra were collected every 2.5^{o}C over a ranger of 10^{o}C and 87.5^{o}C. Peak positions and intensities of the emission spectra were obtained using a mean spectral center of mass method (msm) which overestimates the actual peak positions by about 10 nm.

ANS Fluorescence Spectroscopy:

Unfolding of the protein with increasing temperature was also monitored by fluorescence emission of the extrinsic probe 8-Anilino-1-naphthalene sulfonate (ANS). An optimized 15 molar excess

of ANS was added to the protein solution. The ANS was excited at 375 nm and the emission spectrum was collected from 400-600 nm every 2.5^{o}C over the temperature range of 10 – 87.5^{o}C. Peak intensity of the emission spectra was monitored at 475 nm.

Second Derivation UV Absorbance Spectroscopy:

Changes in the tertiary structure of SP2216 were monitored by second derivation UV absorbance spectroscopy. High resolution absorbance spectra were obtained using an Agilent 8453 UV-Visible absorbance spectrophotometer. Absorbance spectra were recorded from 10 to 90^{o}C at increments of 2.5^{o}C over the wavelength range of 200-400 nm. The second derivative was calculated using a nine-point data filter and third order Savitzky-Golay polynomial with the Chemstation software provided by Agilent. The second derivative data was then imported into origin to calculate peak shifts.

Empirical Phase Diagrams (EPDs):

CD molar ellipticity at 222 nm, intrinsic Trp fluorescence peak intensities and peak shifts, static light scattering and ANS fluorescence peak intensity data sets were used for the construction of the empirical phase diagrams. For SP2216, intrinsic fluorescence spectroscopy could not be used due to the absence of Trp in the protein. Therefore, second derivative UV absorption spectroscopy was used instead for the construction of the phase diagram. A more detailed description of the construction of the phase diagrams can be found in previously published papers. [10-12]

Excipient Screening:

A common buffer consisting of 10 mM sodium acetate, pH 5.5 and 0.067% polysorbate-20 was employed for the excipient screening work. The ionic strength was kept constant at 0.15 with NaCl. In experiments with no NaCl, however, sodium acetate was the sole contributor to the ionic strength lowering the ionic strength significantly.

Intrinsic tryptophan (Trp) fluorescence spectroscopy was used to screen for stabilizers for SP1650 and SP1732 antigens. Circular dichroism spectroscopy was used to screen for stabilizers of SP2216. Fluorescence and CD spectra of each protein in the presence of various GRAS (Generally Regarded as

Safe) excipients were obtained as previously described and thermal melting curves were constructed to determine the melting point (Tm) of each protein in the presence of different excipients. The extent of stabilization by the excipients was measured by their ability to shift the Tm of each protein to higher temperatures compared to protein in the absence of excipient. After stabilizers for all three proteins were identified, studies were performed to optimize their concentrations. Different stabilizers were evaluated in various combinations to determine if any additive or synergistic effects could be obtained for stabilization of the proteins.

Adjuvant Studies:

Experiments in the presence of the adjuvants were conducted by adding Alhydrogel® or Adjuphos® to the protein. The buffer used for the adjuvant studies was 10 mM sodium acetate at pH 5.5, containing 0.067% Tween-20. No sodium chloride was added to decrease the osmolarity of the formulations. Manganese chloride (50 μM) was added to all the formulations due to its impact on the stability of SP1650.

The three protein antigens were first tested separately to determine whether they adsorb preferentially to aluminum hydroxide (Alhydrogel®) or aluminum phosphate (Adjuphos®). This was done by adding 70 μg of protein to 50 μg of adjuvant. The amount of unadsorbed protein was determined by measuring the amount of protein in the supernatant using UV absorbance spectroscopy after centrifugation. An adsorption isotherm was constructed for each of the protein in the presence of 0.25 mg/ml Alhydrogel® at various protein concentrations (0.1 – 0.7 mg/ml at 0.1 unit intervals). Desorption of the proteins from the adjuvants was evaluated in the presence of various concentrations of several desorption agents including sodium chloride, urea, sodium citrate, and guanidine hydrochloride. After suspending the protein-adsorbed adjuvant in the desorption media, the amount of the protein desorbed was measured by UV absorbance spectroscopy after centrifugation.

The thermal stability of the aluminum adjuvant adsorbed protein was assessed by intrinsic fluorescence in the case of SP1650 and SP1732 proteins. The protein (SP1650 or SP1732) was adsorbed

onto Alhydrogel® in a 1 mm cuvette using the procedure described above. The suspension was then allowed to settle for 4 hours. The pellet was then analyzed by intrinsic fluorescence spectroscopy between 10 and 87.5^{o}C at 2.5^{o} intervals. The stability of SP2216 was assessed by FTIR spectroscopy.

FTIR Spectroscopy: FTIR spectra of SP2216 were obtained using a Bruker Tensor-27 FTIR spectrometer (Bruker Optik GmbH, Germany) equipped with a BioATR II cell containing a Zinc Selenide (ZnSe) crystal. The spectra were collected from 4000 to 900 cm^{-1} at temperatures ranging from 10 to 90^{o}C every 2.5^{o}C. Second derivative spectra were calculated using the Savitzky-Golay algorithm. Intensity changes were monitored at 1620 cm^{-1}. Changes at 1620 cm^{-1} are generally associated with vibrations in inter-molecular beta sheet structure that is often prevalent in protein aggregates. [13]

Results

Biophysical Characterization and excipient screening of the three antigens

The biophysical characterization of SP1650 was accomplished using circular dichroism, intrinsic fluorescence, ANS fluorescence spectroscopy, and static light scattering. The data obtained from these methods as a function of pH and temperature are shown in Figure 3.1. Figure 3.1A shows the circular dichroism spectra at various pH values at 10^{o}C. The spectra at pH 4 to 8 display a broad peak with double minima at 208 nm and 222 nm. At pH 3, a significant loss of ellipticity was observed along with the disappearance of the double minima seen at other pH values. CD secondary structure analysis indicated that SP1650 contained approximately 46% α-helices, 26% β sheets and 25% random coil. Figure 3.1B shows the change in circular dichroism signal at 222 nm as a function of temperature for SP1650. Small transitions were seen at about 30^{o}C for SP1650 at pH 3 and 4. At pH 3, another slight transition was observed at about 60^{o}C. At pH 5-8, a sharp decrease in the CD signal was seen at about 50^{o}C. Figure 3.1C shows changes in the tryptophan fluorescence peak position maximum as a function of temperature. At pH 3, a slight transition was again observed at 30^{o}C, with a second transition at about 60^{o}C. SP1650 showed a single transition at about 30^{o}C at pH 4. At pH 5-8, SP1650 displayed a two transition melting

curve, the first of which occurred at about 50^{o}C, followed by a second transition at about 65^{o}C. Figure 3.1D shows the changes in the tryptophan fluorescence peak intensity as a function of temperature. Except for pH 3, which showed no transitions, SP1650 displayed transitions similar to those seen using CD and intrinsic fluorescence spectroscopy. Figure 3.1E shows the changes in ANS intensity as a function of temperature. The ANS intensity at pH 3 is very high even at low temperature, when compared to the other pH values. An increase in intensity was observed at 30^{o}C at pH 4. At the pH values of 5-8, increases in ANS intensity were noticed as early at 45^{o}C. The increase in ANS intensity is thought to correspond to the dye binding to apolar regions of the protein, which are exposed as the protein starts to unfold. Figure 3.1F shows the changes in light scattering intensity. Light scattering was monitored using a second detector 180^{O} to the intrinsic fluorescence detector, and was monitored at 295 nm, which was the incident wavelength used to excite tryptophan residues. No significant increase in light scattering was seen at pH 3. In fact, a slight decrease in scatter intensity was seen for SP1650 at pH 3 at higher temperatures. At pH 4, 5 and 6, an increase in light scattering was observed at 30^{o}C at pH 4, and about 57.5^{o}C at pH 5 and 6. No significant transitions were observed at pH 7 and 8.

An empirical phase diagram (EPD) was constructed using the data shown above (Figure 3.1G). The EPD displays three distinct regions. Region I was identified as the native state of the protein at pH values between 4 and 8 at low temperatures. Based on these data, it appears that SP1650 exists in a conformationally altered state at pH 3 (Region III). Region II was identified as another region at pH values from 4-8 at higher temperatures where the protein was also structurally altered. There appears to be no notable aggregation of the protein at higher temperatures at pH 7-8 (light green), but extensive aggregation at pH 4-6 (darker green).

The EPD suggests that SP1650 is only moderately stable as a function of pH and temperature. In an effort to stabilize the protein further, a library of GRAS excipients were screened to identify potential stabilizers. Figure 3.1H shows the effect of selected compounds on intrinsic fluorescence melts of SP1650. This includes destabilizers such as arginine and histidine, stabilizers such as sorbitol and

dextrose, and excipients that do not affect the stability of the protein such as calcium chloride and dextran-70. The ability of a compound to stabilize SP1650 was measured by its ability to delay the transition seen at about 50^{o}C. The melting temperature (Tm) or the mid-point of the transition was determined by identifying the peak maximum of the first derivative of the melting curve. Table 1 lists the change in Tm of SP1650 for the excipients tested. The concentrations of the most promising stabilizers were then optimized. Stabilizers were also tested in combinations to check for additive or synergistic effects. Table 2 summarizes the changes in Tm of SP1650 at various concentrations of selected excipients, and the Tm of SP1650 for selected excipients tested in combinations are shown in Supplementary Table S1. Manganese chloride and sugars such as sorbitol were shown to best stabilize SP1650. To use the maximum amount of stabilizer, but keep the total solution osmolarity as low as possible, sodium chloride was removed from the formulation buffer.

The biophysical characterization of SP1732 was performed using intrinsic fluorescence, circular dichroism spectroscopy and static light scattering experiments. These data are shown in Figure 3.2A-2E. Extrinsic fluorescence experiments with ANS were not conducted due to the presence of polysorbate-20. Figure 3.2A shows the CD spectra at 10^{o}C for SP1732 at pH values from 3 to 8. No significant differences were seen in the CD spectra for SP1732. Secondary structure analysis of SP1732 CD spectra suggested approximately 82% α-helices, 13% β sheets and 8% random coil. A double minimum was noted at 208 and 222 nm indicative of the presence of alpha helices. Changes in the molar ellipticity at 222 nm as a function of pH and temperature are shown in Figure 3.2B. An increase in CD signal was seen at about 45^{o}C at pH 3, followed by a drastic decrease at about 50^{o}C. The same effect was seen at pH 4 and 5 at about 55^{o}C and 65^{o}C, respectively. The transition in CD signal was seen for pH 6, 7 and 8 only at about 75^{o}C. Figure 3.2C shows the changes in intrinsic fluorescence peak position as a function of pH and temperature. As observed above, the transition at pH 3 starts at lower temperature, near 45^{o}C. This transition was delayed to about 55^{o}C at pH 4, and 65^{o}C at pH 5. At pH 6, 7 and 8 the transition was observed at about 75^{o}C. Very similar trends were noted when analyzing the changes in peak intensity as

well, as shown in Figure 3.2D. Static light scattering data are shown in Figure 3.2E. Similar trends were seen to those described earlier. The formation of protein aggregates was observed at 45^{o}C at pH 3, and at 55^{o}C and 65^{o}C at pH 4 and 5, respectively.

An EPD for SP1732 was constructed using these data (Figure 3.2F). Region I was assigned to the state in which the protein exists in its native form and is most stable. Region III was identified as a region in which large changes in structure occur and aggregation is displayed. In region II, the protein exists in a molten globule-like state, characterized by a loss in the tertiary structure, but maintains the protein's secondary structure. Overall, SP1732 was found to be relatively resistant to changes in pH and temperature. A library of GRAS excipients was screened to determine if any of the compounds were able to further stabilize SP1732. Intrinsic tryptophan fluorescence spectroscopy was again used to screen for potential stabilizers. Candidate stabilizers were selected based on their ability to delay the transition seen at about 72.5^{o}C at pH 6. Due to the incomplete nature of this transition, the onset temperatures of the thermal transitions of SP1732 were used. Supplementary Table S2A lists the transition onset temperatures of SP1732 for all the compounds tested as analyzed by changes in the fluorescence emission peak position and intensity. Sugars such as sucrose, dextrose, and lactose showed a stabilizing effect, whereas, compounds such as cyclodextrins and malic acid produced a destabilizing effect. Selected stabilizers were tested in different concentrations to see if lower amounts of stabilizer were sufficient to stabilize the protein while lowering the osmolarity of the formulations. The effect of excipient concentration on the transition onset temperature of SP1732 is shown in Supplementary Table S2B. The most promising stabilizers were also tested in combinations to check for additive/synergistic effects and these results are shown in Supplementary Table S2C.

The protein SP2216 was characterized in a similar manner using multiple biophysical techniques. Due to the absence of tryptophan residues in the protein, intrinsic fluorescence spectroscopy could not be used. Instead, second derivative UV absorbance spectroscopy was employed, in addition to circular dichroism, extrinsic fluorescence spectroscopy and light scattering methods. Figure 3.3A shows the CD

spectra of SP2216 at different pH values at 10°C. Again, a double minimum was seen at about 208 nm and 222 nm, characteristic of alpha helices. The signal did not vary significantly with changes in pH. CD secondary structure analysis of SP2216 implied that the protein contained roughly 28% α-helices, 38% β sheet, and 38% random coil. Figure 3.3B shows the changes in CD signal at 222 nm as a function of increasing temperature. At all pH values, significant loss in negative ellipticity was evident with transitions initiating at about 15-20°C indicating that SP2216 is an extremely thermolabile protein. The CD melt results suggest that the protein is slightly more thermally stable at about pH 5 and 6 compared to other pH values, based on onset temperatures. Figure 3.3C shows data from static light scattering studies. No significant increase in light scattering intensity was observed at pH values of 6, 7 and 8. At lower pH values, however, significant increase in scattering was observed at about 45°C, indicating aggregation of the protein. At pH 3, the protein displayed the maximum increase in scattering. Figure 3.3D shows the changes in ANS intensity as a function of temperature for SP2216 at the various pH values. It should be noted that the ANS intensity was found to be elevated at 10°C at all pH values examined indicating some level of binding of the dye even at low temperature. Based on the ANS studies, the SP2216 protein was found to be relatively more stable at pH 5 than other pH values with its transition starting at about 35°C. Data obtained from 2nd derivative UV absorbance spectroscopy is shown in Figure 3.3E. The thermal melts show the second derivative peak shifts at 284 nm as a function of pH and temperature. These shifts arise from changes in the environment around the tyrosine residues as the protein unfolds with increasing temperature. The 2nd derivative peak shifts again confirmed that SP2216 displayed changes in its tertiary structure at the relatively low temperatures of about 20-30°C. SP2216 was again found to be relatively more stable at pH 5 by 2nd derivative UV absorbance spectroscopy with the transition starting at about 30°C. At pH 3, SP2216 did not display any detectable transitions. At all other pH values, SP2216 displayed transitions at temperatures ranging from 20-30°C.

The EPD for SP2216 was then constructed using the biophysical data discussed above as shown in Figure 3.3F. The EPD can be divided into three unique structural regions. Region I from pH 5 to 8 at

low temperatures is the region where the protein presumably exists in its native conformation. Increases in temperature at these pH values (region II in the phase diagram) lead to conformational changes in the protein as evidenced by changes in circular dichroism and fluorescence spectra. Region III comprises the pH 3 and 4 states at all temperatures where protein is thermally very labile and is in a variety of non-native aggregation-prone states. Overall, SP2216 was found to be very sensitive to temperature, with changes in structure occurring at room temperature. A library of GRAS excipients was screened using circular dichroism spectroscopy to identify stabilizers. Supplementary Table S3A lists the excipients that were tested along with the Tm and change in Tm for the protein. Sugars and sugar alcohols such as sucrose and sorbitol stabilized SP2216 with an increase in Tm of about 10^{o}C at concentrations of 20% (w/v). Arginine and guanidine were both found to destabilize the protein. Concentration studies revealed a progressive increase in Tm values of SP2216 with increasing concentrations, as shown in Supplementary Table S3B. The effect of using combinations of selected excipients on the Tm of SP2216 is shown in Supplementary Table S3C.

For ease of comparison, Table 3 lists the effect of selected stabilizers and destabilizers on the thermal unfolding temperature (Tm) of each of the three protein antigens. Sugars and sugar alcohols, for example such as sucrose and sorbitol, showed stabilizing effects on the conformational stability of all three proteins. In contrast, additives such as arginine, dextran sulfate, diethanolamine and guanidine destabilized one or more of the three proteins. Interestingly, sodium citrate was able to stabilize SP1650, but not SP1732 and SP2216.

Adjuvant Studies

The binding of all three antigens, SP1650, SP1732 and SP2216 to two different aluminum salt adjuvants, Alhydrogel and Adjuphos, was studied individually. 10 mM sodium acetate buffer at pH 5.5 was used for all the adjuvant studies. Each of the proteins was found to bind preferably to Alhydrogel, with nearly complete binding. Figure 3.4 shows the percent protein bound in the presence of Alhydrogel

and Adjuphos. When 70 μg of each antigen was added to 50 μg of Alhydrogel, over 90% of each antigen was found to rapidly bind (in less than a minute). When added to Adjuphos, however, only 50-60% of the protein was found to be bound. With an isoelectric point (pI) of ~5.1, SP1650 has a slight negative charge at pH 5.5, and hence binds to the positively charged Alhydrogel. SP2216 has a pI of ~5.3, and SP1732 has a pI of ~6.0. Both of these latter proteins thus have low or minimal total negative charge at pH 5.5. Their binding to Alhydrogel may be at least partially due to interactions other than simple electrostatic contacts. Figure 3.5 shows that Alhydrogel demonstrated a high adsorption capacity for all three proteins. 50 μg of Alhydrogel was able to adsorb up to 90 μg of SP1650, SP1732 and SP2216. The anticipated dose in the final vaccine formulation is 600 μg of Alhydrogel with 50 μg of each antigen.

Desorption of each of the absorbed proteins from the surface of the aluminum salt adjuvant was studied in the presence of various agents such as urea, citrate, guanidine hydrochloride, and NaCl. Solutions containing 2M NaCl or 2M urea were not able to desorb significant amounts of protein from the adjuvant. The combination of 2M urea and 1M sodium citrate, however, was able to desorb about 80% of SP1650 from Alhydrogel. This solution, however, was able to desorb only 10-15% of protein in the case of SP1732 and SP2216. A solution containing 2M Guanidine was able to desorb over 80% of SP1732 and SP2216 from Alhydrogel, however, it was unable to desorb significant amounts of SP1650 from the adjuvant. Figure 3.10 shows the amount of protein desorbed. In summary, the protein antigens SP1732 and SP2216 were best desorbed from Alhydrogel using 2M Guanidine, and SP1650 was desorbed using a solution containing 1M sodium citrate and 2M urea.

The conformational stability of SP1650 and SP1732 on the surface of the aluminum salt adjuvant was assessed by intrinsic fluorescence spectroscopy. The position of the emission peak maxima was monitored as a function of temperature. Protein (200 μg/ml) was added to Alhydrogel® (0.5 mg/ml) by the procedure described above, which ensures >90% bound protein. Figure 3.6 shows the melting curve for SP1650 in solution and while adsorbed to the adjuvant surface. In solution, SP1650 shows a transition at about 70^{o}C in the presence of 5% sorbitol and 50 μM $MnCl_2$. When adsorbed onto the adjuvant, the

SP1650 thermal transition initiates much earlier, showing some peak shifts above 30^{o}C. The decrease in stability of the protein on the adjuvant surface was not modified by the addition of previously identified stabilizers. The effect of the addition of sodium phosphate on the stability of the adsorbed SP1650 protein is also shown in Figure 3.6. The addition of as little as 5 mM sodium phosphate was able to delay the transition to about 55^{o}C. When proteins are adsorbed on to Alhydrogel, they are frequently, although not always, destabilized. In contrast, the SP1732 protein was found to be more stable on the surface of the adjuvant. Figure 3.7 shows the intrinsic fluorescence melting curves for SP1732 in solution, and while adsorbed onto the adjuvant. The differences seen in the peak positions probably arise from the nature of the data analysis. The msm method, used to calculate the position of the emission peak maxima, overestimates the peak position by about 8-12 nm. The true emission peak maxima for SP1732 is the same in solution and while adsorbed on the adjuvant, as shown in the representative intrinsic fluorescence spectra of SP1732 at 10^{o}C in solution and bound to the adjuvant in Figure 3.8. No significant differences were seen in the stability of SP1732 upon addition of stabilizers or sodium phosphate.

The stability of SP2216 while adsorbed to Alhydrogel was analyzed by alternative methods other than fluorescence spectroscopy due to the absence of an intrinsic fluorophore. FTIR was employed to access the stability of SP2216 on the surface of the adjuvant. Figure 3.9 shows the second derivative FTIR peak intensity changes at 1620 cm^{-1} as function of temperature. In solution, a small transition is seen at about 40^{o}C. The increase in intensity at 1620 cm^{-1} at 40^{o}C may hint at the formation of intermolecular beta sheets (i.e., protein aggregation). Representative second derivative FTIR spectra of SP2216 at different temperatures are shown in Figure 3.11. In addition to the increasing intensity of the negative peak at 1620cm^{-1}, a decrease in intensity of the peak at 1650cm^{-1}was also observed. Analyses at these wavelengths which reflect α-helical and β-sheet content revealed transitions initiating at similar temperatures as shown in Figure 3.9 (data not shown). When SP2216 is adsorbed to Alhydrogel, the intensity of the thermal transition is lowered, but the structural transition initiates at about the same temperature. The increase in intensity seen may be explained by slight concentration differences or better

packing of the adjuvant on the bioATR II crystal. This result suggests that the adsorption of the SP2216 protein on Alhydrogel does not have a major effect on its stability. The thermal transition of SP2216 adsorbed on the Alhydrogel surface does not seem to be affected by previously identified excipients that stabilized the protein in solution.

Discussion

The structural integrity and conformational stability of three candidate vaccine protein antigens, SP1650, SP2216 and SP1732, were separately characterized in solution using several biophysical techniques and stabilizers were identified for each protein. The stability of the three antigens was then further characterized in the presence of the Alhydrogel aluminum hydroxide adjuvant. Techniques including intrinsic fluorescence, circular dichroism spectroscopy, and light scattering were used to monitor changes in the secondary and tertiary structure, and aggregation state of the three antigens as a function of pH and temperature. The complete data sets obtained using the various spectroscopic methods for each of the three proteins were combined in the form of EPDs to better visualize the data. SP1650 showed transition that represented changes at various levels of structure at about 55^{o}C. SP2216 proved to be a very unstable protein manifesting changes in its conformation even at room temperature. In contrast, SP1732 was seen to be very stable with little to no transition seen until about 70^{o}C. Since SP1732 showed maximum stability at pH 5-6, and the other two antigens were stable in this pH range as well, the three antigens were formulated at pH 5.5 in a sodium acetate buffer. Excipient screening from a library of over 30 compounds revealed sorbitol, trehalose, lactose and sucrose as possible stabilizers for each of the three proteins. These sugars and sugar alcohols probably stabilize the three proteins in solution by the well documented mechanism of preferential hydration.[14-16] Sodium chloride did not seem to have a significant effect on the physical stability of any of the three proteins; therefore, it was removed from the formulations to lower the osmolarity of the solution. The addition of 50 µM manganese chloride produced a dramatic increase in the stability of SP1650, so it was also included. Experiments with lower concentrations of manganese were not conducted. It may thus be possible to obtain a similar degree of stabilization by using the lower

concentrations of manganese. Additionally, zinc may also be evaluated in the future since the SP1650 protein also binds to zinc as well as manganese.[17]

Subunit vaccines are usually insufficiently immunogenic by themselves and therefore require an adjuvant. Common aluminum salt adjuvants such as Alhydrogel and Adjuphos are thought to be most effective with the antigen adsorbed on to the adjuvant surface, although this has been disputed and their mechanism of immunopotentiation is still under active investigation. [18-23] Alhydrogel demonstrated excellent binding properties to each of the three antigens. The addition of NaCl was not sufficient to desorb the protein from the surface of the adjuvant hinting that mechanisms other than simple electrostatic interactions may be at play. All of the proteins were tested for desorption using various agents after 30 minutes of adsorption. The differences in the desorption patterns are presumably due to the differences in structural characteristics of the three proteins. It is usually more difficult to desorb proteins if they are allowed to adsorb to the adjuvant for longer periods of time due to structural transitions as the bound proteins optimize their interactions with the surface. A common desorbing agent was not found for all the three proteins. This result could, in the future, pose some analytical difficulties while studying antigenicity or chemical degradation of the adsorbed antigens, although combinations of the agents found for the individual antigens might be effective. The conformational stability of the adsorbed antigens was studied using intrinsic fluorescence spectroscopy and fourier transform infrared spectroscopy. Tryptophan fluorescence spectroscopy revealed changes in tertiary structure, whereas infrared spectroscopy found alterations in protein secondary structure. Several earlier studies have shown that the protein antigens are often destabilized when adsorbed onto the adjuvant.[21,24,25] In this work, SP1650 was found to be dramatically destabilized when adsorbed to Alhydrogel as seen by the lowering in the onset temperature of the protein's structural transitions. This destabilizing effect was countered by the addition of 5 mM phosphate, which presumably converts some of the aluminum hydroxide to aluminum phosphate and thereby lowering the surface pH.[26] The high surface pH of aluminum hydroxide may induce instability of the adsorbed proteins. The addition of 5 mM phosphate did not affect the

adsorption of the three antigens to Alhydrogel, although higher phosphate concentrations resulted in major losses in binding (data not shown). In contrast, SP1732 was stabilized on the surface of the adjuvant. The thermal transition that initiates at about 70^{o}C for SP1732 in solution does not occur while it is adsorbed to the adjuvant. FTIR was used to study the stability of SP2216 while adsorbed to the Alhydrogel due to the absence of intrinsic fluorescence. Changes in the second derivative peak intensity at 1620 cm^{-1} were monitored as a function of temperature. These changes presumably reflect alterations in the intermolecular beta sheet content of the protein. No significant changes in the stability of SP2216 were observed when the protein was adsorbed to Alhydrogel. This effect might not be observed, however, if the protein structure was analyzed using a technique sensitive to changes in the tertiary structure of the protein.

One potential concern in the development of the trivalent vaccine is the instability of SP2216 protein component. Alterations in this protein antigen's structural integrity were observed as initiating at room temperature. Although several stabilizers were identified that improve the stability of the protein, given the relative instability of SP2216, there could be some benefit in removing this protein from the vaccine from a long term storage stability point of view. At this stage in development, however, SP2216 is still included in the vaccine for examination in initial animal studies due to the degree of the conservation of the protein (~100%) in the different serotypes of S. pneumoniae. This potential utility of this antigen is especially important given the wide serotype variation in the developing world.

In conclusion, candidate formulations of a trivalent recombinant protein vaccine containing aluminum hydroxide adjuvant for protection against *S. pneumoniae* were identified based on a series of preformulation characterization studies as described above. Additives such as sorbitol, sucrose, and trehalose were observed to be good stabilizers for the three antigens at concentrations of 5-15% (w/v). The addition of 50 μM manganese also showed a large increase in physical stability of SP1650. The addition of 5 mM phosphate greatly improved the physical stability of SP1650 on the adjuvant surface and may also help protect the proteins from deamidation, since proteins have been known to undergo

deamidation while adsorbed onto the surface of Alhydrogel due to the high local pH.[26] The next stage of this vaccine formulation development work will require evaluation of immunogenicity data and chemical degradation studies during long term stability studies. A new set of analytical and stability problems will be encountered when the three proteins are actually combined together into a single trivalent vaccine. In particular, the possibility of interaction among the proteins will need to be critically examined. In the combination vaccine, it may be possible to separate the antigens and examine them individually, but analytical methods to test each of the protein antigens in the actual trivalent vaccine still need to be developed. In addition, although aluminum salt adjuvants are the most commonly used adjuvants in current vaccines, additional or alternative adjuvants should be considered in the future to enhance both humoral and cellular immunity.

References

1. Williams WW, Hickson MA, Kane MA, Kendal AP, Spika JS, Hinman AR 1988. Immunization policies and vaccine coverage among adults. The risk for missed opportunities. Ann Intern Med 108(4):616-625.
2. centre WM. 2011. WHO - Pnuemonia Factsheet. ed.
3. Wardlaw TMJ, Emily White; Hodge, Matthew;. 2006. Pneumonia: the forgotten killer of children. ed. p 40.
4. Steven Black JE, Cynthia Whitney, Henry Shinefield. 2008. Pneumococcal conjugate vaccine and pneumococcal common protein vaccines. Vaccines, 4 ed.: Saunders. p 531-567.
5. Girard MP, Cherian T, Pervikov Y, Kieny MP 2005. A review of vaccine research and development: human acute respiratory infections. Vaccine 23(50):5708-5724.
6. Lisa A. Jackson KMN. 2008. Pneumococcal polysaccharide vaccines. Vaccines, ed.: Saunders Elsevier. p 569-604.
7. Black SB, Shinefield HR, Ling S, Hansen J, Fireman B, Spring D, Noyes J, Lewis E, Ray P, Lee J, Hackell J 2002. Effectiveness of heptavalent pneumococcal conjugate vaccine in children younger than five years of age for prevention of pneumonia. The Pediatric infectious disease journal 21(9):810-815.
8. Grijalva CG, Nuorti JP, Arbogast PG, Martin SW, Edwards KM, Griffin MR 2007. Decline in pneumonia admissions after routine childhood immunisation with pneumococcal conjugate vaccine in the USA: a time-series analysis. Lancet 369(9568):1179-1186.
9. Giefing C, Meinke AL, Hanner M, Henics T, Bui MD, Gelbmann D, Lundberg U, Senn BM, Schunn M, Habel A, Henriques-Normark B, Ortqvist A, Kalin M, von Gabain A, Nagy E 2008. Discovery of a novel class of highly conserved vaccine antigens using genomic scale antigenic fingerprinting of pneumococcus with human antibodies. The Journal of experimental medicine 205(1):117-131.
10. Fan H, Ralston J, Dibiase M, Faulkner E, Middaugh CR 2005. Solution behavior of IFN-beta-1a: an empirical phase diagram based approach. Journal of pharmaceutical sciences 94(9):1893-1911.
11. Kueltzo LA, Ersoy B, Ralston JP, Middaugh CR 2003. Derivative absorbance spectroscopy and protein phase diagrams as tools for comprehensive protein characterization: a bGCSF case study. Journal of pharmaceutical sciences 92(9):1805-1820.
12. Maddux NR, Joshi SB, Volkin DB, Ralston JP, Middaugh CR 2011. Multidimensional methods for the formulation of biopharmaceuticals and vaccines. Journal of pharmaceutical sciences.
13. Vonhoff S, Condliffe J, Schiffter H 2010. Implementation of an FTIR calibration curve for fast and objective determination of changes in protein secondary structure during formulation development. Journal of pharmaceutical and biomedical analysis 51(1):39-45.
14. Lee JC, Timasheff SN 1981. The stabilization of proteins by sucrose. J Biol Chem 256(14):7193-7201.
15. Shimizu S, Smith DJ 2004. Preferential hydration and the exclusion of cosolvents from protein surfaces. J Chem Phys 121(2):1148-1154.
16. Uedaira H 2001. Role of hydration of polyhydroxy compounds in biological systems. Cell Mol Biol (Noisy-le-grand) 47(5):823-829.
17. Rosch JW, Gao G, Ridout G, Wang YD, Tuomanen EI 2009. Role of the manganese efflux system mntE for signalling and pathogenesis in Streptococcus pneumoniae. Molecular microbiology 72(1):12-25.
18. Coffman RL, Sher A, Seder RA Vaccine adjuvants: putting innate immunity to work. Immunity 33(4):492-503.
19. Flach TL, Ng G, Hari A, Desrosiers MD, Zhang P, Ward SM, Seamone ME, Vilaysane A, Mucsi AD, Fong Y, Prenner E, Ling CC, Tschopp J, Muruve DA, Amrein MW, Shi Y Alum interaction with dendritic cell membrane lipids is essential for its adjuvanticity. Nat Med 17(4):479-487.

20. Glenny AT, Buttle GAH, Stevens MF 1931. Rate of disappearance of diphtheria toxoid injected into rabbits and guinea - pigs: Toxoid precipitated with alum. The Journal of Pathology and Bacteriology 34(2):267-275.
21. Jones LS, Peek LJ, Power J, Markham A, Yazzie B, Middaugh CR 2005. Effects of adsorption to aluminum salt adjuvants on the structure and stability of model protein antigens. J Biol Chem 280(14):13406-13414.
22. Leroux-Roels G Unmet needs in modern vaccinology: adjuvants to improve the immune response. Vaccine 28 Suppl 3:C25-36.
23. Noe SM, Green MA, HogenEsch H, Hem SL Mechanism of immunopotentiation by aluminum-containing adjuvants elucidated by the relationship between antigen retention at the inoculation site and the immune response. Vaccine 28(20):3588-3594.
24. Iyer V, Liyanage M, Shoji Y, Chichester J, Jones M, Yusibov V, Joshi S, Middaugh CR 2012. Formulation development of a plant-derived h1n1 influenza vaccine containing purified recombinant hemagglutinin antigen. Human Vaccines 8(4).
25. Peek LJ, Martin TT, Elk Nation C, Pegram SA, Middaugh CR 2007. Effects of stabilizers on the destabilization of proteins upon adsorption to aluminum salt adjuvants. Journal of pharmaceutical sciences 96(3):547-557.
26. Wittayanukulluk A, Jiang D, Regnier FE, Hem SL 2004. Effect of microenvironment pH of aluminum hydroxide adjuvant on the chemical stability of adsorbed antigen. Vaccine 22(9-10):1172-1176.

Chapter 4

Preformulation Development of a Multivalent Canine Vaccine Consisting of Three Live Attenuated Viruses

Introduction

Vaccines are widely used in animals to prevent many kinds of diseases. Most of these vaccines were developed and stabilized empirically. Apart from a few exceptions such as the vaccines for rabies and lyme disease, newer technologies such as recombinantly produced proteins have not yet significantly penetrated the veterinary vaccine market.[1] The most common vaccines used in veterinary medicine are based on live attenuated viruses and bacteria, due to their cost effectiveness, high immunogenicity and efficacy. Live attenuated viral strains, however, are not very stable during storage, resulting in short shelf lives as well as loss of potency when exposed to high temperatures.[2] Due to severe requirements to minimize costs of veterinary vaccines, most viral vaccines are not fully characterized from a formulation point of view. The addition of certain low-cost stabilizers might be able to increase the stability of the viral components and thereby significantly increase the shelf life of such vaccines.

A vaccine against three viruses that pose a serious threat to dogs and other animals is employed. These are the attenuated forms of the canine distemper virus (CDV), canine parainfluenza virus (CPI), and canine adeno virus type 2 (CAV2). Canine distemper is caused by the canine distemper virus, which is a paramyxovirus and is closely related to the measles virus.[1,10,11] It is a highly contagious disease observed in dogs and other wildlife worldwide. Apart from dogs, the virus has been known to infect wolves, ferrets, and skunks among others[10]. Prior studies on the distemper virus indicate it to be very thermo-labile with over 50% loss in infectivity within 2 days of exposure to room temperatures[12]. The canine parainfluenza virus is another paramyxoviridae, and is a major cause of lower respiratory infection in dogs. Canine adenovirus type 2 is a non-enveloped virus and is thought it be a potential cause of kennel cough. The combination vaccine, DA2PPC, is currently a core vaccine for dogs administered at 8 weeks of age, with booster doses every year. DA2PPC is effective against the distemper, adenovirus type 2, parvovirus, parainfluenza virus and the canine corona virus.

This work describes a simple cost effective empirical phase diagram-based approach towards the preformulation development of a trivalent live attenuated viral vaccine using biophysical techniques.[3-9]

The empirical phase diagram approach described in this paper has been successfully applied to the preformulation development of therapeutic proteins and vaccines, including antibodies, subunit proteins, viruses, and bacteria.[3-9] The unique feature of this work is the demonstration that a multicomponent vaccine can be separated into its individual antigens, each stabilized and common stabilizers identified which should be effective in the multivalent vaccine.

Materials and Methods

Frozen cell lysates containing the individual viruses, CDV, CPI and CAV2 were received from Merck Animal Health Inc. (Elkhorn, NE). The concentrations of the viruses after purification were determined using a BCA assay. All reagents used in this assay were purchased from Thermo Scientific (Rockford, IL). Citrate-phosphate (20 mM) buffers (pH 5.5, 6.0, 6.5, 7.0, 7.5 and 8.0) at a total ionic strength of 0.15 (adjusted with NaCl) were prepared using citric acid monohydrate (Fisher, Pittsburgh, PA) and sodium phosphate dibasic, anhydrous (Sigma, St. Louis, MO). All excipients were purchased from Sigma (St. Louis, MO) and were analytical grade.

Purification

Purification of Canine Distemper Virus (CDV)

The cell culture medium containing the virus was thawed for 24-36 hours at 4 ^{o}C. The medium was then centrifuged twice at 5,000xg for 20 minutes to pellet particulate matter and cell debris in a bench top centrifuge (Thermo Electron, Model: C5LR). The supernatant was then centrifuged at 40,000xg for two hours to pellet the virus using a Beckman Coulter Optimax ultracentrifuge equipped with a MLA-80 fixed angle rotor. The viral pellet was washed twice and re-suspended in a minimal amount of 20 mM citrate phosphate (CP) buffer containing 2.7% sucrose, pH 7 (I = 0.15). The solution was then filtered using a 0.4 μm filter to remove any remaining viral aggregates that may have formed during the purification process.

The purified virus solution was then stored at 4 ^{o}C. All experiments were conducted within two days due to the instability of the virus.

Purification of Canine Parainfluenza Virus (CPI)

The purification process for the canine parainfluenza virus (CPI) is similar to that for CDV. The cell culture medium was first subjected to same procedures as described above for the CDV. In addition, the filtered viral solution obtained is subjected to further purification using sucrose gradient centrifugation of 20-50% (w/v) in 5% increments. Five hundred μL of each layer were added slowly to maintain the gradient. The filtered viral solution was added to the top of the gradient, which was centrifuged at 40,000xg for 17 hours at 4^{o}C (Beckman Coulter OptimaMax Ultracentrifuge, MLS-50 swinging bucket rotor). The 35-45% sucrose fractions were found to contain a majority of the viral material and were washed with ~10 mL of cold buffer and the virus was pelleted by centrifugation at 40,000xg for 3 hours at 4^{o}C. The pellet was then re-suspended in a minimal amount of buffer to concentrate the viral material. The resulting viral solution was dialyzed against 20 mM CP buffer to remove any trace amount of sucrose.

Purification of Canine Adeno Virus (CAV2)

The cell lysate containing CAV2 was centrifuged at 5,000xg for 25 min at 4 °C. The supernatant was separated and ammonium sulfate was added to the supernatant gradually until 40% saturation was reached. This was followed by a 2 hour incubation period. Precipitated virus samples were separated from the supernatant by centrifuging at 5,000xg for 25 min at 4 °C. The virus precipitate was then reconstituted and dialyzed against 20 mM CP buffer.

Transmission Electron Microscopy (TEM)

Electron microscopy imaging of uranyl acetate-stained virus samples was performed to analyze potential visible structural alterations as a result of the purification process. The virus samples were

subjected to the purification procedures described above and submitted to the Microscopy and Analytical Imaging Lab at the University of Kansas for TEM imaging. The virus samples were subject to negative staining with uranyl acetate and imaging of the samples was performed with a Tecnai G^2 transmission electron microscope (FEI Company, Hillsboro, OR).

SDS-PAGE and Western blot

Virus samples were boiled for 10 minutes in sample buffer containing β-mercaptoethanol before loading onto the 4-12% precast gel (Invitrogen). 20 µL of virus sample was loaded in each well. A 150 V constant voltage was then passed through the gel until the bromophenol blue line marker reached the bottom of the gel. The resulting gel was then stained overnight using 0.1% Coomassie brilliant blue in 10% glacial acetic acid solution. Destaining of the gel was then performed in a solution containing 10% methanol and 7% glacial acetic acid. Silver stain was used in the case of the canine distemper and canine parainfluenza viruses using a silver stain kit (Sigma Aldrich), and the standard protocol was followed. Western blots were performed to test for antigenic peptides from the canine distemper virus. Separated proteins in the gels were transferred to a nitrocellulose membrane electrophoretically at 100 V for 1 hour. The blotted membrane was then washed overnight at 4^oC with the transfer buffer containing 5% milk and 0.1% tween (w/v) to ensure no stray proteins adhere to the membrane. The membrane was then treated with the primary antibody, which was raised against the distemper virus in goats (Merck Animal Health Inc., Elkhorn, NE) for 2 hours at room temperature. The membrane was then washed with the transfer buffer containing 0.1% tween-20 for 5 minutes three times. The bound antibodies were then detected by horseradish peroxidase-conjugated anti-goat secondary antibody (Sigma Aldrich) treated with the 1-Step TMB blotting substrate solution (Thermo scientific). Adequate antibodies were not available for Western blot analysis of the other two viruses.

Dynamic Light Scattering

The hydrodynamic diameter of the three viruses was analyzed using a Dynapro dynamic light scattering instrument (Wyatt Technology, Santa Barbara, CA)). The hydrodynamic diameter was

calculated from the diffusion coefficient by the Stokes-Einstein equation using the method of cumulants (intensity based). The temperature was maintained at 20^{o}C and the pH at 7. Viscosity of the buffer was measured using a SVM-3000 Stabinger viscometer (Anton-Paar, Austria) and the DLS data was corrected for the viscosity as needed.

Biophysical Characterization

Far-UV Circular Dichroism (CD) Spectroscopy

CD spectra were acquired using a Jasco J-810 spectropolarimeter equipped with a 6-position peltier temperature controlled sample cell holder. CD spectra were obtained from 260-190 nm. Melting curves of the proteins were constructed by plotting the CD signal at 222 nm at a 2.5 ^{o}C interval between 10 and 87.5 ^{o}C. In the excipient screening experiments, an Applied Photophysics Chirascan Plus spectropolarimeter (Leatherhead, UK) was employed to obtain the CD spectra. Experimental parameters such as the temperature range and interval times remained the same.

Intrinsic Tryptophan (Trp) Fluorescence Spectroscopy and static light scattering

Intrinsic fluorescence spectra were acquired using a Photon Technology International (PTI) spectrofluorometer (Lawrenceville, NJ) equipped with a turreted 4-position peltier-controlled cell holder. The Trp residues in the various viral proteins were excited at 295 nm, and the emission spectra were collected from 310 to 400 nm. Light scattering data were also collected at 295 nm using a second detector located at a 180^{o} angle to the emission detector. Fluorescence spectra was collected every 2.5 ^{o}C from 10 ^{o}C to 87.5 ^{o}C. Using Microcal Origin 7 software, peak positions and intensities of the emission spectra were obtained using a mean spectral center of mass method (msm) that shifts the actual peak positions by approximately 10-12 nm to the red, but produces better S/N ratios.

Empirical Phase Diagrams (EPDs)

CD molar ellipticity at 222 nm, intrinsic Trp fluorescence peak shifts, and static light scattering data sets were used in the construction of the empirical phase diagrams. Briefly, two indexes were constructed corresponding to the tertiary and secondary structures of the viral proteins. A third index was

constructed based on the aggregation propensity of the viral particles. These three indexes were reduced to RGB values and mapped as a function of pH and temperature to obtain the phase diagrams. Red represents the CD data, green the intrinsic fluorescence data and blue represents the protein association (aggregation) data. In addition, data obtained from the different measurements were normalized to account from slight differences in concentration of the virus, which arise from the different batches of purification.

Excipient Screening

Aggregation Assay (CAV2 and CDV)

Since CAV2 and CDV were both prone to aggregation in solution at elevated temperatures (see results section), an aggregation assay was used for high throughput screening of potential stabilizers for these two live viruses. A library of GRAS (Generally Regarded As Safe) compounds was screened for their ability to inhibit the aggregation propensity of the two viruses. The aggregation was monitored by optical density measurements at 350 nm using a 96-well plate reader (Spectra Max M5, Molecular Devices, Sunnyvale, CA). The aggregation assay was performed at 55 °C (at a concentration of 0.2 mg/ml for CAV2 and 0.5 mg/ml for CDV) in CP buffer. These conditions were selected based upon the apparent phase boundaries observed in the empirical phase diagrams. Virus sample was added to wells containing excipient(s) at the selected pH and incubated at 55 °C for 90 min for CAV2 and 180 minutes for CDV. The optical density was monitored at 350 nm (OD350) every 2 minutes. Samples of virus and buffer with excipient(s) (blanks) were examined simultaneously and served as controls. The measurements were corrected for intrinsic buffer-excipient effects by subtracting values of the blanks prior to data analysis. Each sample was evaluated in triplicate. Percent inhibition of aggregation was calculated employing the following expression:

$$\% \text{ inhibition of aggregation} = 100 - \left[\frac{\Delta OD_{350}\,(E)}{\Delta OD_{350}\,(C)} * 100 \right]$$

where ΔOD350 (E) represents the change in OD350 during heating of the virus containing solution in the presence of the excipient and ΔOD350 (C) is the change in OD350 during heating of virus solution without excipient.

Structural Stability Assay

Compounds which effectively inhibited aggregation of CDV and CAV2 were further investigated for their ability to protect and/or enhance the structural stability of the viruses. The structural stability of the viruses in the presence and absence of selected excipients was monitored by CD (thermal melts at 222 nm) spectroscopy. Combinations of excipients at different concentrations were also studied for their ability to stabilize secondary structure of the viral proteins (CD) and to inhibit aggregation (OD350) at pH 7.0.

CPI Virus Excipient Screening

The CPI virus did not aggregate in solution at elevated temperatures; therefore, the aggregation assay described above was not performed. Instead, intrinsic tryptophan fluorescence peak position measurements were used as an indication of any stabilization effects. 26 GRAS compounds in several variations of concentration and combinations were screened for their ability to increase the melting temperature of the CPI virus at 0.1 mg/mL. The excipients were dissolved in the working buffer (20 mM CP buffer, I = 0.15 (NaCl), 2.71% sucrose, pH 7.0). The working buffer for excipient screening was chosen on the basis of the apparent phase boundaries observed in the empirical phase diagrams and further experimental work.

Excipients effective for all three purified viruses were tested in combination once initial screening studies were completed. A first derivative method using Microcal Origin 7.0 software was used to determine the transition melt temperature (Tm) of the virus in the presence of the different stabilizers. All measurements were made within one week of thawing the purified sample to prevent aggregation of the virus over time.

Results

Each of the three viruses was purified to obtain samples for biophysical characterization and stability assessment. The purified viral samples were first tested using electron microscopy, SDS-PAGE and western blot analysis to confirm the presence of intact viral material after purification. Figures 4.1A, 4.1D and 4.2 outline the data obtained for the canine distemper virus (CDV). Figure 4.1A shows an TEM image of virus particles of about 100-150 nm in diameter, similar to images previously published.[13] Figure 4.1D shows the SDS-PAGE data for the crudely purified virus. The canine distemper virus consists of 7 proteins. The L (180kDa), H (80kDa) and P (70 kDa) proteins as well as the fusion proteins F_0 and F_1 (60 and 40 kDa), N (60 kDa), the Matrix (37kDa) and S proteins (15 kDa) were all present and their size correlates well with that observed in previous studies.[14,15] Several additional bands were also observed, which suggests that not all impurities were removed using the purification process described above. Western blots were used to confirm the presence of antigenic canine distemper proteins using an antibody raised against the distemper virus. The western blot showed 2 bands corresponding to the matrix protein and another at 60 kDa, corresponding to the fusion protein F_0 or the N protein (data not shown).

Dynamic light scattering measurements showed an average diameter of approximately 200 nm for the CDV samples at pH 7. Figure 4.2A shows the circular dichroism spectrum of the distemper virus at 10 ^{o}C and pH 7. A major negative peak was observed at about 208 nm, with a shoulder near 220 nm, hinting at the presence of some α-helical structures in the viral proteins. Figure 4.2B shows the effect of temperature on the CD signal at 222 nm. Although no sharp structural transitions were seen at any of pH

conditions (5.5-8.0), a gradual transition, initiating at about 20 ^{o}C, is observed at all pH values. Figure 4.2C shows the effect of temperature on the position of the fluorescence peak maxima of the viral proteins as a function of temperature. Broad transitions are seen at most pH values, except at pH 8 where a sharper transition initiates at about 50 ^{o}C. Changes in the emission peak maxima presumably reflect changes in the micro environment of the intrinsic (Trp) fluorophores, which in this case are the tryptophan residues in the various viral proteins. A red shift in the intrinsic fluorescence peak position maxima generally indicates the exposure of the apolar Trp residues to a more polar environment suggesting at least partial unfolding of the molecule (Figure 4.2C). Figure 4.2D shows the effect of temperature on the static light scattering intensity at different pH values. An initial decrease in the light scattering intensity was observed until 30 ^{o}C, followed by an increase in scattering intensity. The increase in the scatter intensity at about 35 ^{o}C is consistent with limited aggregation of the virus.

The purification and biophysical characterization data for the canine parainfluenza virus are shown in Figures 4.1B, 4.1E and Figure 4.3, respectively. Figure 1B shows a TEM image of several intact CPI virions and their nucleocapsids. The 35% fraction from the sucrose gradient was run on an SDS-PAGE gel (Figure 4.1E). This gel was compared to that of the human parainfluenza virus, due to lack of prior literature data on the canine parainfluenza virus.[16] The bands corresponding to proteins L, HN, NP, F, P, A and M were all seen in the gel. Slight differences in their size were observed compared to that of the human parainfluenza virus presumably due to differences in protein sequences in the two viruses. Additional bands were observed apart from the major viral proteins indicative of the presence of some residual impurities. DLS measurements were also used to confirm the size of the purified virus. The diameter of CPI was estimated to be about 270 nm, similar to reported values of 150-300 nm in diameter for the human parainfluenza virus.[16] Overall, a significantly improved level of purification of the CPI virus from crude cell lysate was successful while maintaining intact enveloped virus. Figure 4.3A shows the circular dichroism spectrum for the CPI virus at 10 ^{o}C and pH 7. The CD spectrum shows a double minimum around 208 and 222 nm, indicating the presence of alpha helical structure in the viral proteins.

The CD melting curves at 222 nm for the CPI virus are shown in Figure 4.3B. No sudden changes in the ellipticity were noted with increasing temperature at any pH value. Instead, a continual decrease in CD signal initiating at room temperature was observed, indicating a gradual loss of secondary structure in the viral proteins. Figure 4.3C shows the change in the peak position of the emission maximum as a function of increasing temperature at different pH values. A small change in the peak position at all pH values was observed at about 45-50 ^{o}C. The CPI virus was found to be most stable at pH 6 with the transition initiating at about 45^{o}C. The small change in peak position seen at lower temperatures at other pH values was also not observed at pH 6. Static light scattering melts for the CPI virus are shown in Figure 4.3D. No significant increase in the static light scattering intensity was observed at any pH with increasing temperature, indicating no major aggregation events at increased temperature.

The canine adenovirus type 2 (CAV2) was purified using ammonium sulfate precipitation. Figures 4.1C, 4.1F and Figure 4.4 show the purification and the biophysical characterization data for CAV2, respectively. TEM images of CAV2 particles purified using ammonium sulfate precipitation are shown in Figure 4.1C. Several virions of about 80 nm are observed in the TEM image, similar to other values previously reported for adenoviruses.[17] Figure 4.1F shows the SDS-PAGE gel for the purified CAV2. Multiple bands such as PII, PIII, PIIIA, and PV were observed closely matching the protein bands of CAV2 studied previously.[18] The CD spectrum of CAV2 proteins at 10 °C and pH 7 displays a double minimum at approximately 208 and 222 nm (Figure 4.4A) which is again characteristic of high α-helical content. Changes in the CD signal at 222 nm upon heating were monitored for CAV2 (Figure 4.4B). The CD signal decreased with small transitions at all pH values indicating some loss in protein secondary structure upon heating. The midpoint of the thermal transitions occurs at lower temperatures for virus protein at low pH. The transition for the change in the CD signal initiates at about 30 ^{o}C at pH 6, and increases to about 40 ^{o}C at pH values of 7 to 8. The tertiary structure of the CAV2 was studied by measuring the peak shifts in Trp emission as a function of temperature (Figure 4.4C). A red shift was observed in the emission peak maxima beginning at ~30 ^{o}C at each pH. Thus, the CAV2 proteins appear

to begin to unfold around 30 °C and undergo a transition with a Tm of approximately 55 °C. Static light scattering was employed to provide insight into the aggregation behavior of the CAV2 virus in solution. At pH 5.5, 6.0, CAV2 showed greater light scattering intensities even at low temperatures indicating the presence of some aggregation (Figure 4.4D). CAV2 undergoes further aggregation at these pH values with transitions starting as early as 30 °C. The sharp decrease in static light intensity seen after 75 °C may be due to precipitation of CAV2 aggregates. At pH 6.5 and 7.0, aggregation starts at ~ 42 °C as indicated by a sudden increase in static light scattering intensity. CAV2 shows biphasic transitions at pH 7.5 and 8.0 with the first transition starting at ~45 °C and the second one at 65 °C.

The biophysical characterization data for each of the three viruses were compiled to construct the empirical phase diagram (EPD) for each virus as shown in Figure 4.5. The empirical phase diagrams (EPDs) for CDV, CPI virus and CAV2 are shown in Figure 4.5A, 4.5B and 4.5C, respectively. For the construction of the EPDs, data obtained using circular dichroism, static light scattering and intrinsic fluorescence spectroscopy were used with the red representing the CD (secondary structure), green the intrinsic fluorescence (tertiary structure), and blue representing the aggregation of the virus.

The EPD for the canine distemper virus (CDV) is shown in Figure 4.5A. The CDV virus was identified as conformationally stable in region I between pH 6 and 8 at lower temperatures. The viral particles were found to be partially aggregated with its proteins altered in conformation at the lower pH values and at modestly elevated temperatures (region II). Aggregation and unfolding of the viral proteins was observed at high temperatures at all pH values and is shown in region III. Figure 4.5B shows the EPD for the CPI virus. Region I appears to be the region where the CPI virus is most stable. Region II depicts a state of the CPI virus where the viral proteins are in their native state, but a slight swelling of the virus is caused by increasing temperature. Unfolding of the viral proteins was observed at region III. The unfolding of the CPI viral proteins along with possible aggregation is seen in region IV. The empirical phase diagram for CAV2 is shown in Figure 4.5C. The figure shows three distinct regions. Region I at temperature below 40 ^{o}C at all pH values is presumably the native form of the CAV2 virus.

Conformational changes in the CAV2 virus were observed in region II at pH values of 6.5 to 8 and around 55 ^{o}C. CAV2 tends to aggregate at all pH values at higher temperatures as seen in region III.

A common solution pH of 7.0 was selected for further studies with each of the three viruses based on the apparent phase boundaries observed in their respective EPDs (Figure 4.5). To examine the effects of different agents on the stability of the three individual viruses, a library of GRAS compounds including several sugars, sugar alcohols, surfactants, and amino acids among others was tested for stabilizing effects on the viruses. Screening for the canine distemper virus (CDV) and the canine adenovirus (CAV2) employed a kinetic based aggregation method in which the virus was incubated at 55^{o}C in the presence of various compounds. Stabilizers of the canine parainfluenza virus (CPI) were identified using intrinsic Trp fluorescence spectroscopy since the virus did not aggregate significantly at the concentrations tested. Table 1 lists the different compounds tested along with the percent inhibition of aggregation for CDV and CAV2, along with the thermal unfolding (Tm) values in the case of the CPI virus. Figure 4.6A shows representative data from Table 1 in which the increase in optical density at 350 nm for CDV samples when incubated at 55 ^{o}C, was monitored as a function of time in the presence of selected stabilizers and destabilizers. An immediate increase in the optical density at 350 nm was observed in the case of destabilizers like diethanolamine and guanidine while no notable increases in the optical density were seen in the case of stabilizers such as sucrose and sorbitol. Similar results were observed for CAV2 as well with sucrose, sorbitol, dextrose and lysine inhibiting temperature induced aggregation (Table 1).

Compounds that showed a positive effect on the inhibition of aggregation were selected to further study their effect on the stability of the three viruses. For this, circular dichroism spectroscopy was used to determine the effect of the selected compounds on stabilizing the secondary structure of the viral proteins. Table 2 summarizes the thermal unfolding values for each of the three viruses at different concentrations of sucrose and sorbitol. Figure 4.6C shows the effect of increasing the concentration of sorbitol on the CD signal at 222 nm of the CDV virus. Maximum stabilization effects were seen in the samples containing the highest concentrations of sorbitol. Sorbitol at concentrations of 25% showed no

major signal changes in the circular dichroism signal up to about 40 ^{o}C. The same was found to be true in the case of sucrose and trehalose as well. For the CPI virus, Figure 4.6B shows the intrinsic fluorescence melts in the presence of various selected stabilizers and destabilizers. Tm values were calculated from the first derivative of the peak position melting curves as shown in Figure 4.6D. Again, sugars and sugar alcohols showed promising stabilizing properties with increases in the thermal unfolding (Tm) values of about 5^{o}C. Similar to the CDV and CAV2, the maximum stabilization of the CPI virus was achieved at the highest concentrations of sorbitol and sucrose tested as seen in Table 2.

In summary, sorbitol and sucrose proved to be common stabilizers for all three viruses. Some stabilizers such as trehalose and proline had positive effects on CDV and the CPI virus, but negative effects on CAV2. Sorbitol at concentration of 25% (w/v) proved to be most effective at stabilizing the viruses individually from aggregation and the viral proteins from temperature induced conformational changes.

Discussion

The purification procedure for each of the three viruses yielded viral samples of sufficient purity to enable their individual biophysical characterization. The EM images of the three viruses show primarily intact viral particles. Dynamic light scattering also finds the size of viral particles are in line with previously published data. SDS-PAGE gels showed several bands for each virus corresponding to the known molecular weight of the viral proteins. Western blot experiments of the canine distemper virus showed two bands corresponding to the matrix protein, and the fusion (F_0) or the neuramidase (N) protein. Western blot data for the other two viruses were not available due to the lack of adequate primary antibodies.

The biophysical characterization of the three viruses was performed individually using circular dichroism and intrinsic fluorescence spectroscopy, and static light scattering experiments. Circular dichroism and fluorescence spectroscopy were used to study changes in different levels of structure

(secondary and tertiary) of the viral proteins while static light scattering experiments analyzed the aggregational propensity of the viruses. Although the results reflect the sum of the effects of temperature and pH on all the proteins in each virus, they still serve as a useful measure of the overall stability of the virus even if their effects on individual viral proteins cannot be resolved. Stabilizers which were capable of enhancing the aggregational stability and the conformational stability for all the three viruses were identified.

The data obtained from circular dichroism spectroscopy, intrinsic fluorescence spectroscopy and static light scattering were combined in the form of a three-index empirical phase diagram to better understand the effect of temperature and pH on the gross structure of the viruses. The empirical phase diagrams for each of the viruses indicate that each virus is very thermo-labile. Changes in the distemper virus were seen initiating at about 30^{o}C, with the CDV virus aggregating at around 45^{o}C. The canine parainfluenza virus was found to be even more sensitive to temperature with changes initiating below room temperature. Partial unfolding of the viral proteins was observed at about 50^{o}C with the CPI virus aggregating at about 65^{o}C. Of the three virus, the CAV2 proved to be the most resistant to temperature induced changes by maintaining its native state to about 45^{o}C at pH 6.5-7.5. Aggregation of this virus was observed only at about 70^{o}C over this pH range. CAV2 was observed to be more unstable at lower pH, with aggregation occurring as low as 40^{o}C at pH 5.5 and 6. It is important to note that CAV2 is a non-enveloped virus, which may account for some of the observed differences in stability.

CDV and CAV2 viruses were prone to aggregation at elevated temperature and therefore, a kinetic based aggregation assay was employed to screen for potential stabilizers. Circular dichroism was further used to study the effect of the potential stabilizers on the secondary structure of the viral proteins from these two viruses. Screening of over 30 GRAS excipients yielded several common stabilizers such as sucrose, sorbitol, and lysine among others. These stabilizers were able to not only prevent these viruses from aggregating, but to also provide structural stability to the viral proteins. Several of excipients, however, such as dextran sulfate, were not able to conformationally stabilize the structure of the viral

proteins even though they inhibited aggregation (Table 1). Based on these data, a vaccine consisting of the above mentioned attenuated viruses should therefore benefit from the addition of stabilizers such as sucrose or sorbitol. Sucrose and sorbitol probably stabilize the viral particles by non-specific processes such as the well documented preferential hydration mechanism.[19-21] Specific interactions should not be ruled out, however, since sialic acid, which is the natural ligand of the hemagglutinin (or the hemagglutinin-neuraminidase) protein in the distemper and the parainfluenza virus, bears some structural resemblance to stabilizing sugars. The amount of sucrose and/or sorbitol that can be added to the formulation may be limited by solution osmolarity. For example, the osmolarity of a formulation must be considered due to the potential for pain and discomfort at the site of injection. Cell lysis has also been shown to occur with the use of formulation with high osmolarity values. Higher values than those used in humans may potentially be usable in these animal vaccines.

When the three live attenuated viruses are mixed together to make a trivalent vaccine, the possibility of the viruses interacting with each other should be examined carefully. The lack of analytical assays at this point to probe the different viruses individually in the mixture makes it impossible to study each of the three viruses simultaneously. Therefore, it may be necessary to develop chromatographic separations to examine the biophysical properties of the individual viruses from the trivalent mixture. Ultimately, in vitro cell-based and animal potency studies will be necessary to decide on the best formulation and dosage criteria for this trivalent live virus vaccine. Additionally, spray drying or freeze drying of the final formulation may be performed to further stabilize the three live viruses during long term storage.

References

1. Chalmers WS 2006. Overview of new vaccines and technologies. Veterinary microbiology 117(1):25-31.
2. Brandau DT, Jones LS, Wiethoff CM, Rexroad J, Middaugh CR 2003. Thermal stability of vaccines. Journal of pharmaceutical sciences 92(2):218-231.
3. Fan H, Kashi RS, Middaugh CR 2006. Conformational lability of two molecular chaperones Hsc70 and gp96: Effects of pH and temperature. Archives of Biochemistry and Biophysics 447(1):34-45.
4. Fan H, Vitharana SN, Chen T, O'Keefe D, Middaugh CR 2007. Effects of pH and Polyanions on the Thermal Stability of Fibroblast Growth Factor 20. Molecular Pharmaceutics 4(2):232-240.
5. Harn N, Allan C, Oliver C, Middaugh CR 2007. Highly concentrated monoclonal antibody solutions: Direct analysis of physical structure and thermal stability. Journal of pharmaceutical sciences 96(3):532-546.
6. Nonoyama A, Laurence JS, Garriques L, Qi H, Le T, Middaugh CR 2008. A biophysical characterization of the peptide drug pramlintide (AC137) using empirical phase diagrams. Journal of pharmaceutical sciences 97(7):2552-2567.
7. Ramsey JD, Gill ML, Kamerzell TJ, Price ES, Joshi SB, Bishop SM, Oliver CN, Middaugh CR 2009. Using empirical phase diagrams to understand the role of intramolecular dynamics in immunoglobulin G stability. Journal of pharmaceutical sciences 98(7):2432-2447.
8. Iyer V, Liyanage M, Shoji Y, Chichester J, Jones M, Yusibov V, Joshi S, Middaugh CR 2012. Formulation development of a plant-derived h1n1 influenza vaccine containing purified recombinant hemagglutinin antigen. Human Vaccines 8(4).
9. Kissmann J, Joshi SB, Haynes JR, Dokken L, Richardson C, Middaugh CR 2011. H1N1 influenza virus-like particles: physical degradation pathways and identification of stabilizers. Journal of pharmaceutical sciences 100(2):634-645.
10. Harder TC, Osterhaus AD 1997. Canine distemper virus--a morbillivirus in search of new hosts? Trends in microbiology 5(3):120-124.
11. Martella V, Elia G, Buonavoglia C 2008. Canine distemper virus. The Veterinary clinics of North America Small animal practice 38(4):787-797, vii-viii.
12. Webster AC 1975. The adverse effect of environment on the response to distemper vaccination. Australian veterinary journal 51(10):488-490.
13. Norrby E, Friding B, Rockborn G, Gard S 1963. The Ultrastructure of Canine Distemper Virus. Archiv fur die gesamte Virusforschung 13:335-344.
14. Campbell JJ, Cosby SL, Scott JK, Rima BK, Martin SJ, Appel M 1980. A comparison of measles and canine distemper virus polypeptides. The Journal of general virology 48(1):149-159.
15. Stephenson JR, ter Meulen V 1979. Antigenic relationships between measles and canine distemper viruses: comparison of immune response in animals and humans to individual virus-specific polypeptides. Proceedings of the National Academy of Sciences of the United States of America 76(12):6601-6605.
16. Cowley JA, Barry RD 1983. Characterization of human parainfluenza viruses. I. The structural proteins of parainfluenza virus 2 and their synthesis in infected cells. The Journal of general virology 64 (Pt 10):2117-2125.
17. Schoehn G, El Bakkouri M, Fabry CM, Billet O, Estrozi LF, Le L, Curiel DT, Kajava AV, Ruigrok RW, Kremer EJ 2008. Three-dimensional structure of canine adenovirus serotype 2 capsid. Journal of virology 82(7):3192-3203.
18. IV FWP. 1999. Characterization of the Adenovirus Protease Activity in Adenovirus Gene Therapy Preparations. Department of biology, ed.: Seton Hall University.
19. Lee JC, Timasheff SN 1981. The stabilization of proteins by sucrose. J Biol Chem 256(14):7193-7201.
20. Shimizu S, Smith DJ 2004. Preferential hydration and the exclusion of cosolvents from protein surfaces. J Chem Phys 121(2):1148-1154.

21. Uedaira H 2001. Role of hydration of polyhydroxy compounds in biological systems. Cell Mol Biol (Noisy-le-grand) 47(5):823-829.

Chapter 5

Conclusions

Conclusions

Over the past couple of decades, the pharmaceutical industry has tried to move away from traditional whole organism-based vaccines to sub-unit protein-based vaccines. There are several advantages to this such as increases in stability, better molecular definition and ease of manufacturing. There are, however, some drawbacks as well which include the low immunogenicity associated with sub-unit protein vaccines. Despite this, there are several sub-unit vaccines on the market today, and several more being developed. In the last three chapters, I have described the formulation development of three vaccines: a protein subunit influenza vaccine, a trivalent subunit pneumococcal vaccine and a trivalent live attenuated viral vaccine against three canine viruses.

In chapter 2, I discussed the development of a protein subunit vaccine towards the 2009 pandemic H1N1 flu strain of swine origin utilizing the hemagglutinin surface antigen. One of the major problems we encounter with influenza vaccines is the time involved with their development. Presently, it takes about 9 months to develop a seasonal influenza vaccine. In the event of a pandemic, thousands of lives may be lost in this time period. By recombinantly producing the hemagglutinin antigen in tobacco plants, we should be able to significantly speed up the manufacturing process. Additionally, we may be able to identity formulation conditions of the vaccine within a few weeks using the empirical phase diagram approach. This was done using several biophysical techniques such as circular dichroism, intrinsic and extrinsic fluorescence spectroscopy and light scattering. Each of these techniques is used to study a different aspect of protein structure. From the initial characterization studies, HAC1 was found to be most stable at pH 7 and 8 and at temperature below 40^{o}C. It was also established that HAC1 was found to be in a conformationally altered state at lower pH values. These pH-dependent changes in conformation are fairly common with many viral surface antigens undergoing pH dependent conformational changes which help the virus infect their host cells.

Since HAC1 was found to be most stable at pH 7, it was formulated in a 20mM imidazole buffer to screen for excipients. Intrinsic fluorescence spectroscopy was used to screen for stabilizers from a

library of GRAS compounds. Traditionally used kinetic based aggregation assays were not used in this case since HAC1 did not aggregate significantly at acceptable temperatures. Sucrose, sorbitol, trehalose and other sugars and sugar alcohols proved to be to most promising stabilizers. These compounds were able to stabilize HAC1 conformationally as well as inhibit aggregation. Surfactants such as polysorbate-20 and polysorbate-80 also were efficient in protecting the protein against aggregation. The concentrations of these potential stabilizers were optimized to determine if they can impart similar stabilizing effects at lower concentrations. The increase in thermal stability was found to be concentration dependent for stabilizers tested. Additionally, combinations of these stabilizers were tested to check for additive or synergistic effects. Only slight increases in thermal stability were observed when combinations of stabilizers were tested. Based on the increase in thermal stability of the protein and the required osmolarity of the formulations, 15% sorbitol, 10% sorbitol with 5% sucrose and 10% dextrose were chosen as the most ideal formulations for HAC1 in solution.

The addition of aluminum salt adjuvants was also tested to boost the immunogenicity of vaccine. HAC1 showed high binding affinity towards Alhydrogel. One hundred micrograms of Alhydrogel was able to adsorb up to 160ug of HAC1. Saturation of the binding of HAC1 to Alhydrogel was not achieved over the concentration range examined. It was also found to be difficult to desorb HAC1 from the surface of the adjuvant. Such desorption of the antigen from the adjuvant may be important to search for possible chemical degradation of the protein during storage. A combination of 1M citrate and 2M urea was identified as a possible desorption agent because it was able to desorb over 80% of the adsorbed protein. The conformational stability of the protein was found to be affected by adsorption to the adjuvant. This appears to be the result of an optimization of the protein's conformation on the adjuvants surface in order to reduce its free energy. Many of the stabilizers such as sorbitol and sucrose, which were identified as stabilizing the protein in solution also helped to stabilize the protein on the adjuvant surface. This, however, was not to the same extent as that observed in solution. The addition of 5mM sodium phosphate helped improve the stability of the adsorbed HAC1. No significant desorption of the HAC1 from the

adjuvant was observed in the presence of any of the stabilizers. In addition to excipients, the effect of heat treatment or "annealing" was tested to see if any increase in stability could be obtained. No significant conformational changes were observed until when HAC1 was exposed to temperatures of 40^{o}C for 10 minutes. Therefore, three formulations were found to stabilize HAC1 in the presence of the adjuvant. These were 15% sorbitol with 5mM phosphate and 0.01% tween-80, 5mM phosphate alone and HAC1 annealed at 40^{o}C.

These formulations, along with the recommended solution formulations were tested in mice to see which produced the highest antibody titer. As expected, the formulations with Alhydrogel produced the greatest antibody response. It was also observed that 0.5mg/ml Alhydrogel was sufficient to elicit this antibody response. Among the non-adjuvanted formulations, 15% sorbitol showed the highest antibody titers. A more thorough study will be required to test for any differences observed in the use of the different excipients. This vaccine was entered into phase I human trials in September 2010, which were completed in May 2011. HAC1 was found be safe and well tolerated at all dosage levels, with and without adjuvant. Preliminary reports suggest the immune response was highest in presence of the adjuvant.

Chapter 3 discusses the development of a trivalent protein sub-unit vaccine against *S. pneumoniae*. One of the major problems faced with this bacterium is its wide serotype distribution, which makes it hard to develop a single effective vaccine that could be used worldwide. In chapter 3, we explored the formulation development of three protein antigens – SP1650, SP1732 and SP2216. Varying stability profiles were observed for each of the three antigens. SP1732 was seen to be very stable, with no conformational differences observed until 70^{o}C. SP1650 was relatively unstable, showing protein conformational changes and aggregation at about 45^{o}C. SP2216 was found to be very unstable with conformational changes occurring below room temperature. These stability profiles were reflected in the empirical phase diagrams produced for each of the three proteins.

In a manner similar to HAC1, the three proteins were screened for stabilizers from a library of GRAS compounds. During this process the proteins were dialyzed into a 10mM sodium acetate buffer containing 150 mM NaCl and 0.067% tween-20 at pH 5.5. This buffer was identified by our collaborators at Intercell AG previously for the three antigens. Sorbitol and sucrose, along with other sugars and sugar-alcohols were identified as potential common stabilizers for all three proteins. Manganese chloride was also able to significantly stabilize SP1650. The presence of manganese was able to increase the thermal transition temperature ofSP1650 by almost 15^{o}C. The concentrations of these potential excipients were optimized to lower the osmolarity of the formulations. These stabilizers were also tested in combinations to search for additive or synergistic effects. Only the excipients that were able to stabilize all three proteins independently and simultaneously were chosen since all three antigens will be formulated together in a trivalent vaccine. The presence or absence of NaCl did not significantly affect the thermal transition temperatures of any of the three proteins, although a decreased extent of unfolding was observed in the case of SP1650. Five percent sorbitol with 10% trehalose, 10% trehalose and 5% sorbitol were identified as perspective stabilizers for the top three formulations recommended for the trivalent vaccine. In addition, 50um manganese chloride was recommended for the combined formulations due to its ability to drastically stabilize SP1650. NaCl was not included in the list of recommended components for the trivalent vaccine. This also helped lower the osmolarity of the formulations.

All three antigens showed high affinity towards Alhydrogel, even though the pI of the three proteins is on either side of the formulation pH. This suggests that there may be other mechanisms affecting the adsorption process apart from simple electrostatic interactions. The three antigens bound weakly to Adjuphos with less than 60% of the total antigen binding. Near-saturation of binding to Alhydrogel of each antigen was observed in the adsorption isotherms. 50ug of Alhydrogel was able to adsorbed almost 90ug of each antigen. The final dosage form is expected to contain about 50ug of each antigen in 600ug of Alhydrogel. At these concentrations, each of the three proteins should be completely bound to the adjuvant. A common desorption agent was not identified for all the proteins. Two molar

guanidine, however, was able to desorb over 80% of SP2216 and SP1732 from Alhydrogel. Similar levels of desorption of SP1650 required the use of a combination of 1M urea and 2M sodium citrate. The three antigens displayed different stability profiles when adsorbed on to the adjuvant. SP1650 was dramatically destabilized. This destabilization was partially offset by the addition of sodium phosphate at a concentration of 5mM. The secondary structure of SP2216 was found not to be perturbed when adsorbed on to the adjuvant as assessed by FTIR spectroscopy. On the other hand, SP1732 was found to be stabilized by its adsorption on to Alhydrogel as observed by temperature dependent intrinsic tryptophan fluorescence spectroscopy. This illustrates that the stability profile of the antigens while adsorbed to the adjuvant tends to be antigen specific.

When these three antigens are eventually combined to make a trivalent vaccine, the possibility of interaction between the three antigens needs to be explored. Due to a lack of assays to explore this aspect at this time, efforts are being undertaken to identify and develop assays that can be used to study all three antigens simultaneously. Additionally, animal studies are yet to be completed using the trivalent vaccine. These studies are on scheduled to be undertaken in 2013 by PATH.

The empirical phase diagram approach used to formulate the previous two vaccines was also used to formulate a trivalent live attenuated viral vaccine. This vaccine consists of attenuated forms of the canine distemper virus, canine parainfluenza virus and the canine adenovirus type 2. Each of the three viruses was purified to the maximum possible extent to enable an exploration of the biophysical properties of the three viruses. Canine adenovirus was purified using ammonium sulfate precipitation. The other two viruses were purified using ultracentrifugation. Additionally, a sucrose gradient was also employed in the case of the canine parainfluenza virus for further purification. Due to severe aggregation of the virus at low pH, the empirical phase diagrams for all three viruses was constructed between pH range of 5.5 to 8, at 0.5 pH unit intervals. Since all three viruses were most stable at about pH 7, a citrate phosphate buffer at pH 7 with 150mM NaCl was employed for further excipient screening studies. Again,

only the excipients that were able to stabilize all the three viruses were selected. Sorbitol and sucrose proved to be the most potent stabilizers of all three viruses.

Because osmolarity of the formulation is less of a concern in animal vaccines, concentrations of stabilizers were increased to as much as 25% w/v in some cases. It was recommended that the cell lysates of the three viruses be combined in the presence of high concentrations of these stabilizing sugars. These studies illustrate the important result that the EPD approach is useable even in the case of complex molecular entities such as viruses. This may be at least partially due to the dominance of their physical properties by only one or a few proteins which are sensitive to the immunogenicity of the virus.

Further studies on this vaccine were performed by Intervet Inc., and improvements over previous commercial formulations have yielded over a year of viral stability and activity in solution. This may enable the use of solution vaccines in addition to the currently marketed freeze dried form, which requires reconstitution prior to administration of the vaccine.

With the experience gained with the formulation development of several vaccines, I would like to highlight a couple of areas where focus would be required to obtain a more ideal formulation. A third of all proteins contain a metal binding site. The presence of the metal ion can, in many cases, dramatically increase the thermal stability of the protein. An easy and obvious pathway to identify potential metals that can stabilize a protein therapeutic would be to screen each metal individually. This can sometimes be quite tedious and time consuming. It is possible to predict metal binding sites by several algorithms available online. Additionally, it may also be worthwhile to search for known proteins with similar sequences to identify potential metal binding sites.

Another aspect to consider is the osmolality of vaccine formulations. Once developed, these vaccines will be injected in millions of children and adults across the world. If these administrations have high osmolarity, they can cause pain and discomfort at the site of injection. Cell lysis has also been known to occur under such conditions. An effective formulation strategy that considers osmotic effects

can help lower such harmful side effects, while maximizing stability and immunogenicity. For instance, the removal of sodium chloride greatly reduced the osmolarity of the formulation of the trivalent recombinant protein based pneumococcal vaccine. The osmolarity reduced by the removal of sodium chloride may be replaced with suitable concentrations of a stabilizer to further increase stability of the vaccine.

Many of the vaccines developed today are multivalent. They have more than one component to produce a broad immunogenic response. Unfortunately, this can lead to interactions between the multiple components in the vaccine. When multivalent vaccines such as the live attenuated viral vaccine or the trivalent recombinant protein based pneumococcal vaccine are developed, it is important to consider and characterize the interactions between the various components of the vaccine and alter formulations to decrease such interactions if they are undesirable.

As more recombinant protein based vaccines continue to be developed, novel adjuvants are being identified. The aluminum salt adjuvants prevalent today may not be the ideal adjuvants for future or current vaccines. With each novel adjuvant, the formulation approach will need to be molded to best characterize the interactions between the adjuvants and the antigens and to optimize such effects.

Future Studies

In case of each of the three vaccines formulations developed, there are several studies yet to be completed before work can continue further. These future studies have been discussed for each project. For the influenza vaccine, the animal studies showed high antibody titer in the presence of Alhydrogel. Initial phase I clinical trials showed the vaccine was safe in all doses tested. Currently phase II clinical trials are underway to establish the efficacy of the vaccine. Results from this study should be available within the next year. Phase III clinical trials for the vaccine still need to be initiated. In addition, the effects of newer adjuvants should be tested to determine if the vaccine can be made more immunogenic.

The trivalent pneumococcal vaccine has yet to be tested in an animal model. Upon successful completion of initial animal studies, the vaccine will then need to be subjected to clinical trials in which its safety and efficacy will be tested in humans. Also, with the presence three individual proteins in the vaccine, the potential for interactions between the proteins need to be studied. This was not performed in this study due to a lack of assays to explore these aspects. Such assays are, however, being currently developed.

The trivalent live attenuated viral vaccine has been proven to be stable and active for over a year. Since this is not a human vaccine, extensive clinical trials need not be undertaken. Their efficacy in protecting dogs against the different diseases is being studied currently.

In conclusion, the biophysical EPD-based approach described in this thesis is shown to be both efficient and effective methodology for characterization and stabilization for a variety of different vaccines. Although it continues to be refined, it currently offers an important addition to the tool kit of vaccine formulation development.

Tables

Table 1.1: The effects of vaccines have had on the number of deaths caused by several deadly diseases in the United States.

Disease	**Number of deaths**	
	Before Vaccine	After Vaccine
Paralytic Polio	30,000	0
Rubella	100,000	10
Pertusis	100,000	<10,000
Mumps	100,000	100
Measles	1,000,000	10
Diptehria	100,000	0

Table 1.2: Different types of vaccines elicit different types of immune response.

Vaccine	Type	Type of Immune Response
Diphteria Toxoid	Toxoid	Humoral
Hepatitis A	Killed	Humoral
Hepatitis B	VLP	Humoral
Influenza	Subunit	Humoral
Measles	Live Attenuated - Viral	Humoral + Cellular
Mumps	Live Attenuated - Viral	Humoral + Cellular
HPV	VLP	Humoral
Pneumoccal PS	Subunit Conjugate	Humoral
Polio	Killed	Humoral
Rabies	Killed	Humoral
Rubella	Live Attenuated - viral	Humoral
TB (BCG)	Live Attenuated - Bacterial	Humoral + Cellular
Varicella	Live Attenuated - Viral	Humoral + Cellular

Table 1.3: Selected marketed vaccines that contain aluminum salt adjuvants along with their dosages. AAHS is a proprietary aluminum salt adjuvant manufactured by Merck.

Trade name	Vaccine	Adjuvant	Al per dose
Daptacel	Diphteria, Tetanus and pertusis	Adjuphos	0.33
Prevnar	Pneumoccoccal 7-Valent	Adjuphos	0.125
Biothrax	Antrax	Alhydrogel	0.6
Gardasil	HPV	AAHS	0.225
Twinrix	Hep A	Alhydrogel and Adjuphos	0.45
Recombivax HB	Hep B	AAHS	0.5

Table 2.1. Effect of GRAS compounds on the conformational stability (T_m-Trp) and aggregation (T_m-SLS) of HAC1 as determined by intrinsic fluorescence and static light scattering. The effect of each compound on the aggregation and conformational stability of the protein is represented as a change in T_m. Compounds that inhibit aggregation and enhance stability have increased T_m values, while compounds that induce aggregation and reduce conformational stability produced decreased T_m values.

Excipient	**T_m (°C)-Trp**	**Excipient**	**T_m (°C)-SLS**
HAC1	53.9	HAC1	57.0
20% Dextrose	58.2	0.1% Tween 80	64.0
20% Sorbitol	58.1	20% Dextrose	63.5
20% Sucrose	57.1	20% Sorbitol	62.8
20% Glycerol	56.5	20% Sucrose	61.0
20% Lactose	56.2	0.3M Lysine	60.0
0.15M Malic Acid	55.3	20% Glycerol	60.0
0.1% Tween 80	55.0	20% Lactose	59.9
20% Trehalose	54.8	0.15M Lactic Acid	59.8
0.2M Sodium Citrate	54.1	0.1% Pluronic F-68	58.9
0.3M Lysine	53.9	0.1% Tween 20	58.5
0.3M Glysine	53.8	5% γ-cyclodextrin	58.0
0.15M Lactic Acid	53.6	0.15M Glutamic Acid	57.9
0.1% Pluronic F-68	53.6	0.1% Brij 35	57.9
5% γ-cyclodextrin	53.2	0.07M Aspartic Acid	57.5
0.15M Glutamic Acid	53.2	2.5% α-cyclodextrin	57.5
0.3M Proline	53.1	5% β-cyclodextrin	57.5
0.1% Tween 20	53.0	20% Trehalose	57.5
0.1% Brij 35	53.0	0.3M Diethanol Amine	57.1
0.07M Aspartic Acid	53.0	0.3M Arginine	57.0

2.5% α-cyclodextrin	53.0	0.3M Glysine	56.1
0.015M Calcium Chloride	52.7	0.3M Proline	56.0
5% β-cyclodextrin	52.3	0.15M Malic Acid	55.2
0.3M Diethanol Amine	51.5	7.5E-6M Dextran Sulfate	55.0
0.3M Arginine	51.5	0.2M Sodium Citrate	55.0
7.5E-6M Dextran Sulfate	50.8	0.015M Calcium Chloride	53.8
0.3M Guanidine	49.0	0.3M Guanidine	53.1

Table 2.2. Effect of the concentration of selected GRAS compounds on the aggregation (T_m-SLS) and the conformational stability (T_m-Trp) of HAC1 as determined by intrinsic fluorescence and static light scattering.

Excipient	**T_m (°C)-Trp ***	**Excipient**	**T_m (°C) –SLS ***
HAC1	54.6	HAC1	54.5
20% Sorbitol	59	20% Sorbitol	58.5
15% Sorbitol	57.8	15% Sorbitol	58.9
10% Sorbitol	56.9	10% Sorbitol	56.9
20% Dextrose	58.9	20% Dextrose	62.8
15%Dextrose	57.3	15% Dextrose	61
10% Dextrose	57	10% Dextrose	60
20% Sucrose	58.1	20% Sucrose	59.9
15% Sucrose	56.2	15% Sucrose	59
10% Sucrose	55.5	10% Sucrose	57.5
20% Glycerol	57.4	20% Glycerol	59
15% Glycerol	56.6	15% Glycerol	58.5
10% Glycerol	57	10% Glycerol	59.5
0.1% Tween-80	55	0.1% Tween-80	64
0.05% Tween-80	53.6	0.05% Tween-80	57.4
0.01% Tween-80	53.2	0.01% Tween-80	62

* The precision of these values is estimated to be ±0.5^{o}C based on two independent measurements.

Table 2.3. The effect of combinations of stabilizing GRAS compounds on the aggregation (a) and the conformational stability (b) of HAC1 as determined by intrinsic fluorescence and static light scattering.

(a)

Excipient	Concentration	Excipient	Concentration	T_m (^oC) –SLS*
Sucrose	15%	Tween-80	0.05%	61
Dextrose	10%	Glycerol	5%	60.8
Dextrose	10%	Sorbitol	5%	60.5
Glycerol	10%	Sucrose	5%	59.8
Sorbitol	10%	Sucrose	5%	58.9
Sorbitol	15%	Tween-80	0.05%	58.5

(b)

Excipient	Concentration	Excipient	Concentration	T_m (^oC)-Trp*
Dextrose	10%	Glycerol	5%	57.6
Dextrose	10%	Sorbitol	5%	57.2
Sorbitol	10%	Sucrose	5%	56.8
Glycerol	10%	Sucrose	5%	56.5
Sucrose	15%	Tween-80	0.05%	56.5
Sorbitol	15%	Tween-80	0.05%	54.5

* The precision of these values is estimated to be $\pm 0.5^oC$ based on two independent measurements.

Table 2.4. Formulations tested in mouse immunogenicity study

Group	Antigen	Buffer	Components	Alhydrogel®
1	HAC1*	10 mM imidazole, 150 mM NaCl, pH 7.0	15% sorbitol	None
2			10% sorbitol, 5% sucrose	
3			10% dextrose	
4			15% sorbitol, 0.01% Tween-80, 5 mM phosphate	0.5 mg/ml of aluminum
5			5 mM phosphate	
6	HAC1* treated at 40 °C		None	
7	HAC1*	Saline	None	1.8 mg/ml of aluminum
8	NA	Saline	None	

* 18 μg/dose

Table 2.5. Mean HAI antibody titers and seropositive rates

Group		**1**	**2**	**3**	**4**	**5**	**6**	**7**	**8**
Mean ± SE*	Day 35	304 ± 138	26 ± 6	154 ± 68	576 ± 288	800 ± 214	320 ± 88	800 ± 214	10 ± 0
% responders**		100	40	80	100	100	100	100	0
Mean ± SE*	Day 70	130 ± 53	30 ± 6	46 ± 15	704 ± 251	960 ± 202	640 ± 263	1280 ± 0	10 ± 0
% responders**		80	40	60	100	100	100	100	0

***** Mean HAI titers (± standard error) on day 35 or 70 (post second vaccination)
** % animals with HAI titers ≥40 on day 35 or 70 (post second vaccination)

Table 3.1: Thermal unfolding temperature (Tm) values for SP1650 in the presence of various stabilizers and destabilizers in a 10mM sodium acetate buffer at pH 5.5.

Excipient	Tm (°C)
Protein	59.1
50 μM Manganese Chloride	70.0
20% Lactose	68.4
20% Dextrose	66.5
0.2 M Sodium Citrate	64.0
20% Trehalose	63.1
20% Sorbitol	62.2
20% Sucrose	62.2
10% Mannitol	61.6
0.3 M Glycine	61.0
20% Glycerol	60.0
0.15 M Glutamic Acid	60.0
5% 2-OH propyl γ-cyclodextrin	59.9
7.5E-6 M Dextran T70	59.5
0.3 M Proline	59.3
0.015 M Calcium Chloride	59.3
0.07 M Aspartic Acid	59.2
0.15 M Lactic Acid	59.2
5% 2-OH propyl β-cyclodextrin	56.4
0.3 M Histidine	55.1
7.5E-6 M Dextran Sulfate	55.0
0.3 M Diethanolamine	54.3
0.3 M Arginine	51.5
0.3 M Guanidine	51.5

Table 3.2: Thermal unfolding temperature (Tm) values for SP1650 in the presence of selected stabilizers at various concentrations in a 10mM sodium acetate buffer at pH 5.5. Duplicate measurements were made for all combinations. The standard error was calculated to be below ± 0.5^{o}C.

Excipient	Concentration	Tm (^{o}C)
SP1650		59.1
Sodium Citrate	0.05 M	60.1
	0.1 M	60.7
	0.15 M	62.5
	0.2 M	63.9
Lactose	5%	59.8
	10%	61.3
	15%	62.5
	20%	67.6
Sorbitol	5%	60.4
	10%	62.0
	15%	63.9
	20%	66.0
Trehalose	5%	60.0
	10%	60.9
	15%	61.5
	20%	63.2
Sucrose	5%	58.4
	10%	59.3
	15%	60.1
	20%	62.2

Table 3.3: Thermal unfolding temperature (Tm) values for three protein antigens (SP1650, SP1732 and SP2216) in the presence of selected stabilizers in a 10mM sodium acetate buffer at pH 5.5. *Reproducible transitions were not available for SP1732 in the presence of arginine

Excipient	SP1650 Tm (°C)	SP1732 T_{onset} (°C)	SP2216 Tm (°C)
Protein	59.1	70.0	33.8
50 µM Manganese Chloride	70.0	70.0	33.8
20% Lactose	68.4	72.5	44.3
20% Dextrose	66.5	72.5	43.3
0.2 M Sodium Citrate	64.0	67.5	33.3
20% Trehalose	63.1	72.5	42.2
20% Sorbitol	62.2	72.5	42.6
20% Sucrose	62.2	72.5	38.8
10% Mannitol	61.6	72.5	38.0
7.5E-6 M Dextran Sulfate	55.0	60.0	32.5
0.3 M Dietanolamine	54.3	65.0	31.2
0.3 M Arginine	51.5	NT*	27.0
0.3 M Guanidine	51.5	70.0	25.5

Table 4.1: The effect of different GRAS compounds on the physical stability of three purified live attenuated canine viruses. The ability to inhibit aggregation of the canine distemper virus (CDV) and the canine adenovirus (CAV2) was measured in a 20 mM citrate phosphate buffer at pH 7. Standard error was calculated to be ±5% based on three individual experiments for the CDV and CAV2. The thermal unfolding temperature (Tm) values for CPI virus in the presence of different excipients were measured by intrinsic fluorescence spectroscopy with the precision of the data on the order of ±0.5^{o}C. ND stands for no data.

Excipient	% Inhibition of CDV	% Inhibition of CAV2	Tm (^{o}C) for CPI
Virus Alone	0	0	52.8
0.2M Sodium Citrate	113	14	56
0.3 M Arginine	108	45	49.9
7.5E-6 M Dextran Sulfate	94	66	52.9
20% Dextrose	77	69	57.0
10% 2-OH propyl g-CD	73	11	52.6
20% Sucrose	69	67	57.3
20% Sorbitol	67	114	57.5
20% Glycerol	62	38	56.3
0.3M Lysine	62	85	53.3
10% 2-OH propyl β-CD	55	18	50.9
20% Trehalose	53	-47	55.0
10% Mannitol	53	ND	55.0
.15M Malic Acid	48	8	52.6
.15M Lactic Acid	41	-26	52.6
.15M Aspartic Acid	40	-52	52.6
0.3M Guanidine	27	-111	47.2
0.3M Dietanolamine	17	26	52.3
0.3M Proline	17	-46	52.6
0.1% Tween 80	16	63	52.6
0.3M Glycine	15	ND	51.3
.15M Ascorbic acid	14	ND	52.6
7.5E-6 M Dextran T70	6	-27	52.6
0.1% Brij 35	5	14	51.3
0.1% Tween 20	0	21	52.7
0.1% Pluronic F-68	0	-2	52.6

Table 4.2: The effect of concentration of selected stabilizers on the thermal unfolding temperature (Tm) values of CDV, CPI and CAV2 viruses as determined by circular dichroism spectroscopy (in the case of CDV and CAV2) and intrinsic fluorescence spectroscopy (in the case of CPI) in a 20 mM citrate phosphate buffer at pH 7. Standard error was calculated to be ±0.5^{o}C. ND stands for no data.

Excipient	Tm (°C) for CDV	Tm (°C) for CPI	Tm (°C) for CAV2
CDV2	49.4	52.7	56.0
25% Sorbitol	62.5	55.8	57.0
20% Sorbitol	56.4	57.5	ND
15% Sorbitol	55.6	55.3	59.1
10% Sorbitol	53.6	54.6	57.5
5% Sorbitol	52.5	52.8	55.0
25% Sucrose	54.9	56.8	56.5
20% Sucrose	54.2	56.8	ND
15% Sucrose	49.8	55.2	56.5
10% Sucrose	51.1	54.4	53.0
5% Sucrose	50.0	53.9	56.1

Figures

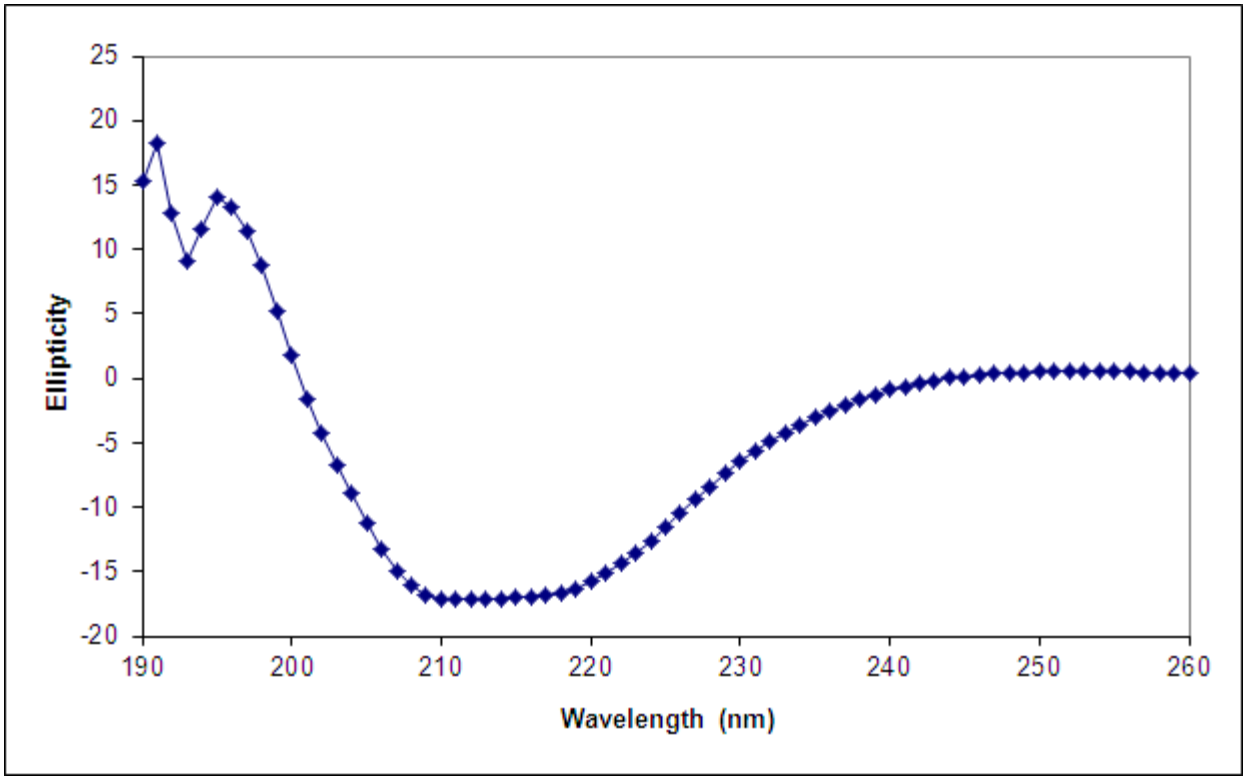

Figure 2.1. Circular dichroism spectrum of HAC1 at 10 °C.

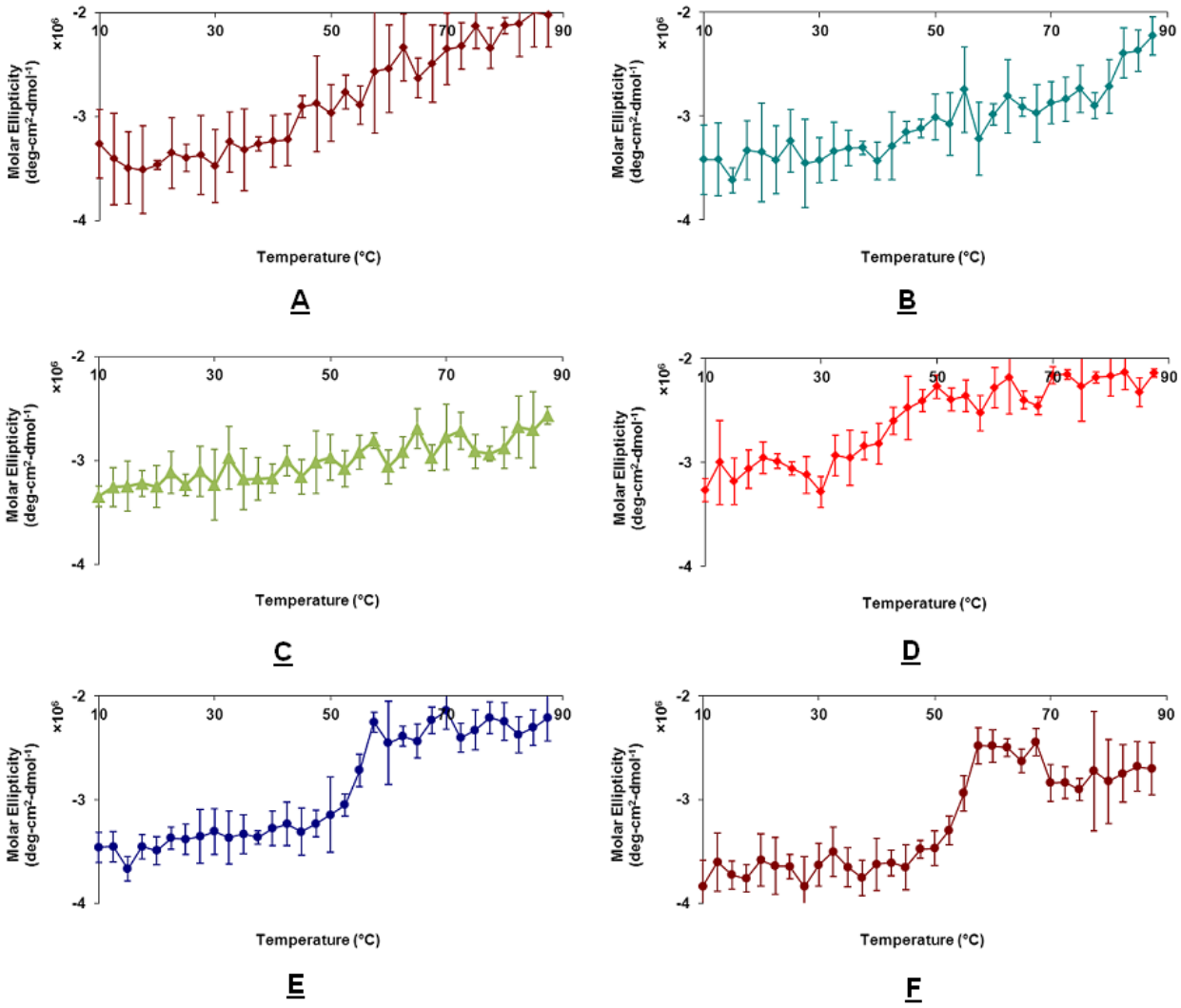

Figure 2.2. Circular dichroism thermal melt plots of HAC1 in imidazole buffer. The molar ellipticity at 222 nm was monitored as a function of temperature for six pH conditions—pH 3.0 (A), 4.0 (B), 5.0 (C), 6.0 (D), 7.0 (E) and 8.0 (F).

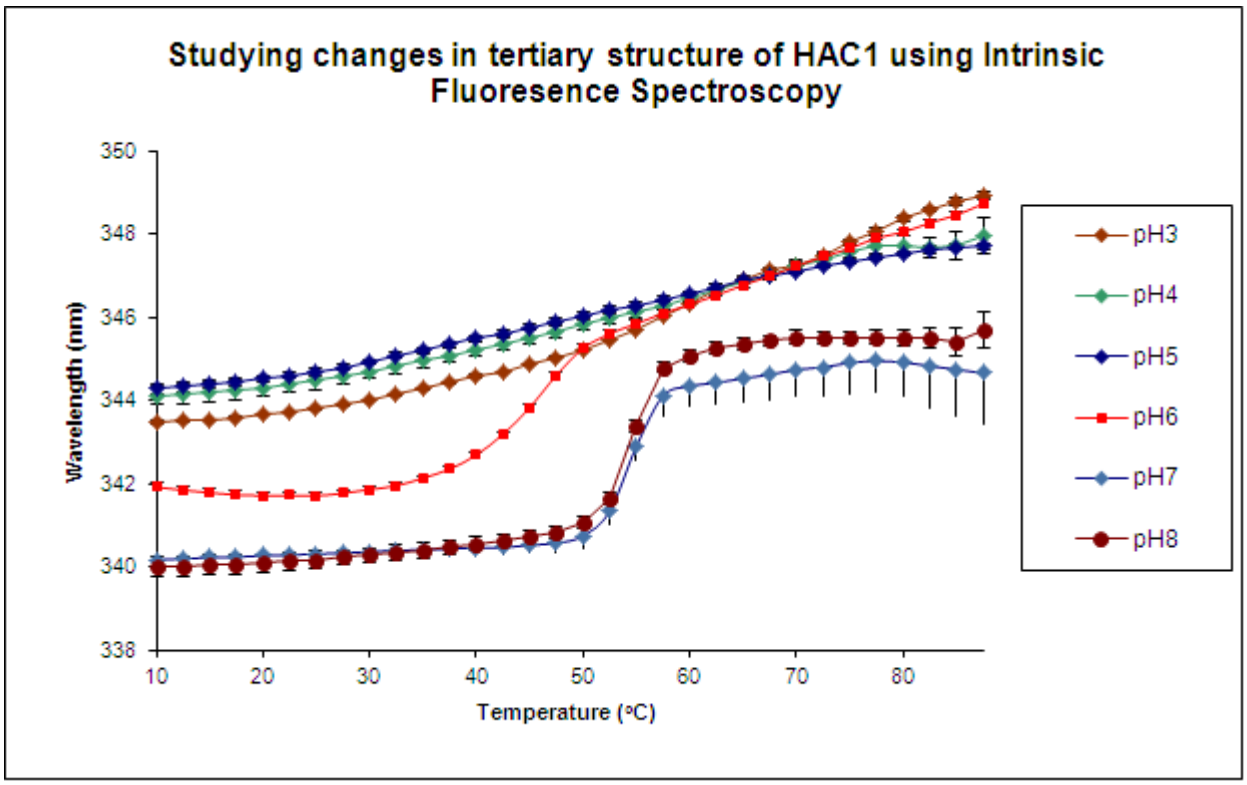

Figure 2.3. Intrinsic fluorescence peak position changes as a function of temperature for the pH range 3.0-8.0. Peak positions are determined by the mean spectral center of mass (msm) method, which shifts the actual peak positions by 8-10 nm towards the red.

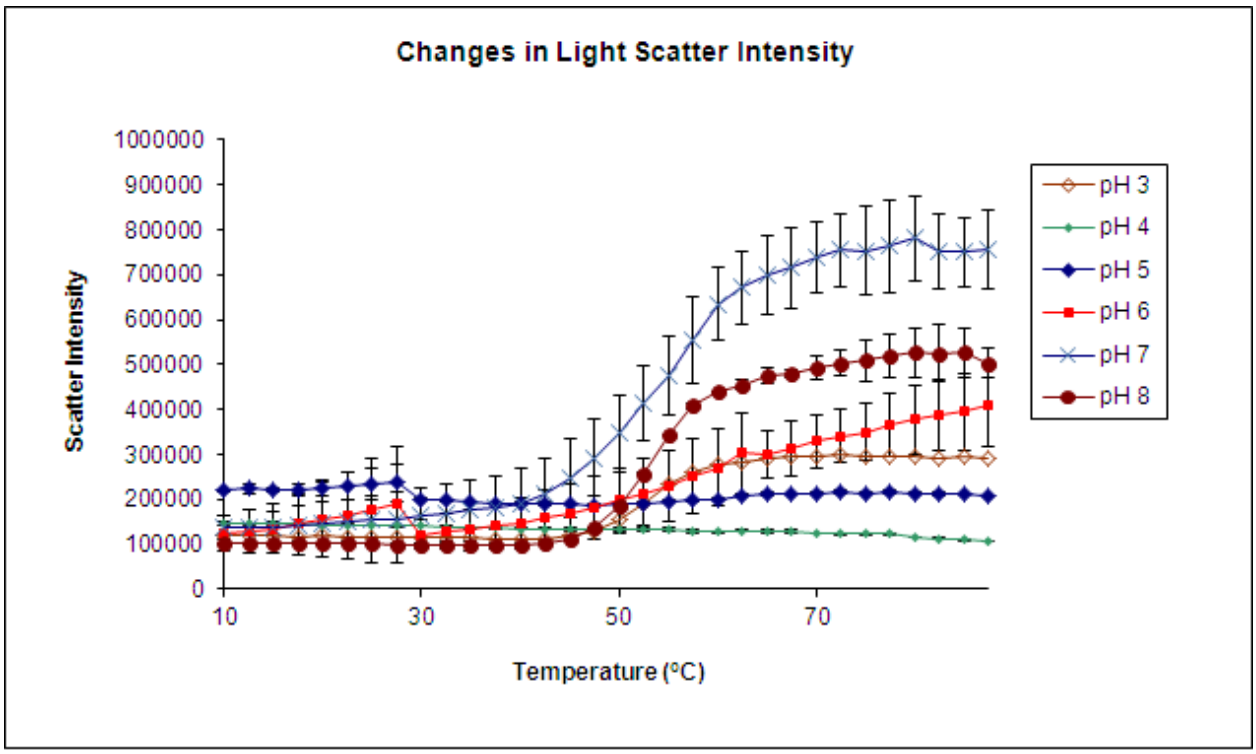

Figure 2.4. Static light scattering intensity changes as a function of temperature for the pH range 3.0-8.0. Static light intensity was determined by monitoring scattered light at the fluorescence excitation wavelength (295 nm).

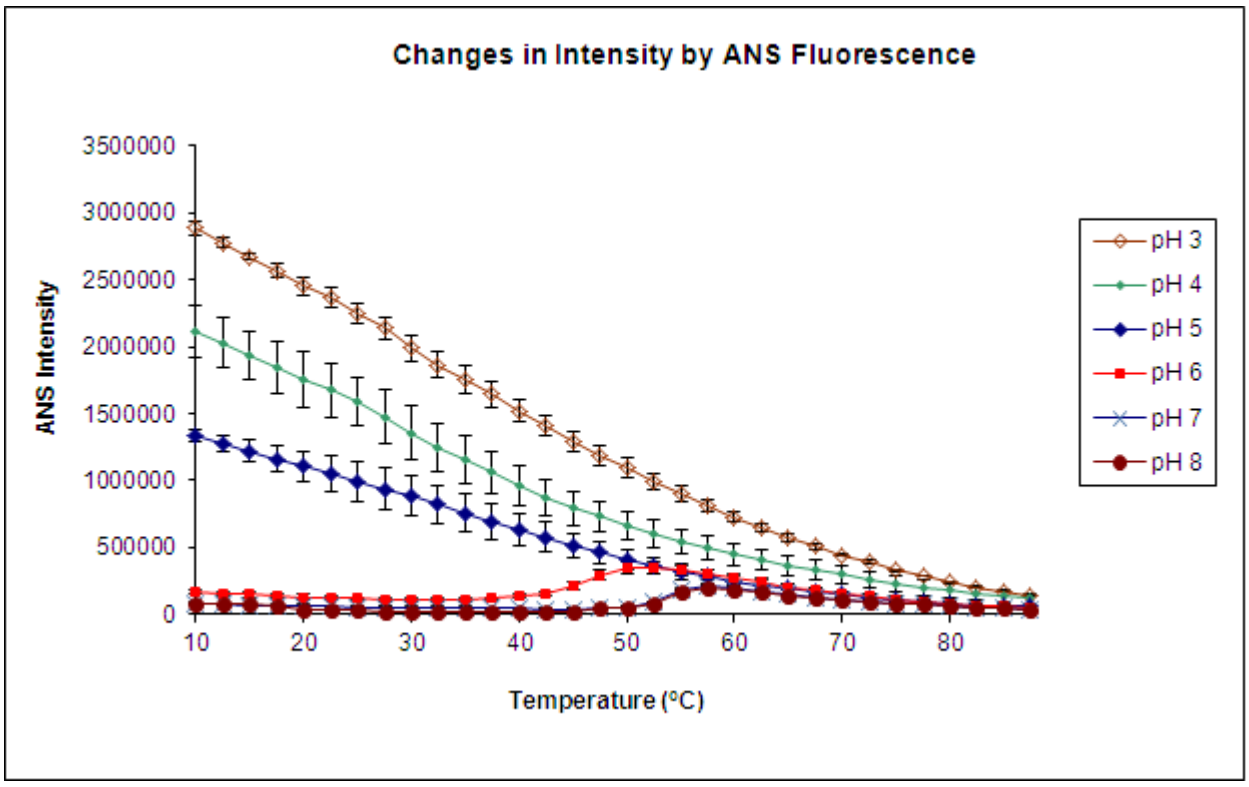

Figure 2.5. ANS fluorescence intensity changes as a function of temperature for the pH range from 3.0-8.0 for HAC1. Peak intensities are determined by the mean spectral center of mass (msm) method.

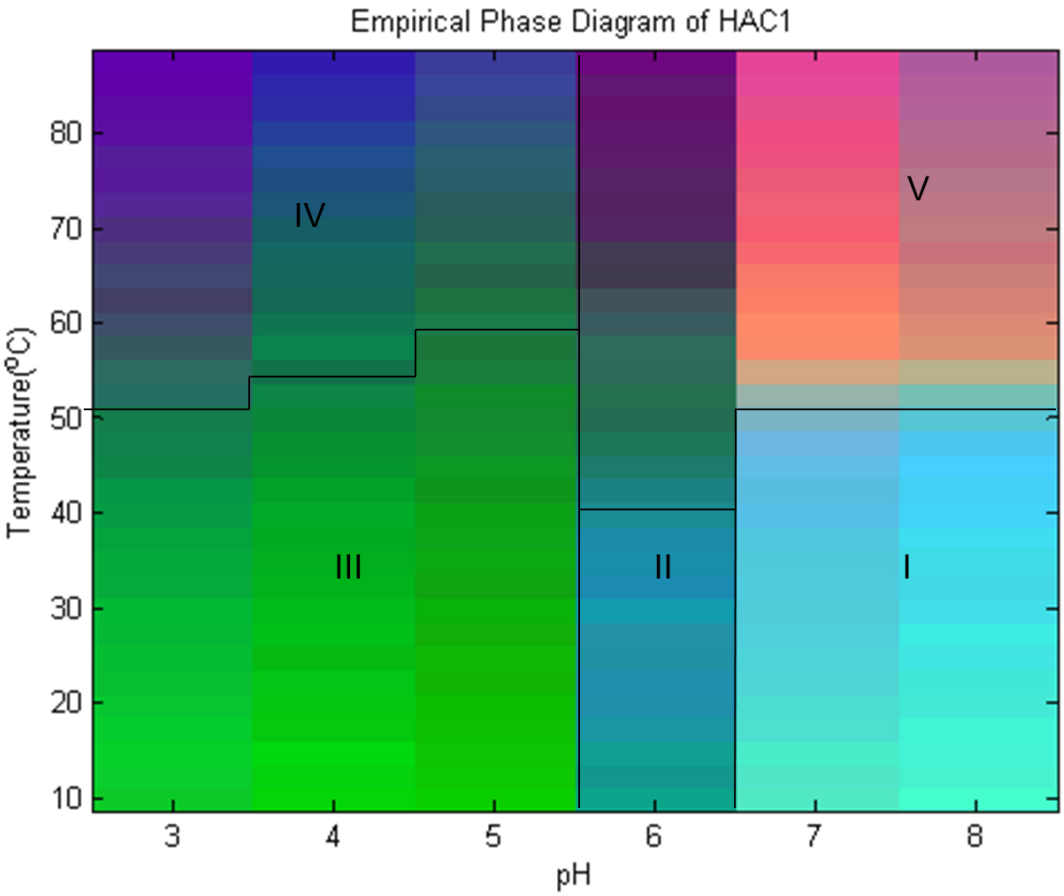

Figure 2.6. An empirical phase diagram (EPD) constructed using intrinsic and extrinsic fluorescence, circular dichroism and static light scattering techniques for HAC1.

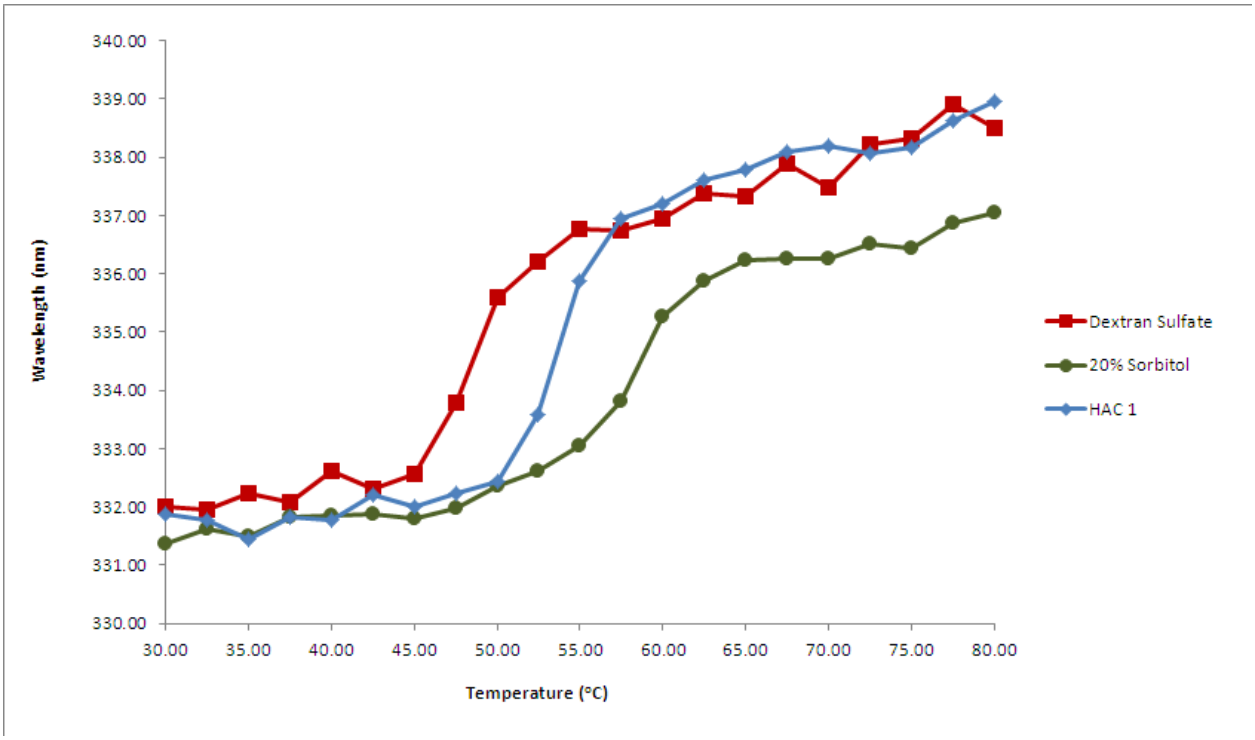

Figure 2.7. Comparison of thermal unfolding profiles of HAC1 in the presence of selected different stabilizers and destabilizers. Excipients are prepared in imidazole buffer (10 mM imidazole, pH 7.0, I=0.15 M adjusted with NaCl).

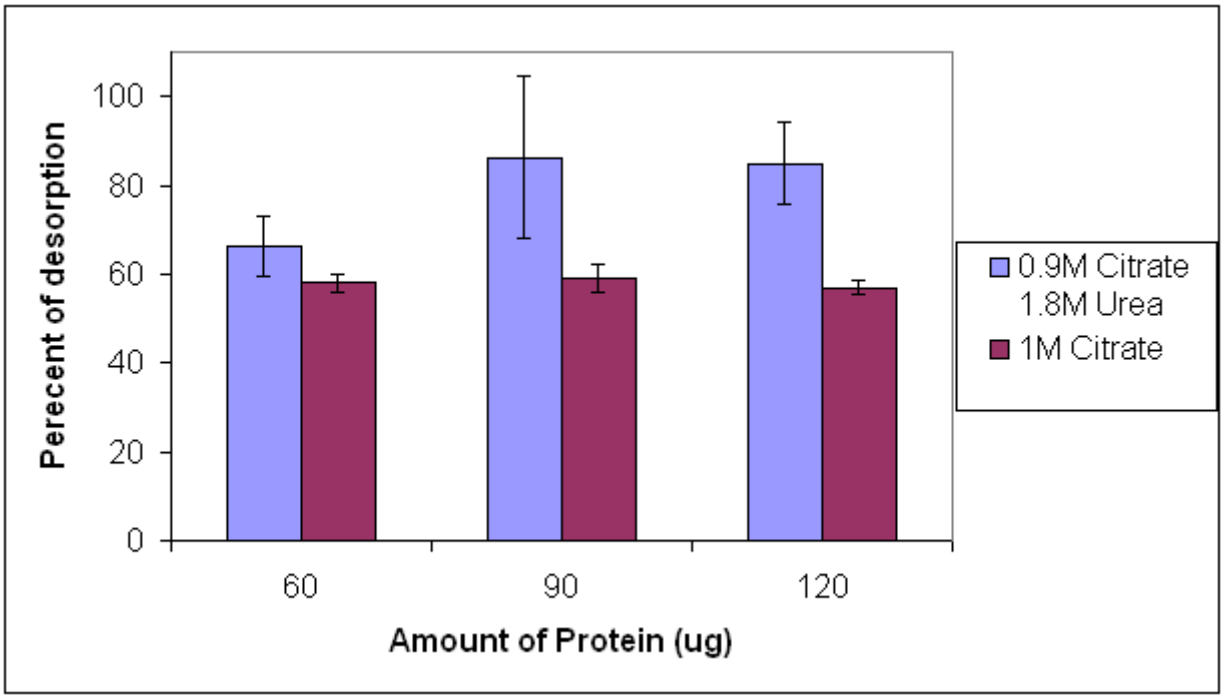

Figure 2.8. Desorption of HAC1 from adjuvant surface. Over 80% of HAC1 is desorbed from Alhydrogel® in the presence of a combination of 0.9 M sodium citrate and 1.8 M urea. The error bars reflect the standard deviations based on three different experiments.

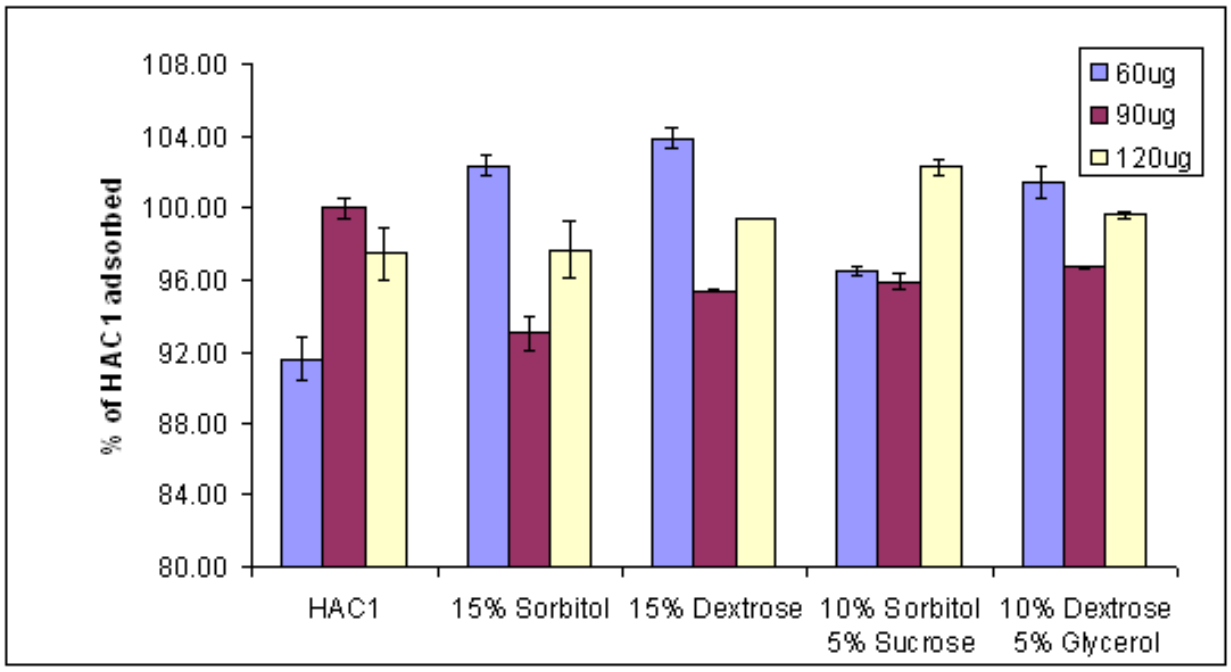

Figure 2.9. Effect of selected stabilizers on the adsorption of HAC1 onto Alhydrogel®. Alhydrogel® was added to the mixture of HAC1 and the excipient. The error bars reflect the standard deviations based on three different experiments

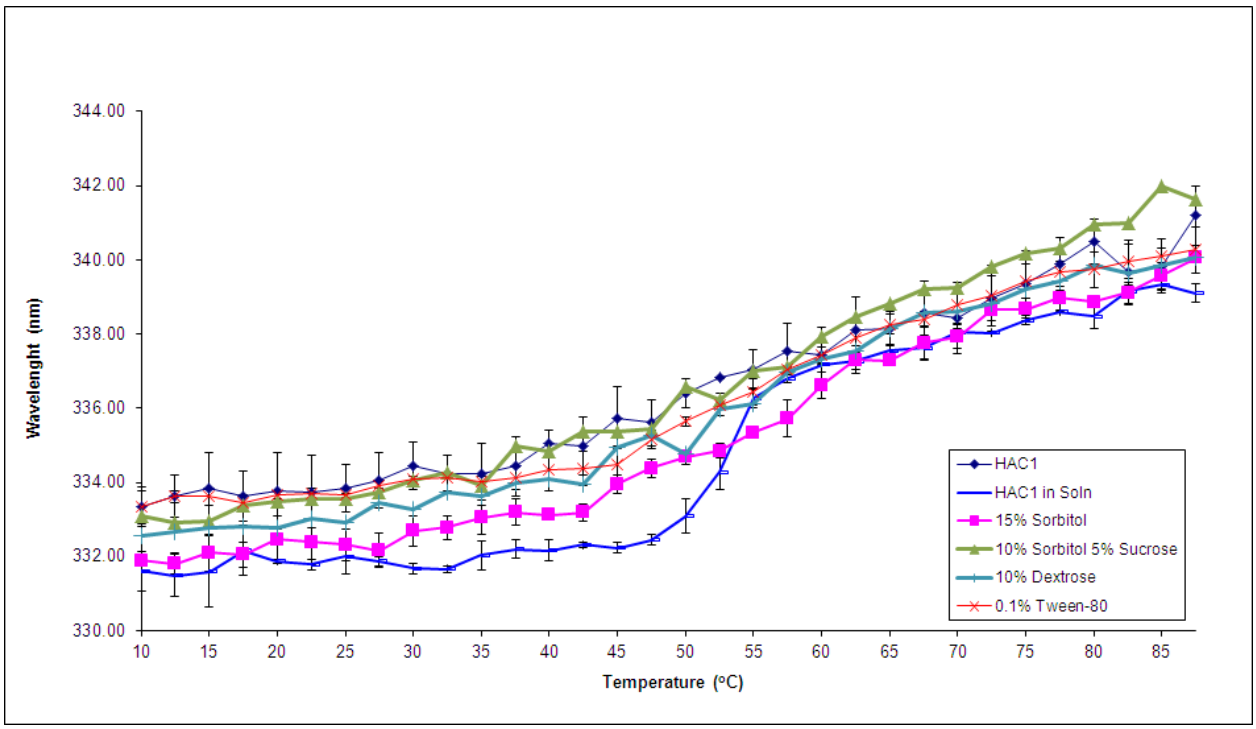

Figure 2.10. Intrinsic fluorescence based melting curves of HAC1 in the presence of selected excipients and Alhydrogel®. The excipients shown here were selected by screening in liquid formulations.

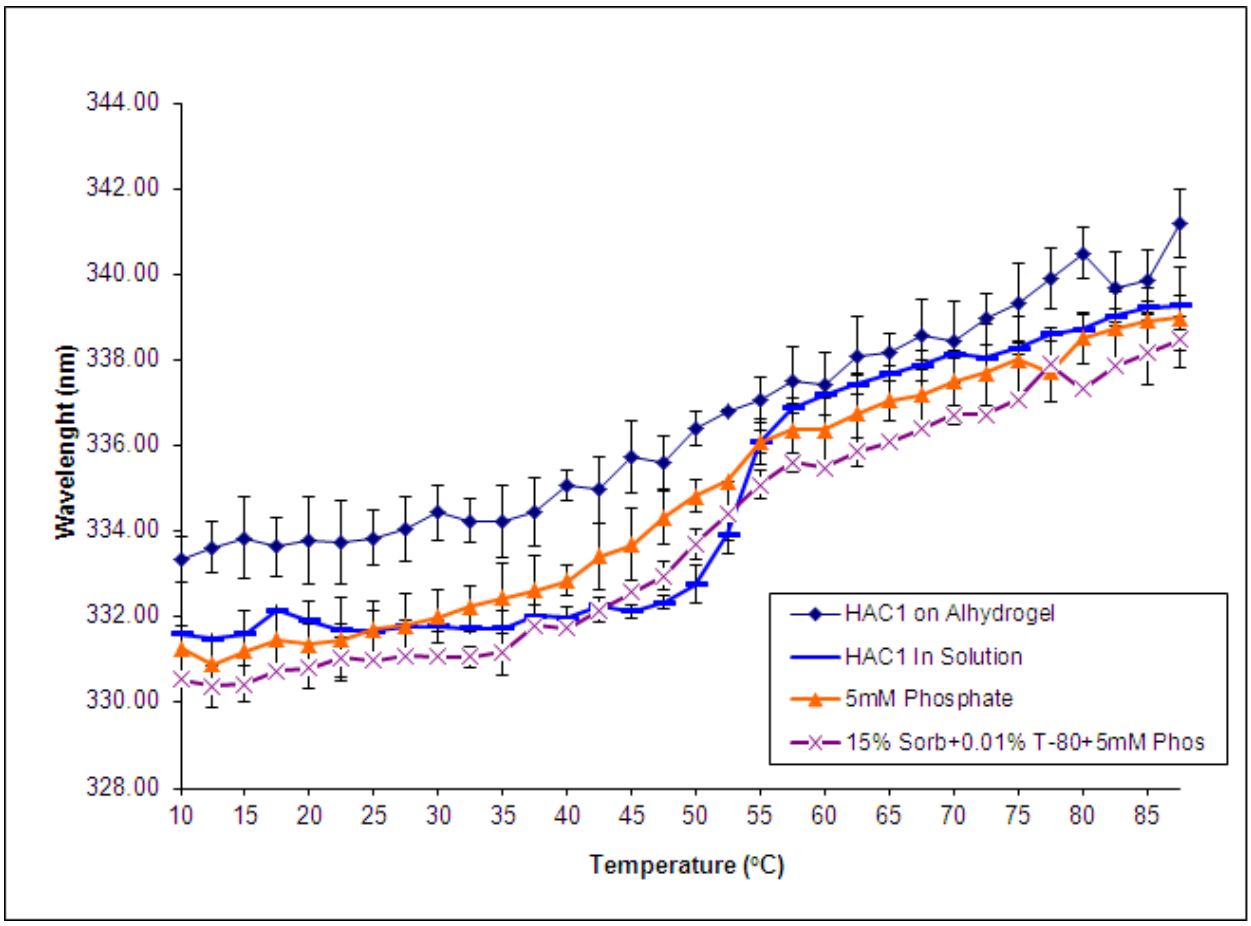

Figure 2.11. Intrinsic fluorescence based melting curves of HAC1 in the presence of best stabilizers identified for adjuvanted formulation. The error bars reflect the standard deviations based on three different experiments.

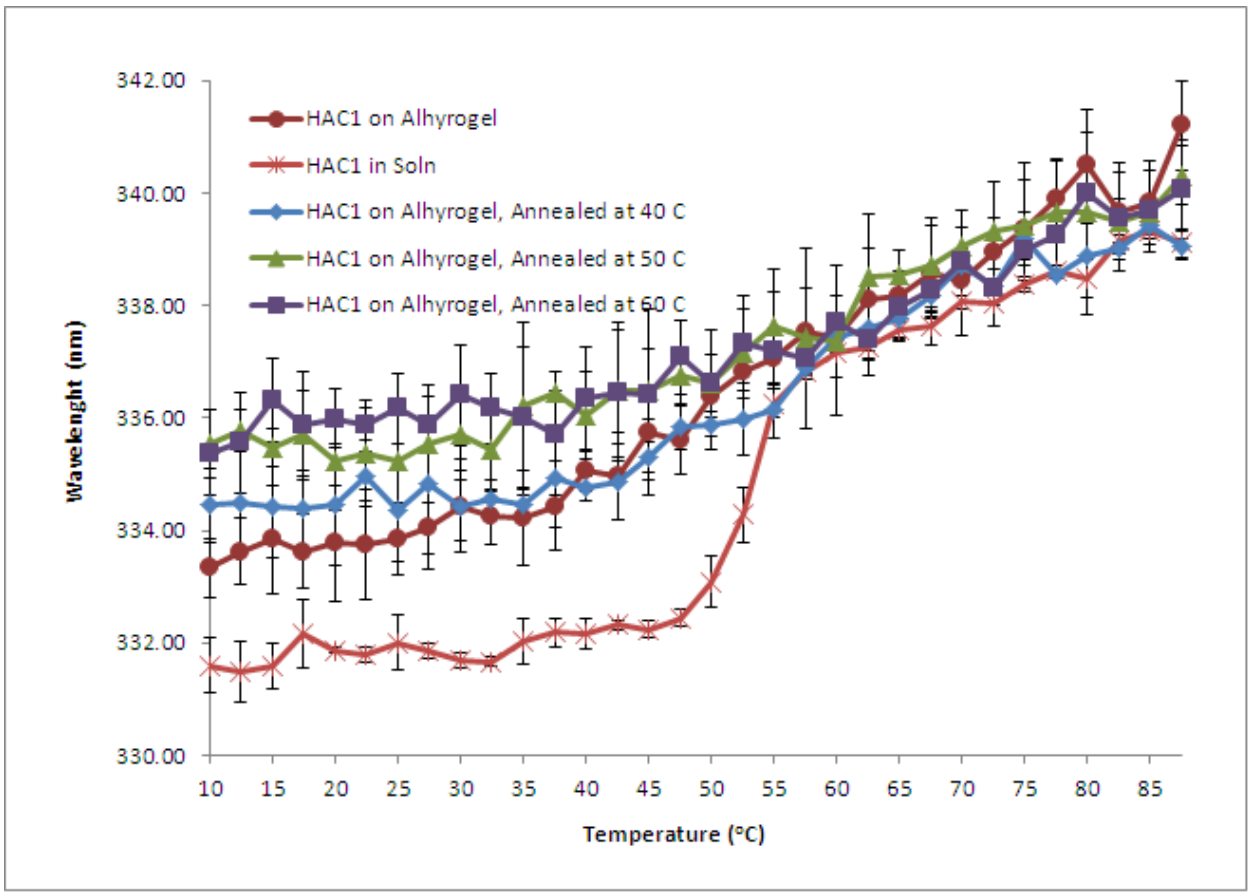

Figure 2.12. Intrinsic fluorescence based melting curves of annealed HAC1 in the presence of Alhydrogel®.

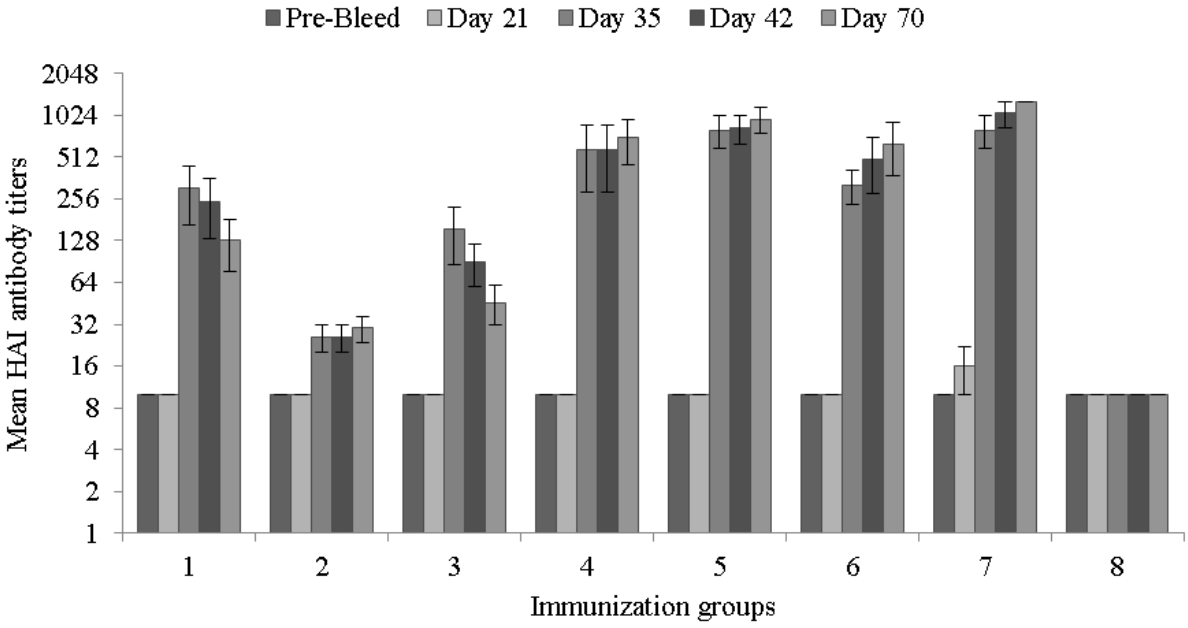

Figure 2.13. Hemagglutination-inhibition (HAI) antibody titers in sera from immunized mice. HAI titers are expressed as mean titers for each immunization group with standard deviations. Samples without detectable HAI were assigned a titer of 1:10.

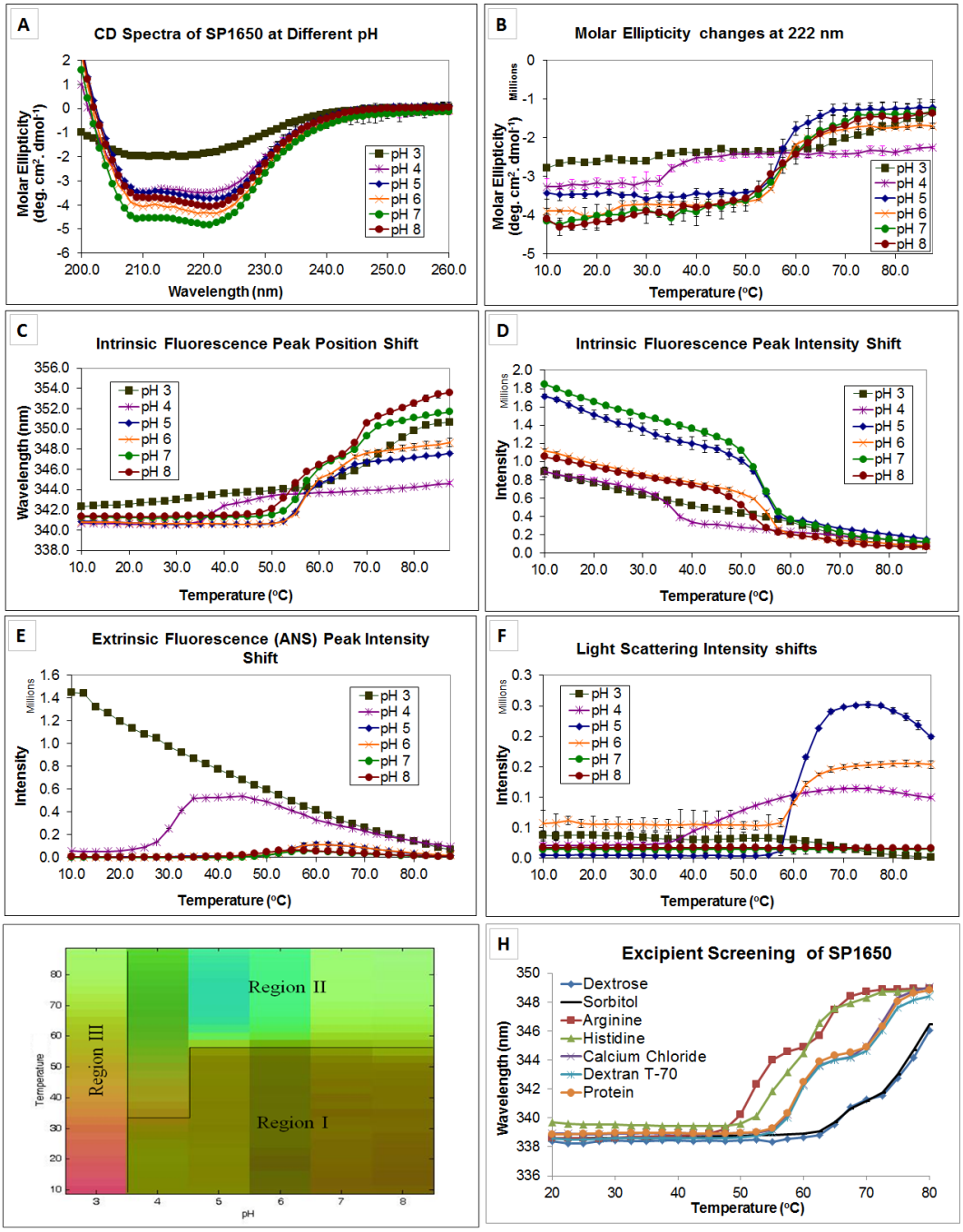

Figure 3.1: Biophysical characterization and excipient screening for protein antigen SP1650. (A) CD spectra of SP1650 at different pH values at 10°C, (B) CD melts of SP1650 at different pH values, (C) Intrinsic fluorescence peak position shifts for SP1650 as a function of pH and temperature, (D) Intrinsic fluorescence peak intensity changes for SP1650, (E) Extrinsic fluorescence peak intensity changes for SP1650 using ANS, (F) Static light scattering intensity shifts as a function of pH and temperature, (G) Empirical phase diagram for SP1650, and (H) Intrinsic fluorescence peak position shifts for SP1650 in the presence of selected excipients.

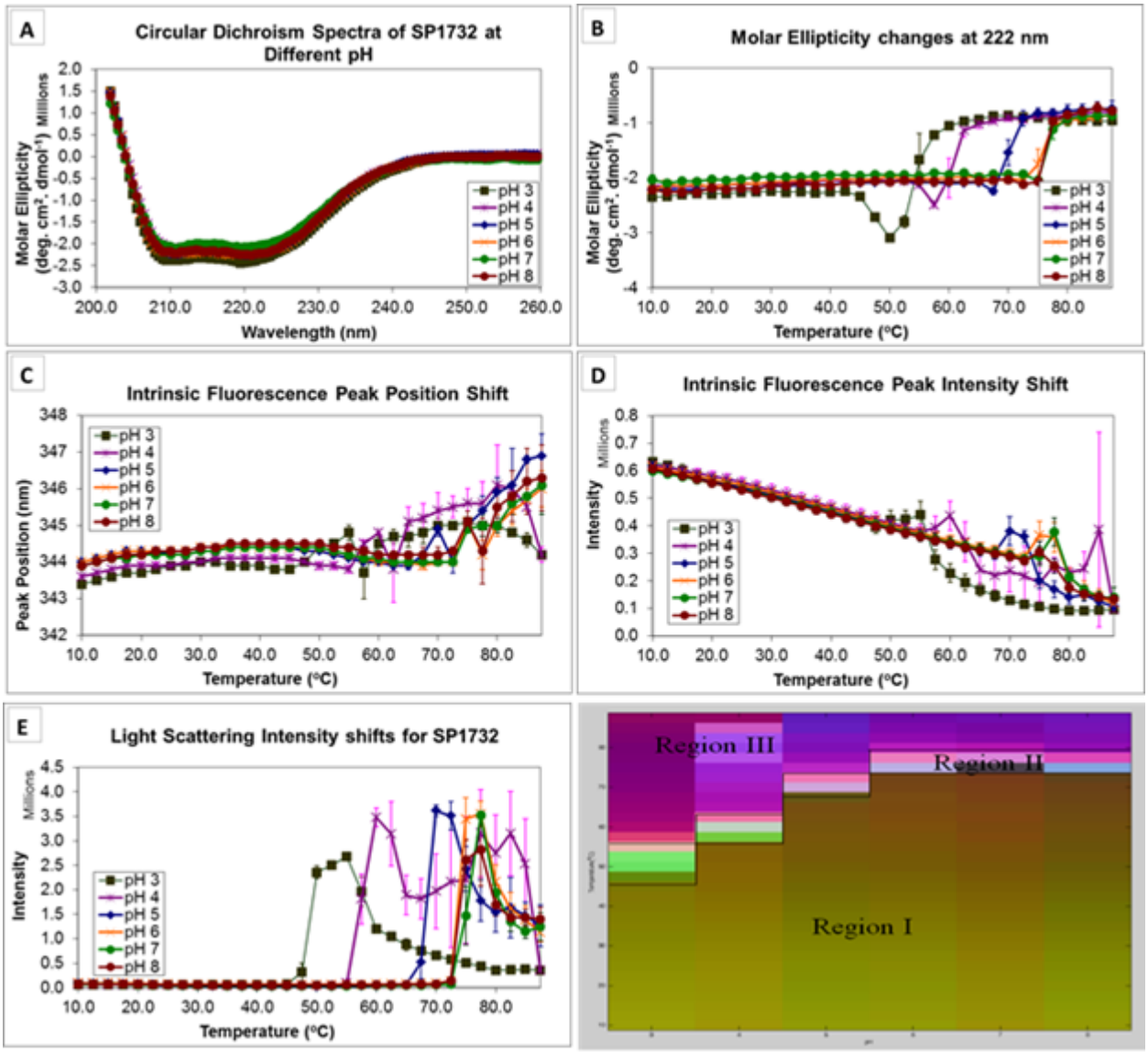

Figure 3.2: Biophysical characterization and excipient screening for protein antigen SP1732. (A) CD spectra of SP1732 at different pH values at 10°C, (B) CD melts of SP1732 at different pH values, (C) Intrinsic fluorescence peak position shifts for SP1732 as a function of pH and temperature, (D) Intrinsic fluorescence peak intensity changes for SP1732, (E) Static light scattering intensity shifts as a function of pH and temperature, and (F) Empirical phase diagram for SP1732.

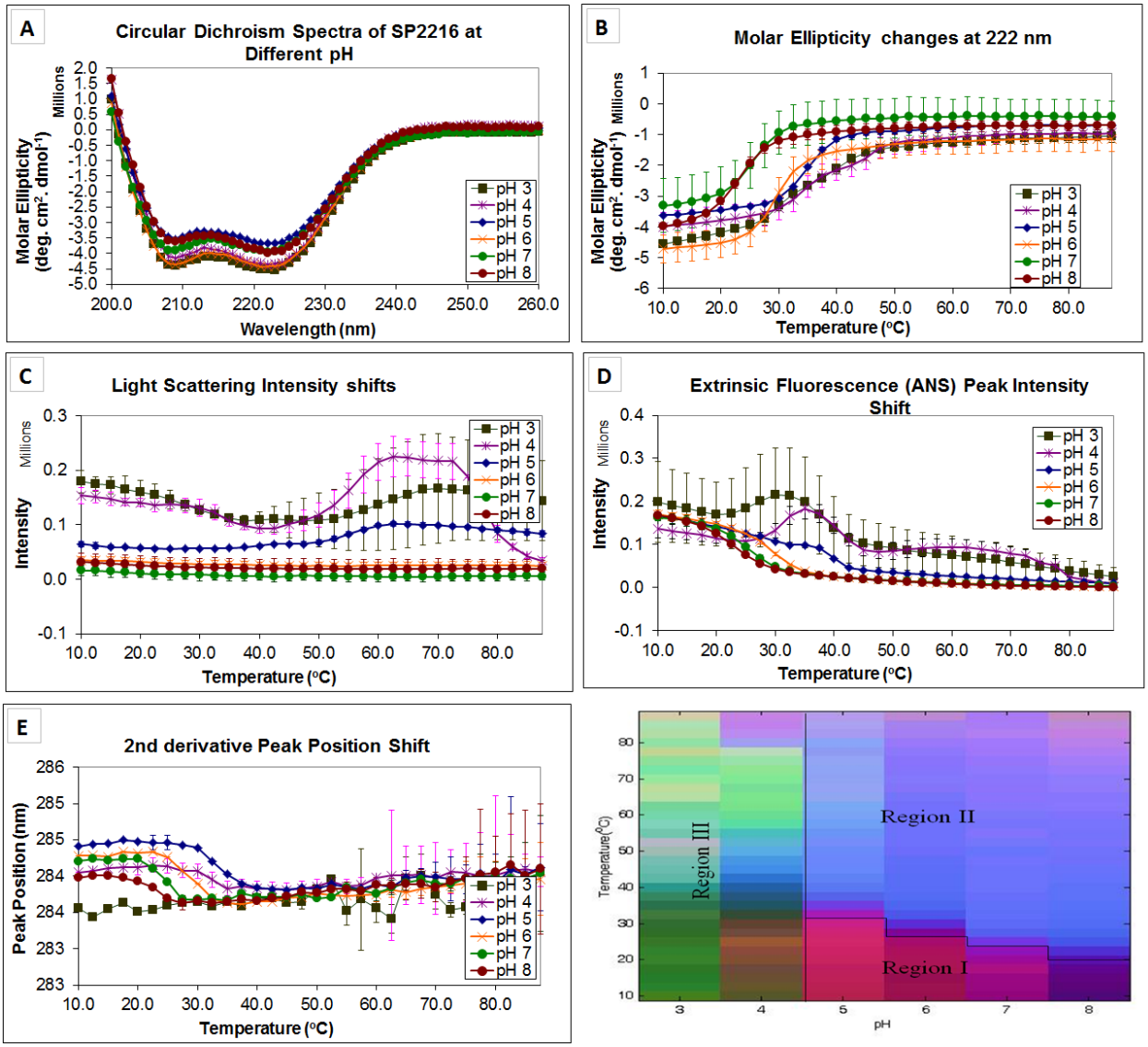

Figure 3.3: Biophysical characterization and excipient screening for protein antigen SP2216. (A) CD spectra of SP2216 at different pH values at 10°C, (B) CD melts of SP2216 at 222 nm at different pH values, (C) Static light scattering intensity shifts as a functions of pH and temperature, (D) Extrinsic fluorescence peak intensity changes using ANS, (E) second derivative UV melts of SP2216 as a function of pH and temperature, and (F) Empirical phase diagram for SP2216.

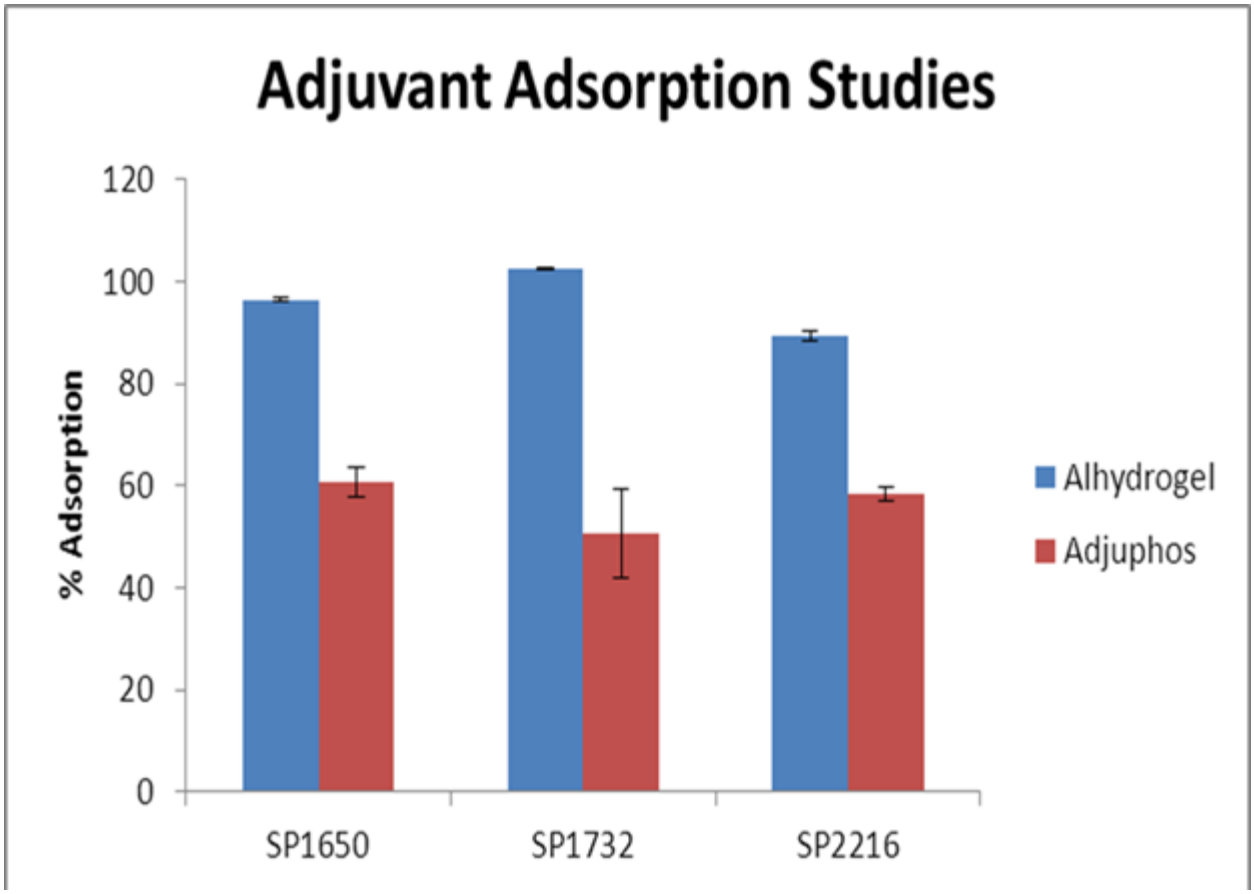

Figure 3.4: Percent adsorption of the three protein antigens (SP1650, SP1732, SP2216) to two different aluminum salt adjuvants, Alhydrogel and Adjuphos. 70 µg of protein was adsorbed onto 50 µg of adjuvant in a 10 mM sodium acetate buffer at pH 5.5.

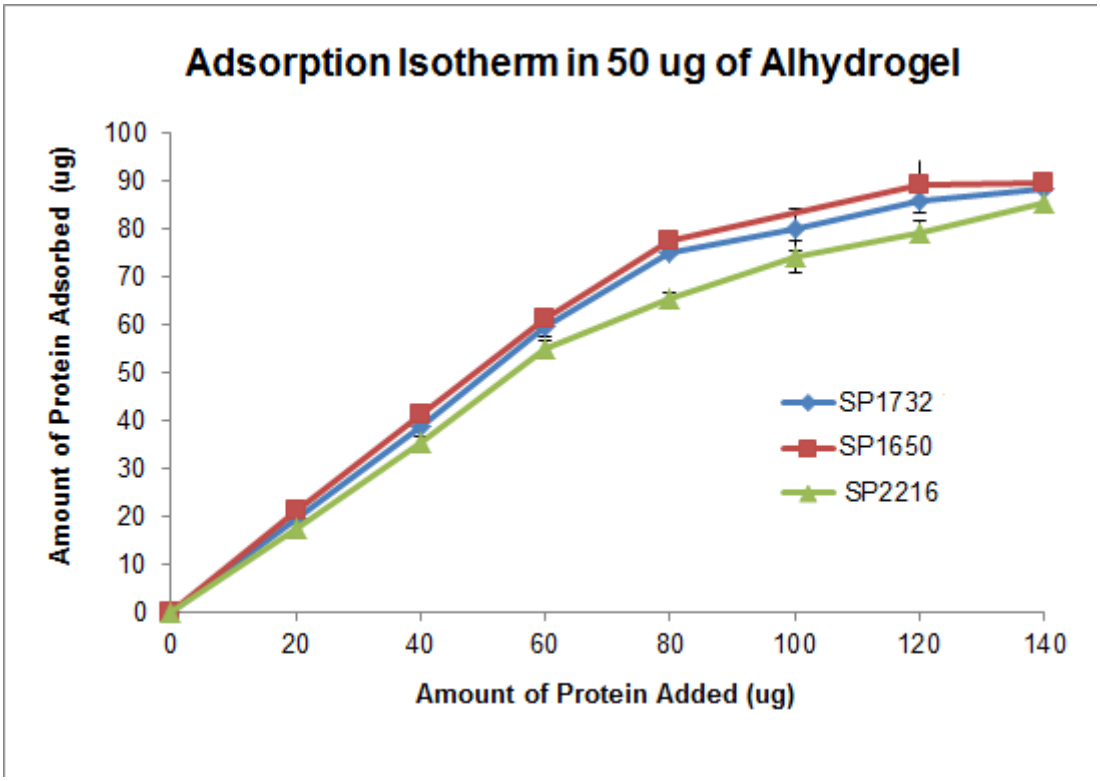

Figure 3.5: Adsorption isotherms for the three protein antigens (SP1650, SP1732, SP2216) to aluminum hydroxide adjuvant (Alhydrogel) in a 10 mM sodium acetate buffer at pH 5.5.

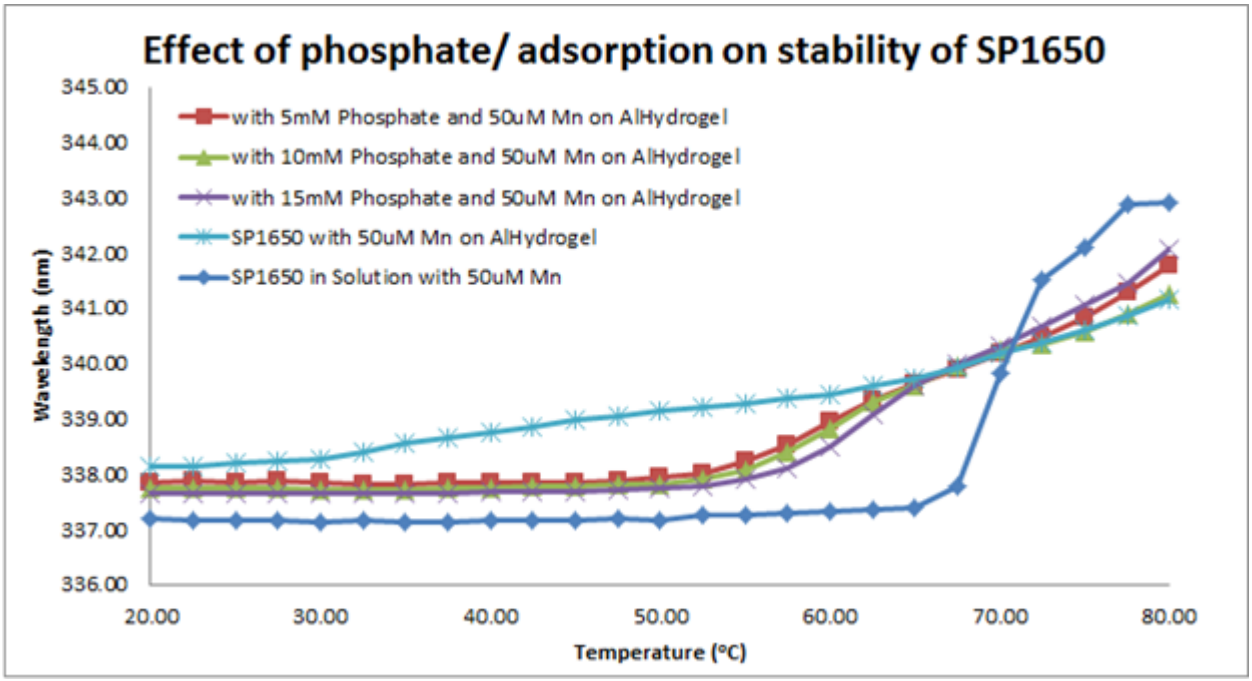

Figure 3.6: Intrinsic fluorescence emission maximum as a function of temperature for SP1650 in solution and while adsorbed to Alhydrogel in a 10 mM sodium acetate buffer at pH 5.5. The effect of manganese on protein stability in solution and in presence of Alhydrogel is shown along with the effect phosphate on the stability of the adsorbed protein.

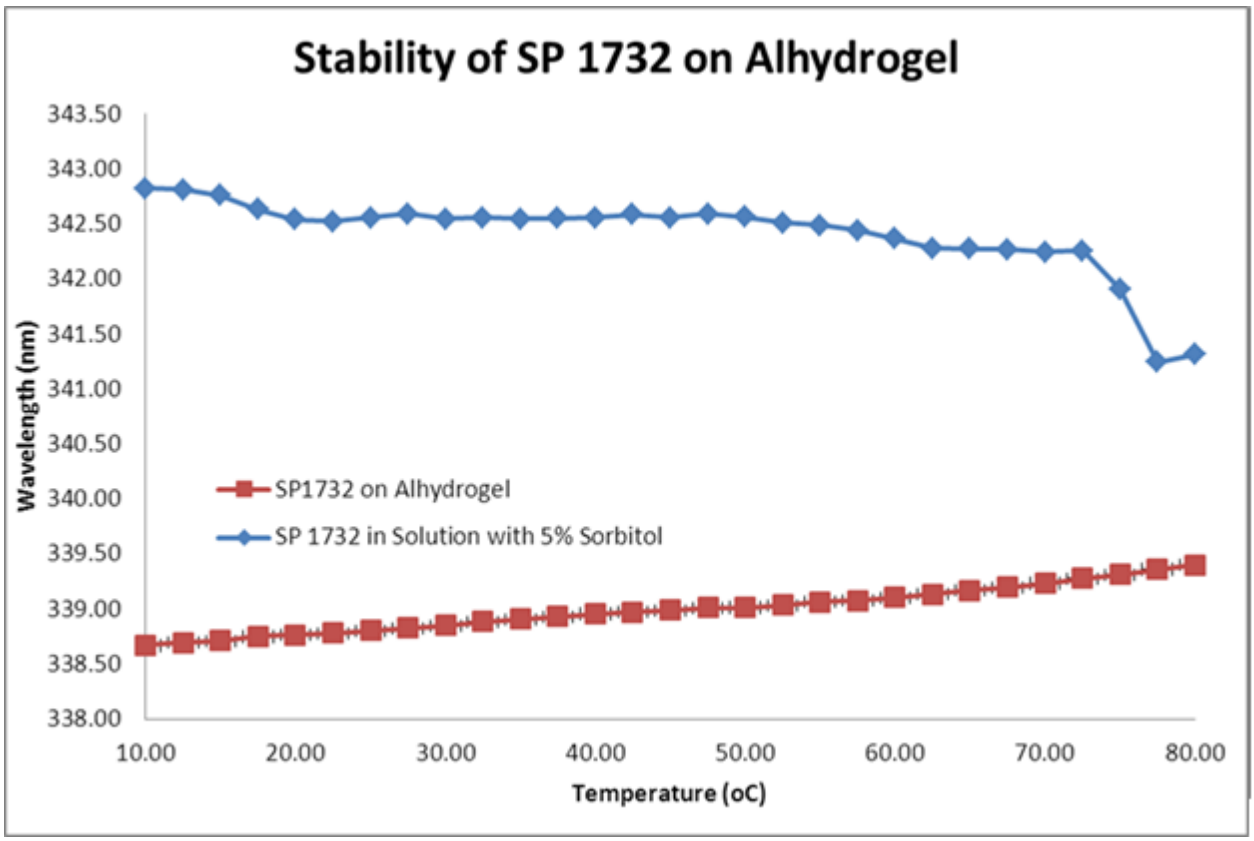

Figure 3.7: Intrinsic fluorescence emission maximum as a function of temperature for SP1732 in solution and on Alhydrogel in a 10 mM sodium acetate buffer at pH 5.5.

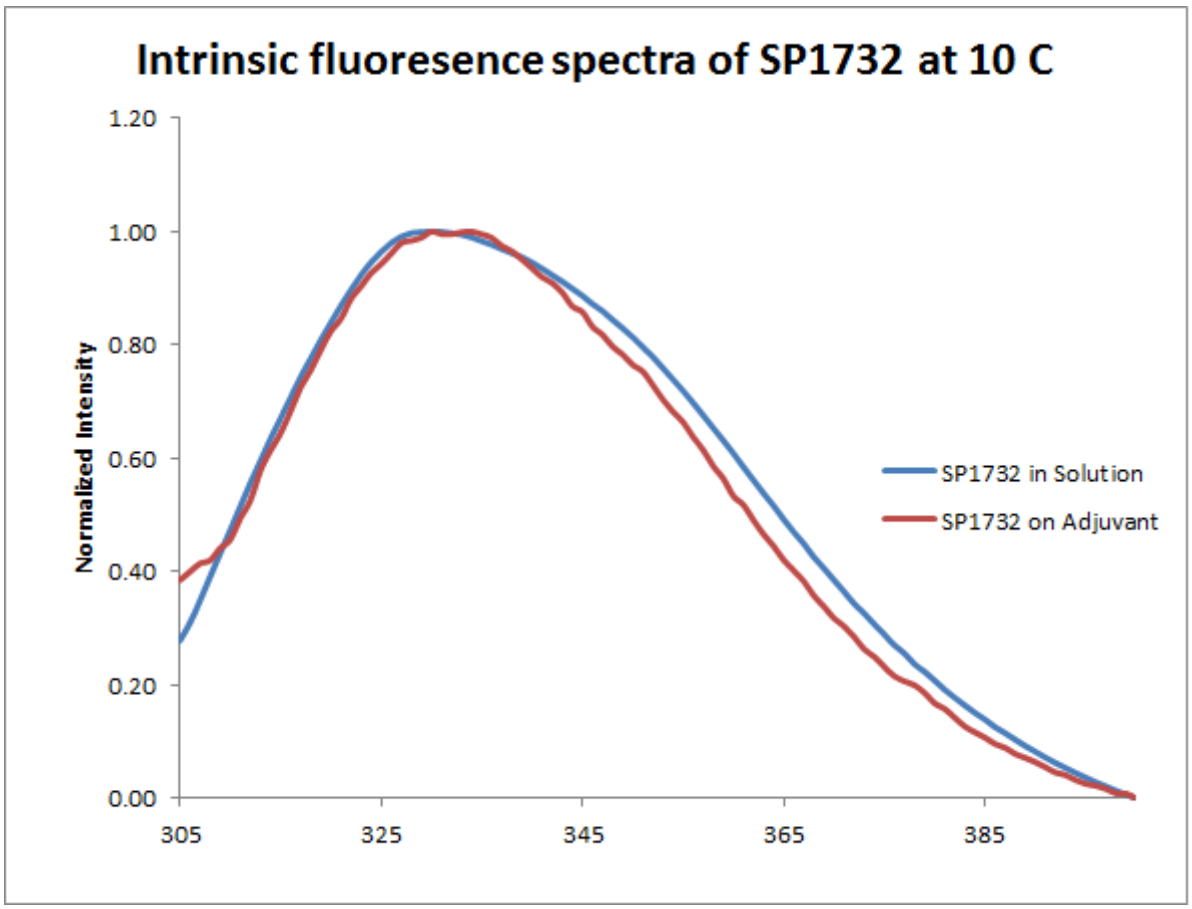

Figure 3.8: Representative tryptophan fluorescence spectra of SP2216 at 10°C in solution and adsorbed to the adjuvant.

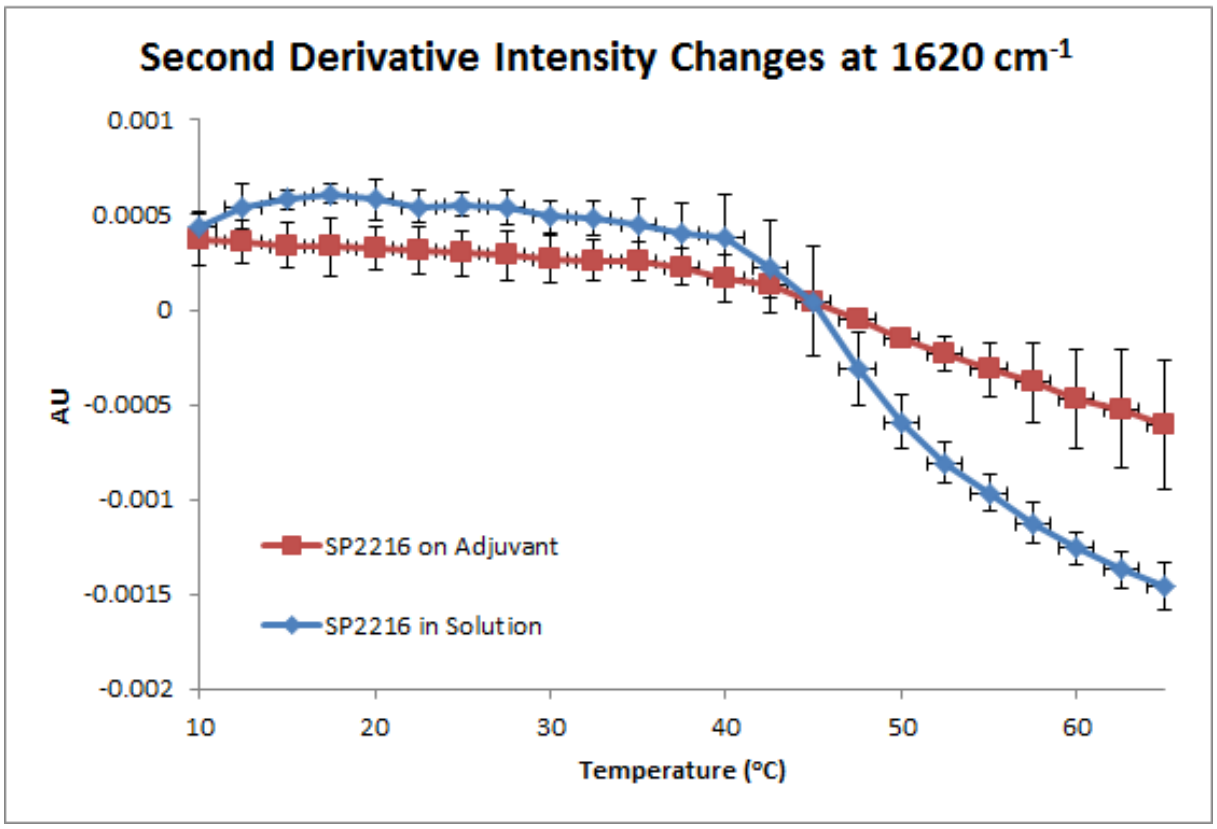

Figure 3.9: FTIR Second derivative peak intensity changes at 1620 cm^{-1} as a function of temperature for SP2216 in solution and on Alhydrogel in a 10 mM sodium acetate buffer at pH 5.5.

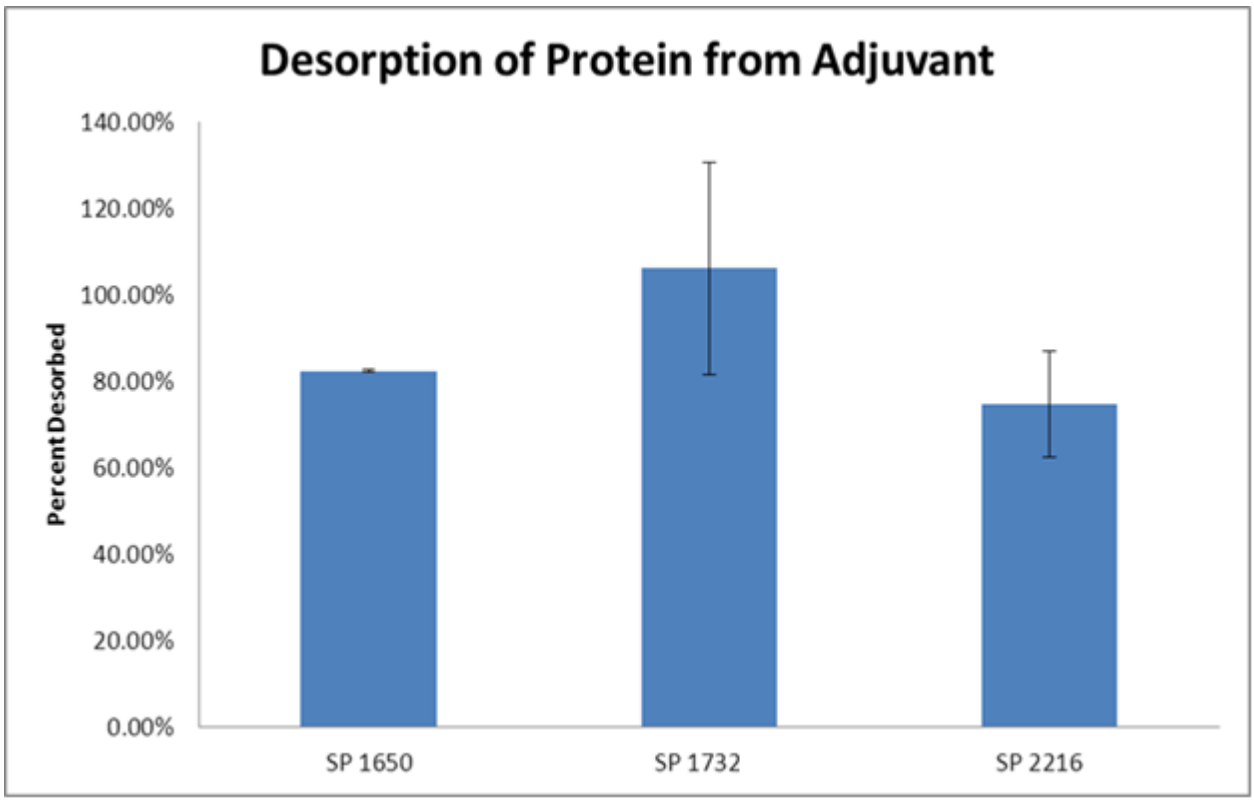

Figure 3.10: Desorption of the three protein antigens from aluminum hydroxide adjuvant (Alhydrogel). SP1650 was desorbed from adjuvant using a solution containing 1M sodium citrate and 2M urea. SP1732 and SP2216 were desorbed using 2M Guanidine.

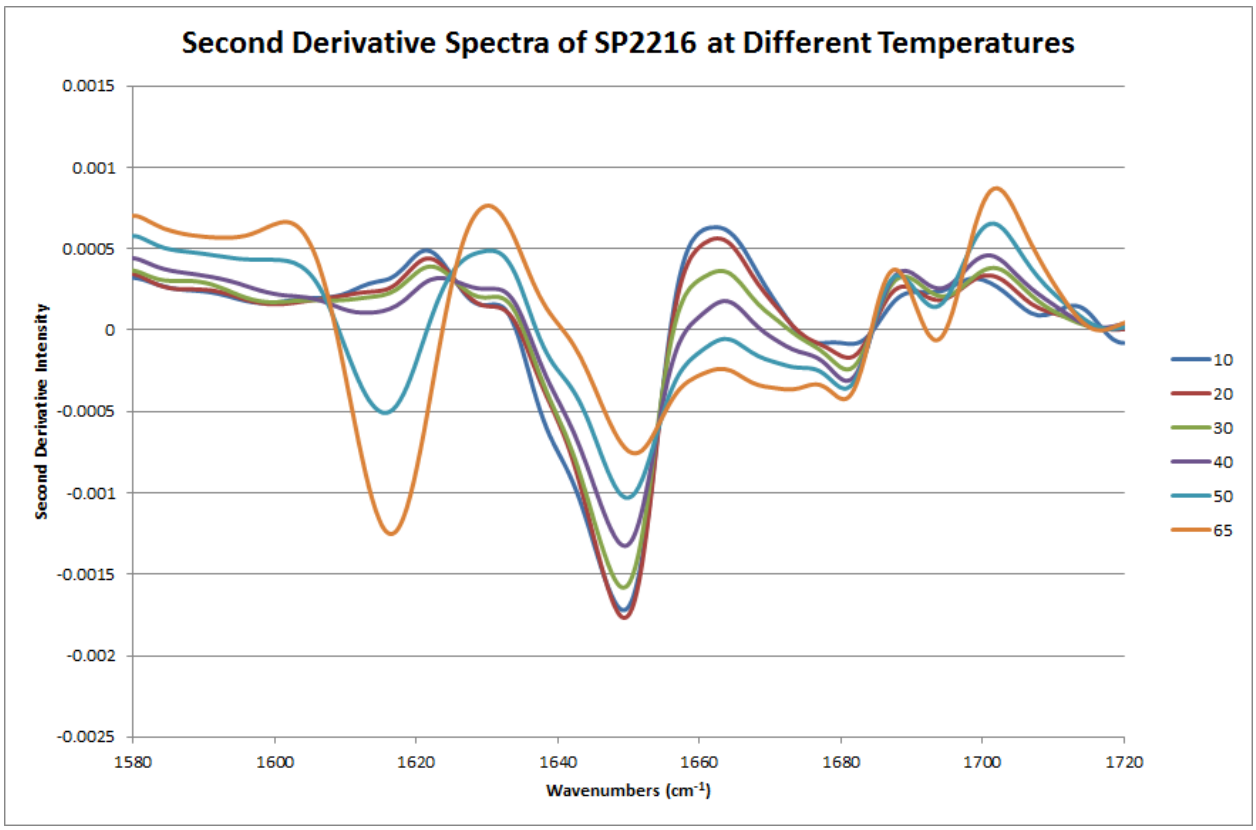

Figure 3.11: Representative second derivative FTIR spectra of SP2216 at different temperatures in a 10mM sodium acetate buffer at pH 5.5.

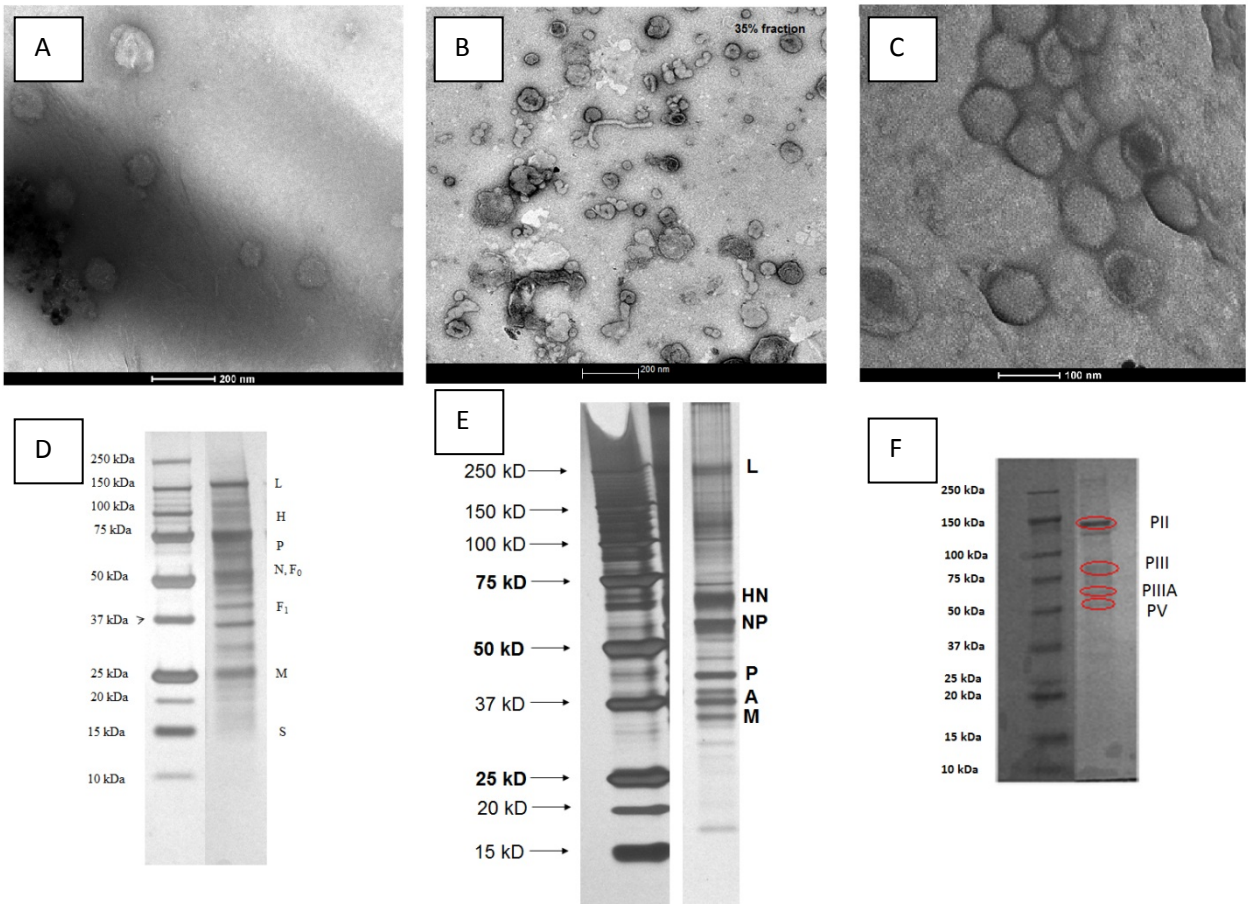

Figure 4.1. TEM images of three live attenuated canine viruses after purification (A) CDV,(B) CPI and (C) CAV2, along the SDS-PAGE gel image of the individual purified virus samples (D) CDV,(E) CPI and (F) CAV2. The marker for the gels is shown on the left along with the virus samples on the right.

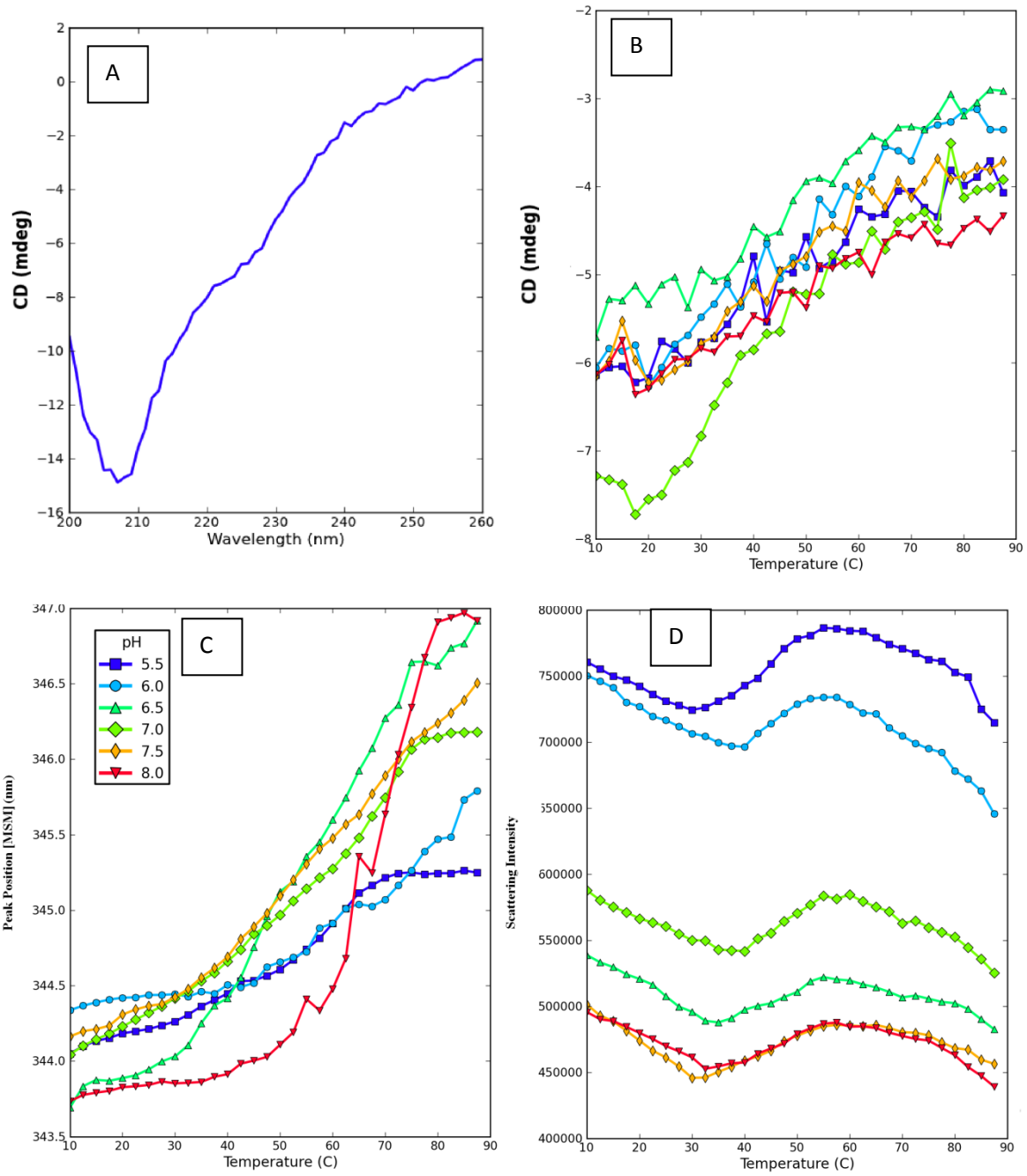

Figure 4.2. Biophysical characterization data for the purified canine distemper virus in a 20 mM citrate phosphate buffer. (A) CD spectrum of CDV at pH 7 and 10^{o}C. (B) CD signal at 222 nm, (C) changes in fluorescence peak position as analyzed by MSM, and (D) changes in the static light scattering intensity at different pH values as a function of temperature. Error bars are not included for clarity of data.

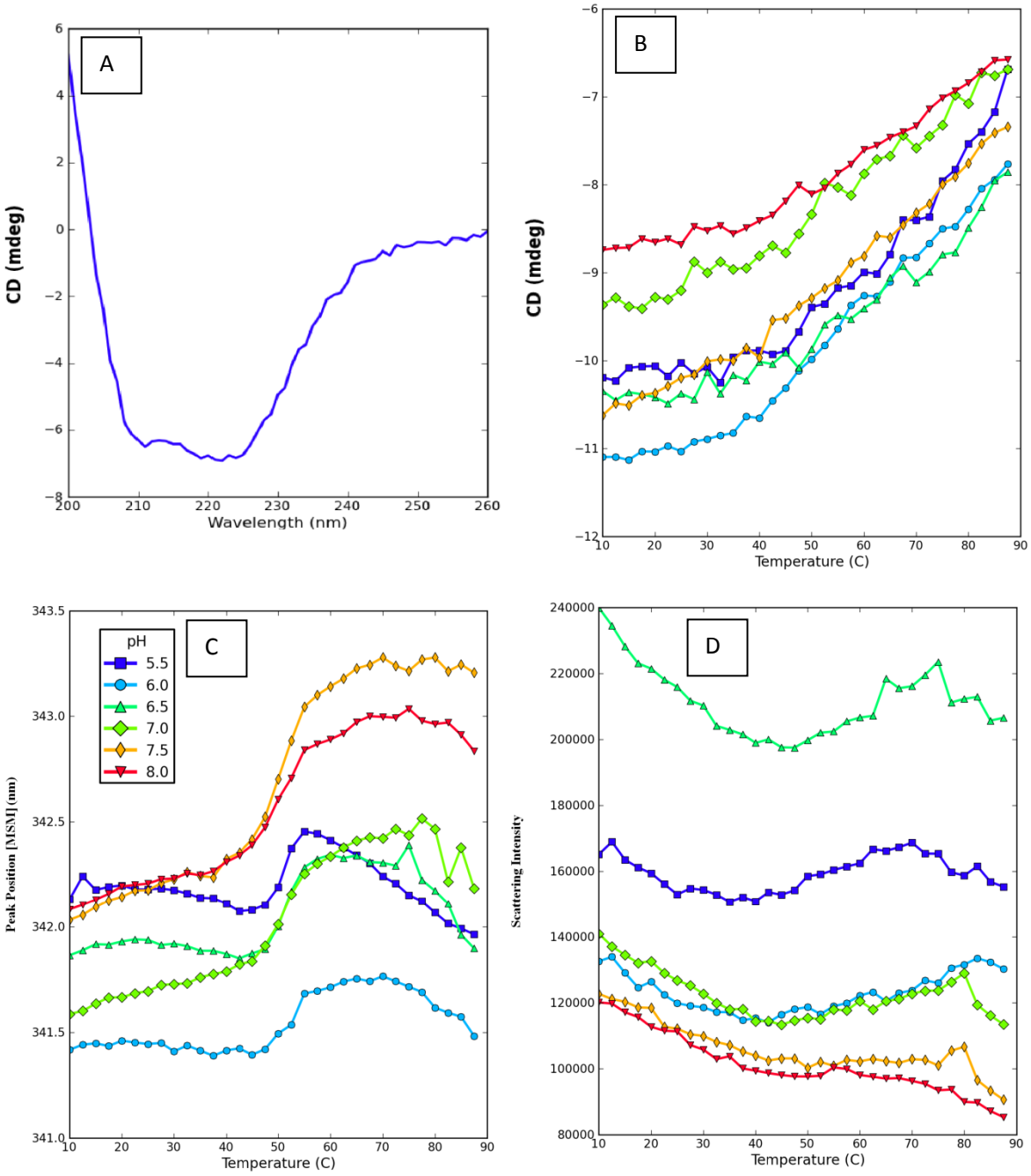

Figure 4.3. Biophysical characterization data for purified canine parainfluenza virus in a 20 mM citrate phosphate buffer. (A) CD spectrum of CPI at pH 7 and 10°C. (B) CD signal at 222 nm, (C) changes in fluorescence peak position as analyzed by MSM, and (D) changes in the static light scattering intensity at different pH values as a function of temperature. Error bars are not included for clarity of data.

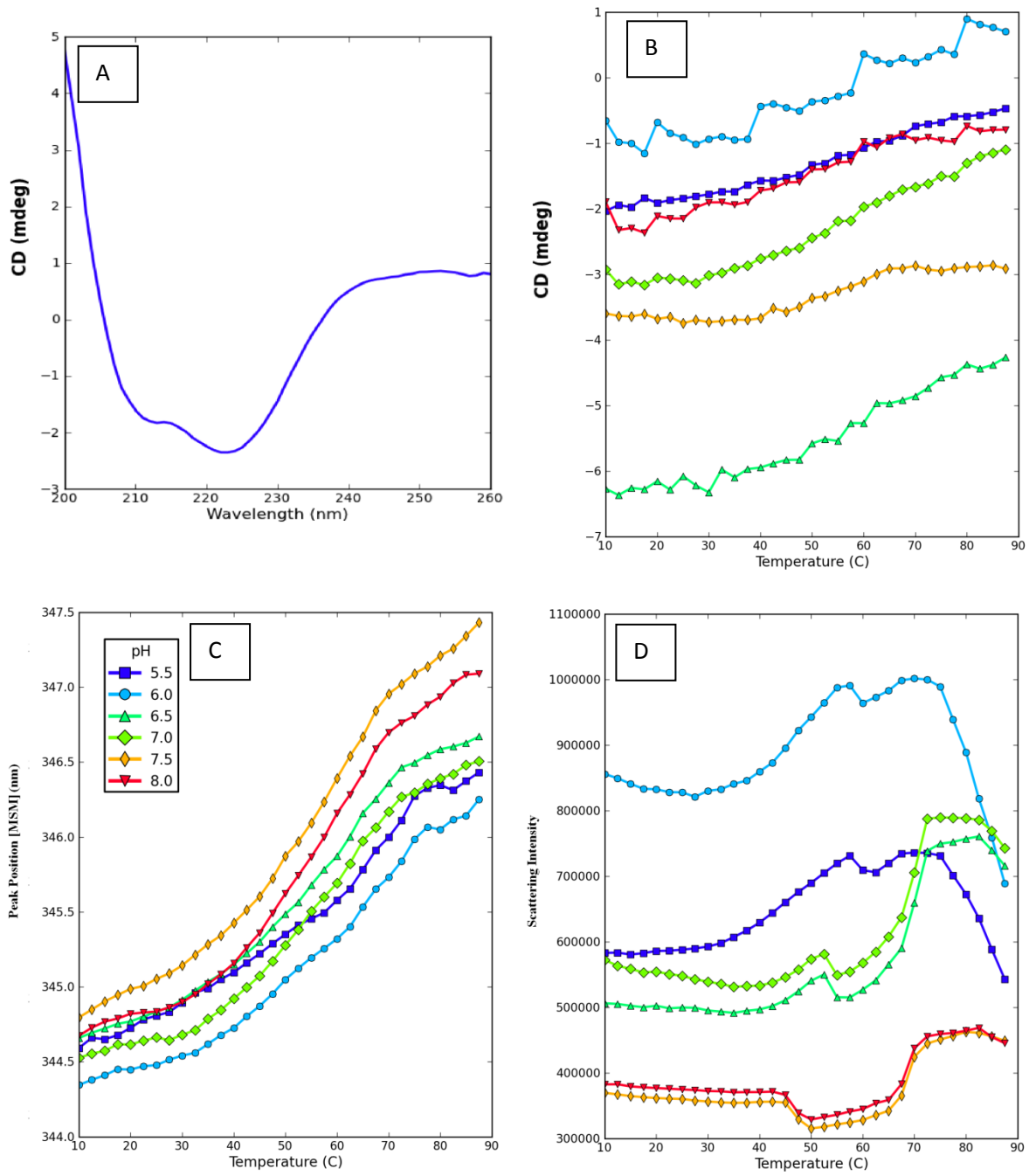

Figure 4.4. Biophysical characterization data for purified canine adenovirus type 2 in a 20 mM citrate phosphate buffer. (A) CD spectrum of CAV2 at pH 7 and 10°C. (B) CD signal at 222 nm, (C) changes in fluorescence peak position as analyzed by MSM, and (D) changes in the static light scattering intensity at different pH values as a function of temperature. Error bars are not included for clarity of data.

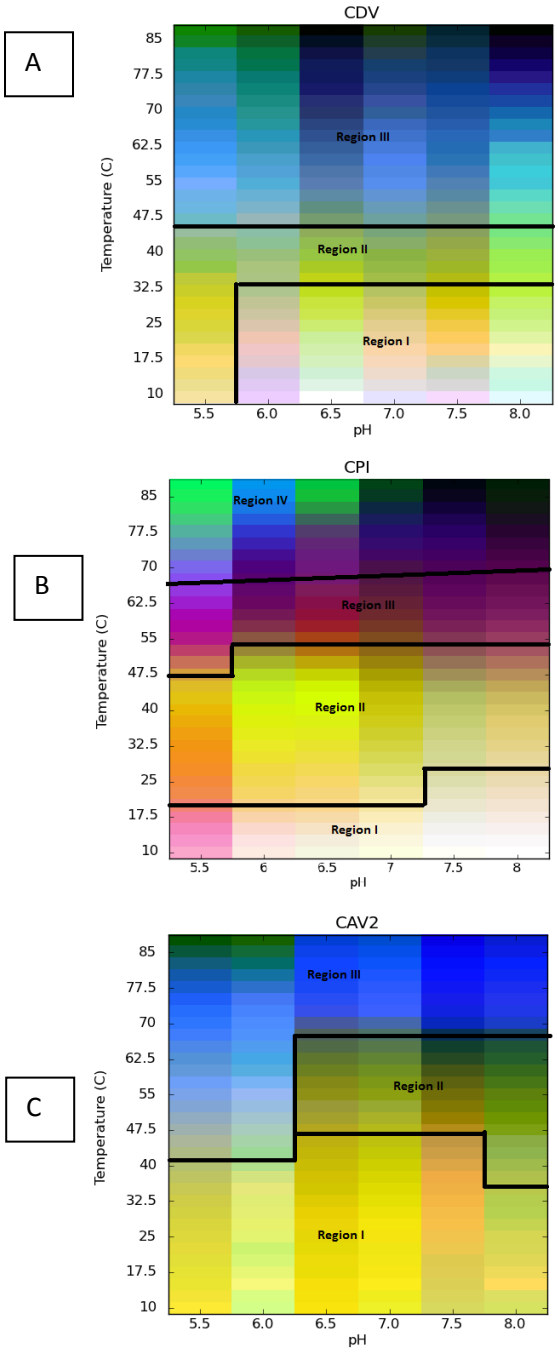

Figure 4,5. Empirical phase diagrams constructed for three different purified live attenuated canine viruses: (A) CDV (B) CPI and (C) CAV2. The red color represents the CD (secondary structure) data, the green represents the intrinsic fluorescence (tertiary structure) data and the blue represents the protein association (aggregation) data. The white and yellow regions represent the native state of the virus. The blue regions represent an aggregated state of the virus, pink region in the CPI virus represents a state where the viral proteins of the virus are unfolded.

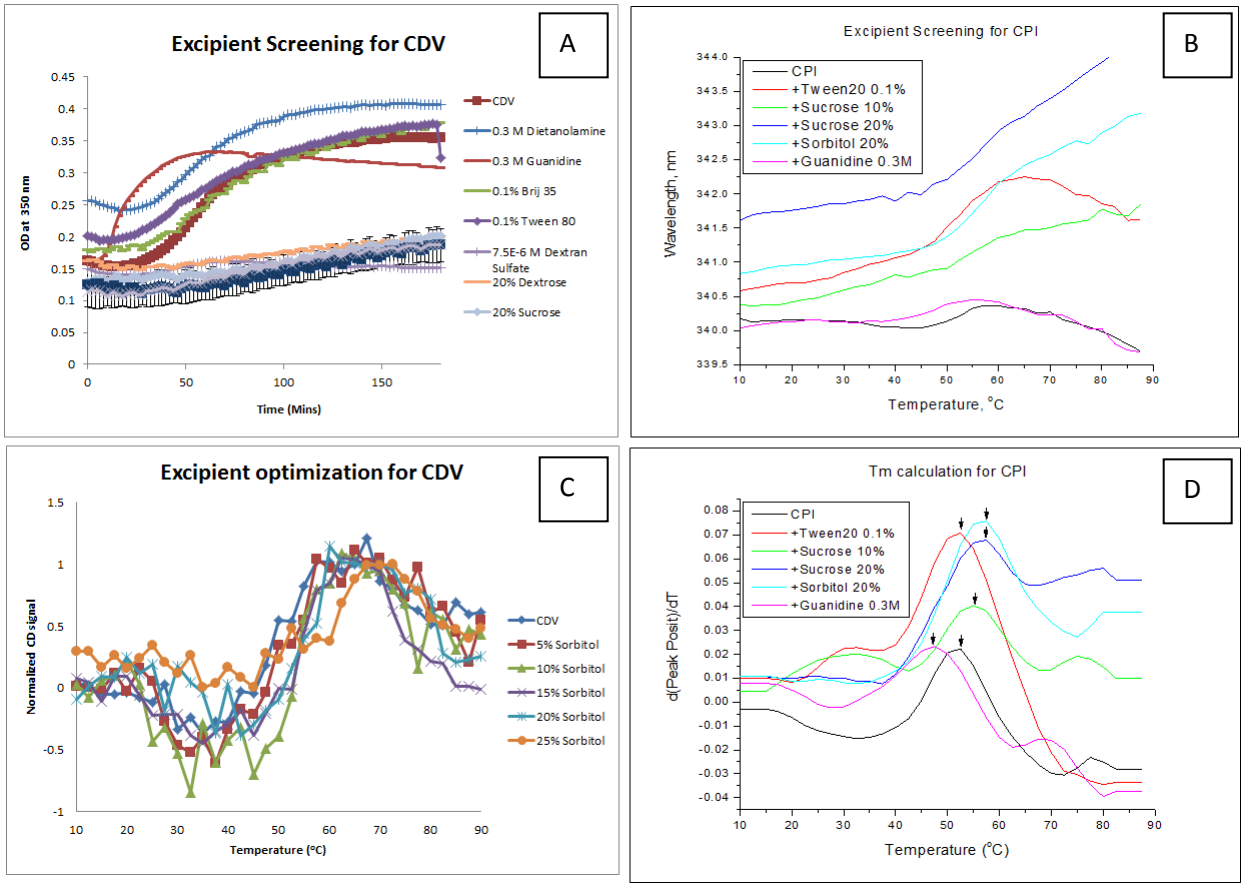

Figure 4.6. Excipient screening data for two purified live, attenuated canine viruses. (A and C) CDV virus stability as monitored by aggregation at OD350nm and thermal unfolding temperature (Tm) by circular dichroism. (B and D) CPI virus stability monitored by Tm values from fluorescence spectroscopy. Virus samples contained indicated level of excipients in a 20 mM citrate phosphate buffer at pH 7.